Functional roles of *rx3* and Shh in the hypothalamus of the zebrafish

Thesis presented for the degree of PhD

by Victor Muthu

at

The Centre for Developmental Genetics,
Department of Biomedical Science,
University of Sheffield

October 2010

PAGE NUMBERING AS ORIGINAL

Acknowledgements

Being the only person in the lab to work on a new model was never an easy task and was in fact very challenging and demanding. But I could never have gotten to this stage without, first and foremost, my supervisor Prof. Marysia Placzek who has supervised and supported me in many ways throughout the past three years, and very diligently providing feedbacks and thoughts into the experiments and data described in this thesis. I would hence like to extend my sincere gratitude, appreciation and heartfelt thanks to Marysia. Another individual who deserves recognition and appreciation is Dr. Kyoji Ohyama for his feedback, encouragement and open discussion of my work. Very special thanks go also to my two brilliant and wise advisors Dr. Freek van Eeden and Dr. Vincent Cunliffe for their expert inputs into my work especially those pertaining to zebrafish techniques and methods. I would also like to thank members of the Placzek lab and many individuals at the CDBG (scientists and non-scientists alike) especially Dr. Tanya Whitfield and Dr. Henry Roehl for kindly allowing me to use consumables and equipment in their lab; as well as the zebrafish aquaria staff for their support.

Of course, everything would not be possible at all without the love and encouragement from my lovely wife, Puneet, who has been the essence of my inspiration throughout my scientific career from the lecture halls during my bachelor's to the completion of this thesis. It is also a pleasure to be working alongside her from the beginning of our PhDs to the completion of our theses; her thoughts and ideas on my work were crucial and extremely valuable. Our newborn baby boy, Raphael, provided me with much joy and excitement especially during the stressful times of writing this thesis. I would also like to extend my thanks and hugs to my parents and siblings for just being them; always smiling and encouraging.

My thanks also go to Asst. Prof. Rudolf Meier (NUS, Singapore) and Asst. Prof. Klaus Heese (NTU, Singapore) for their very helpful and constant advice on my career path and scientific interests.

Finally and most importantly, I would to thank the Lord Almighty for providing me the opportunity to serve him through the knowledge of science and for keeping me in good health and faith throughout my studies here.

List of abbreviation

ADH	Anterior dorsal hypothalamus
AP	Anterior-posterior
BMP	Bone Morphogenetic Protein
BrdU	Bromodeoxyuridine
CNS	Central nervous system
CNTF	Ciliary neurotrophic brain factor
Cyc-t	Cyclopamine treated embryos
DV	Dorso-ventral
DTJ	Diencephalic-telencephalic junction
FGF	Fibroblast growth factor
ISH	In situ hybridization
LHN	Lateral hypothalamic nucleus
NSC	Neural stem cells
NPC	Neural progenitor cells
NC	Notochord
Phos-H3	Phospo-histone 3
PTC	Patched
PM	Prechordal mesoderm or prechordal mesendoderm
POMC	Propiomelanocorticotropin
PVH	Posterior ventral hypothalamus
RMS	Rostral migratory stream
Rx	Retinal homeobox gene / protein
SHH	Sonic hedgehog
SU embryos	SU5402 treated embryos
TBX	T-box transcription factor
3V	3rd ventricle

Table of Contents

List of Figures and Boxes

Materials and Methods

Result Chapters

Chapter 1

Abstract

The *rx/Rax* gene is a conserved homeobox transcription factor that is known to play an important role in the development of the eye. Mutations in *rx/Rax* gene manifest in the congenital loss of eyes known as anophthlamia or the development of small-eyes; microphthlamia. Despite numerous literatures describing the expression of Rx/Rax in the anterior hypothalamus of several model organisms, its function there is still hugely unknown and remains to be investigated. In order to gain insight into the role of *rx*, I have performed experiments aimed at understanding the signalling events governing the expression and function of *rx3*, a homologue of *rx/Rax*, in the anterior hypothalamus of the embryonic zebrafish model system.

Several studies have shown the reduction of *pomc* expressing neurons in the arcuate nucleus of the hypothalamus when the function of *rx3/Rax* is compromised. Here I have shown that *rx3* may, together with the signalling molecule sonic hedgehog (Shh), act to specify and promote the differentiation of progenitor cells to the Pomc cell fate. The functional loss of either *rx3* or Shh leads to a decrease in the number of *pomc* expressing neurons in the arcuate nucleus; located adjacent to the *rx3* and *shh* expressing domains at the anterior hypothalamus. Further analyses reveal that *rx3* and Shh may mutually activate each other's expression during the early establishment of the anterior dorsal hypothalamus. Experiments also show that Fgf may operate upstream of *rx3* to regulate its expression; as well as the number of *pomc* positive cells in the arcuate nucleus. These studies show for the first time, a role for *rx3* in the development of the anterior hypothalamus and the differentiation of *pomc* positive progenitors in the arcuate nucleus through its interaction with Shh.

Additionally, I have found the signalling factors Shh and Fgf3 to be maintained in the adult zebrafish hypothalamus. Furthermore, I have evidence to suggest a role for Shh in governing the proliferation of neural progenitor cells in the medial hypothalamus of the adult zebrafish. This study is the first to investigate neural stem/progenitor cells in the hypothalamus of the adult zebrafish.

Introduction

Introduction

1. The hypothalamus: embryo and adult

The hypothalamus is situated within the ventral forebrain and links the nervous and the endocrine systems. It is primarily responsible for regulating physical homeostasis, circadian rhythms and behavioural responses and co-operates with other regions of the brain to govern emotions such as fear and anger. Anatomically, the hypothalamus is comprised of retrochiasmatic, medial and mamillary regions, which occupy, respectively, the anterior, medial and posterior hypothalamus. Together these regions form a major portion of the ventral diencephalon and are bounded anteriorly by the optic chiasm and posteriorly by the hypothalamic /thalamic boundary.

Although the hypothalamus is undoubtedly one of the most important tissues of the nervous system, the mechanisms that underlie its development are still rather poorly understood – perhaps not surprising given its complexity. Only of late has research begun to indicate the role of intricate molecular pathways in its induction and patterning.

1.1 Functional overview of the hypothalamo-neuroendocrine axis

In amniotes, the hypothalamus connects to the pituitary or hypophysis via the infundibulum, an outgrowth of the ventral diencephalic floor commonly known as the pituitary stalk. The hypothalamus regulates the function of the pituitary through the release of neurohormones and neurotransmitters from two major groups of neurosecretory neurons: parvocellular neurons, which control the anterior pituitary (adenohypophysis) and magnocellular neurons, which innervate the posterior pituitary (neurohypophysis). Magnocellular neurons consist of large-sized cells, mainly in the supraoptic nucleus and periventricular nuclei. Parvocellular neurons are comprised of small neurons, largely found within the paraventricular nuclei of the hypothalamus (see Table 1 for full list of hypothalamic nuclei).

Hypothalamic Nucleus	Function
Anterior nucleus	▪ Temperature regulation – cooling of the body ▪ Reproduction and parental behaviour ▪ Control of the autonomic nervous system
Supraoptic nucleus Paraventricular nucleus	▪ Control of water balance via kidney ▪ Control of reproductive organs during ovulation and copulation ▪ Control of milk flow in mammals ▪ Contraction of uterus in mammals ▪ Social and parental behaviour ▪ Control of the autonomic nervous system
Posterior nucleus Mammillary body	▪ Temperature regulation- warming of the body ▪ Control of autonomic nervous system
Suprachiasmatic nucleus	▪ Pacemaker for the biological rhythms
Arcuate nucleus	▪ Control of synthesis and release of anterior pituitary hormones
Ventromedial nucleus Dorsomedial nucleus	▪ Feeding behaviour ▪ Aggression ▪ Control of autonomic nervous system

Table 1: The major nuclei in the hypothalamus of vertebrates and their main functions. (**Source:** *Comparative Vertebrate Neuroanatomy, 2005*[1])

Magnocellular neurons connect directly with the neurohypophysis, whereas, at least in amniotes, the connection of parvocellular neurons to the adenohypophysis is indirect (Figure 1). Magnocellular neurons project their axons through the infundibulum into the neurohypophysis, where their secretions of oxytocin and vasopressin are released directly into the blood stream for general circulation, hence 'direct connection'. In contrast, parvocellular neurons terminate their projections in the anterior-dorsal infundibulum, at a point that will form the future

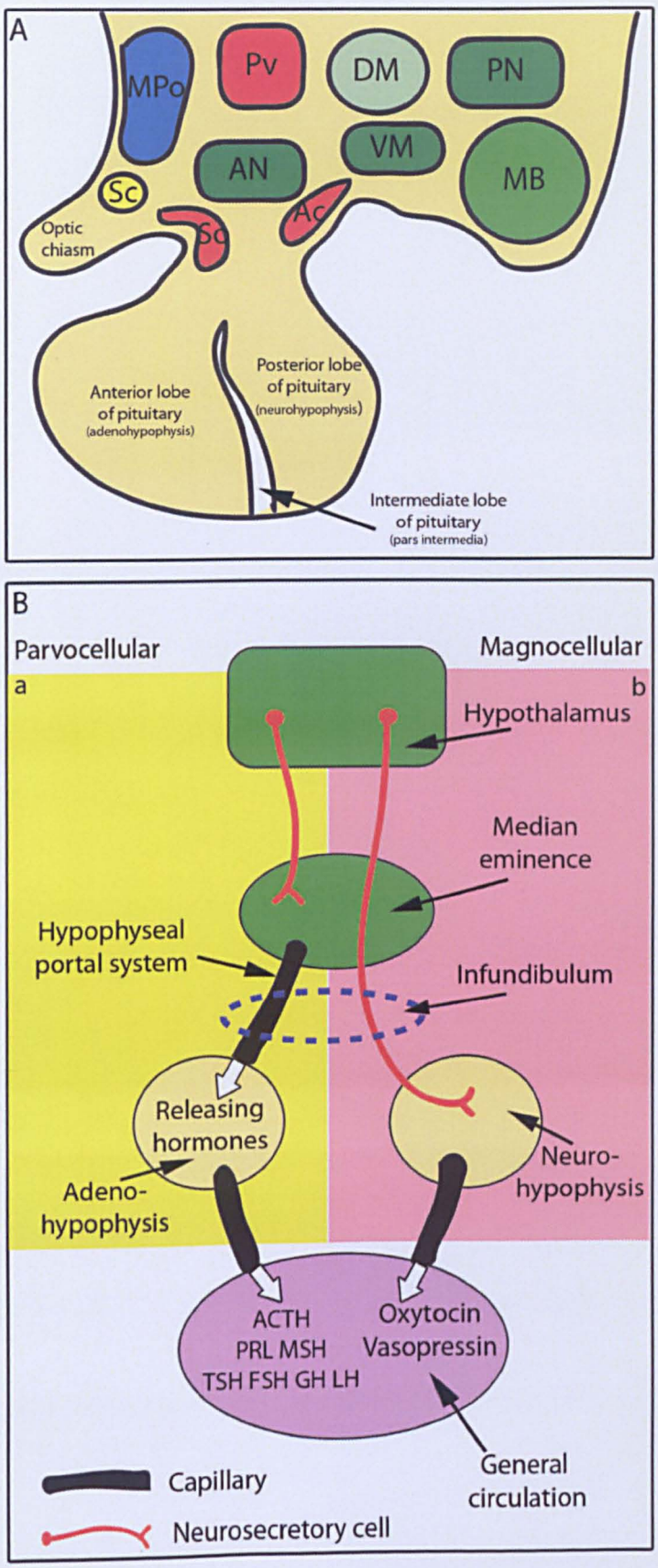

Figure 1: (A) Schematic representation of the major nuclei in the adult mammalian hypothalamus. Abbreviations: Ac, arcuate nuclues; AN, anterior nucleus; DM, dorsomedial nucleus; MB, mammillary body; MPo, medial preoptic nucleus; PN, posterior nucleus; Pv, paraventricular nucleus; Sc, supra-chiasmatic nucleus; So,, supraoptic nucleus; VM, ventromedial nucleus. Anterior to the left. (B) Schematic diagram of the hypothalamic hypophyseal portal system. Panel a, indirect link (parvo-cellular neurons); panel b; direct link (magnocellular neurons). Both figures are adapted from [1].

median eminence – a plexus of nerve terminals and portal capillary vessels (Figure 1). Parvocellular neurons release two main classes of hormones: releasing hormones and inhibiting hormones, which are picked up by the network of capillaries in the median eminence. This network forms part of the hypophyseal portal system, which then transports the hormones into the adenohypophysis, hence 'indirect connection'. Depending on which of the two classes are released, a variety of hormones are then either suppressed or released into the general circulation by the adenohypophysis. The full list of hormones from the hypothalamus and the target adenohypophyseal hormones can be found in Table 2.

Hypothalamic Releasing Hormone	Pituitary Hormone	Target Endocrine Gland
Gonadotropic releasing hormone (GnRH)	▪ Follicle stimulating hormone (FSH) ▪ Luteinizing hormone (LH)	▪ Testis ▪ Ovary
Corticotropin releasing hormone	▪ Adrenocorticotropic hormone (ACTH)	▪ Adrenal cortex
Thyrotropin releasing hormone (TRH)	▪ Thyroid stimulating hormone	▪ Thyroid
Prolactin releasing factor (PRF) and Prolactin release-inhibiting hormone (PIH)	▪ Prolactin (PRL)	▪ Ovary ▪ Mammary gland
Melanocyte stimulating hormone releasing factor (MRF) and Melanocyte stimulating hormone release-inhibiting factor (MIF)	▪ Melanocyte stimulating hormone (MSH)	▪ Pigment cells
Growth hormone releasing hormone (GHRH) and Somatostatin (SOM)	▪ Growth hormone (GH)	▪ Skeleton
Hormones produced in the hypothalamus and transported to the posterior pituitary (neurohypophysis) where they are secreted.	▪ *Oxytocin (isotocin in fish)*	▪ *Uterus* ▪ *Mammary gland* ▪ *Social behaviour*
	▪ *Vasopressin*	▪ *Kidney, blood pressure* ▪ *Social behaviour*

Table 2: Some of the major hypothalamic and pituitary hormones that are released into the general circulation and their target non-endocrine glands and organs (**Source:** *Comparative Vertebrate Neuroanatomy, 2005*[1])

The zebrafish similarly possesses both magnocellular and parvocellular axons. As in amniotes, magnocellular axons project directly to the neurohypophysis, releasing hormones directly into the portal vasculature. However, in contrast to the amniote, the fish does not appear to have an extended infundibulum, nor a median eminence. Instead, parvocellular axons are believed to project directly to the adenohyphysis, the releasing hormones acting directly on adenohypophyseal cells, without an intermediate transport via a portal capillary network.

Despite these intrinsic differences, the core mechanisms for establishing the hypothalamic-hypophyseal system appear to be conserved in fish and chick. In both species, FGF ligands secreted by the medial ventral midline or forming pituitary stalk of the zebrafish/chick hypothalamus play a critical role in axon and vasculature guidance. *In vitro* analyses in the chick, and *in vivo* analyses in the zebrafish show that FGFs exert long-range chemoattractive effects on both hypothalamic neurosecretory axons and the endothelial vasculature, attracting them to the medial ventral midline/pituitary stalk. Thus, in both fish and chick, the mechanisms underlying the functional hypothalamic-hypophyseal-pituitary axis appear to be conserved[2].

1.2 Development and patterning of the CNS

The formation of the central nervous system (CNS) including the hypothalamus is a complex event that occurs in several intricate steps. It begins with the formation of the neural plate through cell-cell interactions between the dorsal mesendoderm with the overlying ectoderm during late gastrulation; a process whereby the three distinct germ-layers (i.e. ectoderm, mesoderm and endoderm) are formed. In higher vertebrates, the neural plate folds into the neural tube through the process of neurulation (Figure 2). The future CNS including the brain and spinal cord are derived from the neural tube. These steps are described in detail below.

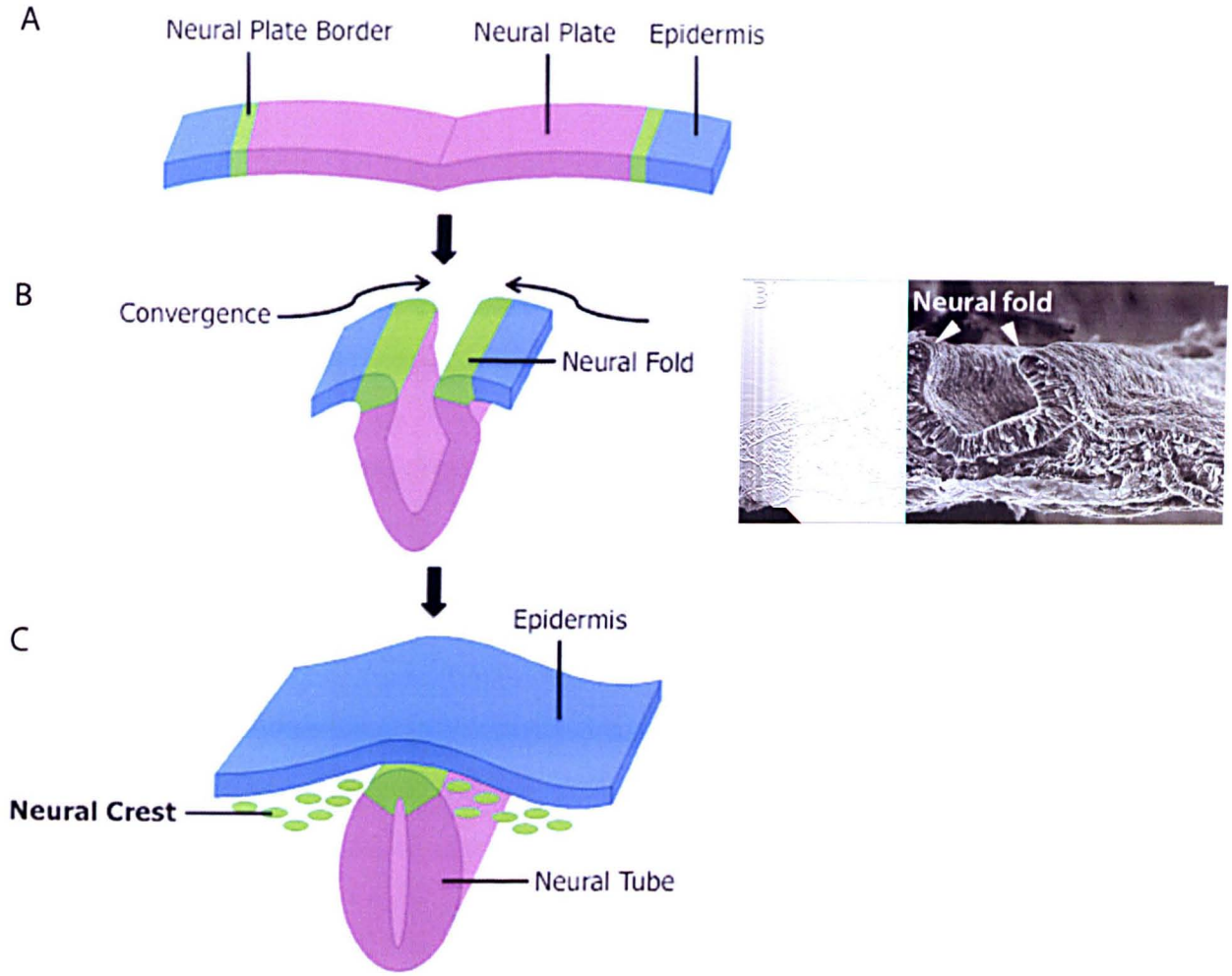

Figure 2: Formation of the neural tube. (A,B) The neural plate invaginates ventrally to form the U-shaped fold. (B,C) The neural folds come into contact at the midline and fuse before fully invaginating ventrally to form the neural tube. (B') Electron microscopy scanned image of the invaginating neural tube.

Image sources:

i) Images A-C are obtained from [149].

ii) Image B' is obtained from [150].

1.2.1 Induction of the neural plate from ectoderm

Studies performed in a variety of species, most notably, *Xenopus*, demonstrate a key role for the mesodermal layer in inducing neural plate from ectoderm. Experiments conducted by Hans Spemann and Hilde Mangold in 1924 point to the existence of a group of mesoderm cells that function as 'organizers' for the overlying ectoderm to adopt the neural fate. This group of cells is now known as the 'Spemann organizer' in the Xenopus[3]; its functional counterpart in amniotes is known as the Node or Hensen's node[4] (Figure 3). The Spemann organizer functions to inhibit the signalling molecule BMP4 by secreting BMP antagonists such as chordin and noggin. Upon inhibition of BMP4, the ectoderm thickens and forms the neural plate. The indirect induction of the dorsal ectoderm to a neural fate (neurectoderm) by the Spemann organizer via inhibitory mechanism suggests that the ectoderm would adopt a neural fate by default if not induced by BMP. The default neural fate of the ectoderm potentially underscores the importance of the nervous system as an evolutionary conserved 'master structure' without which control over other parts of the body would be impossible to achieve.

1.2.2 Neural plate to neural tube

The neural plate is organized along the principle rostrocaudal (anteroposterior) and mediolateral axes. The former is also termed the neuraxis, and corresponds to the main body axis. As outlined above, in many vertebrates, the neural plate subsequently folds to form the neural tube. Folding of the neural plate is made possible when cells throughout the neurectoderm lose their cuboidal shape typical of embryonic epithelia and take on a tall columnar, pseudostratified arrangement. The shape change causes the elevation of the margins on either side of the now U-shaped neural plate (Figure 2). The ends of these margins are known as the neural folds. These ends eventually meet at the dorsal midline margin and coalesce through the process of neurulation to form the rod-like neural tube. There are two distinct forms of neurulation that takes place in different parts of the neural tubes a) primary and b) secondary neurulation.

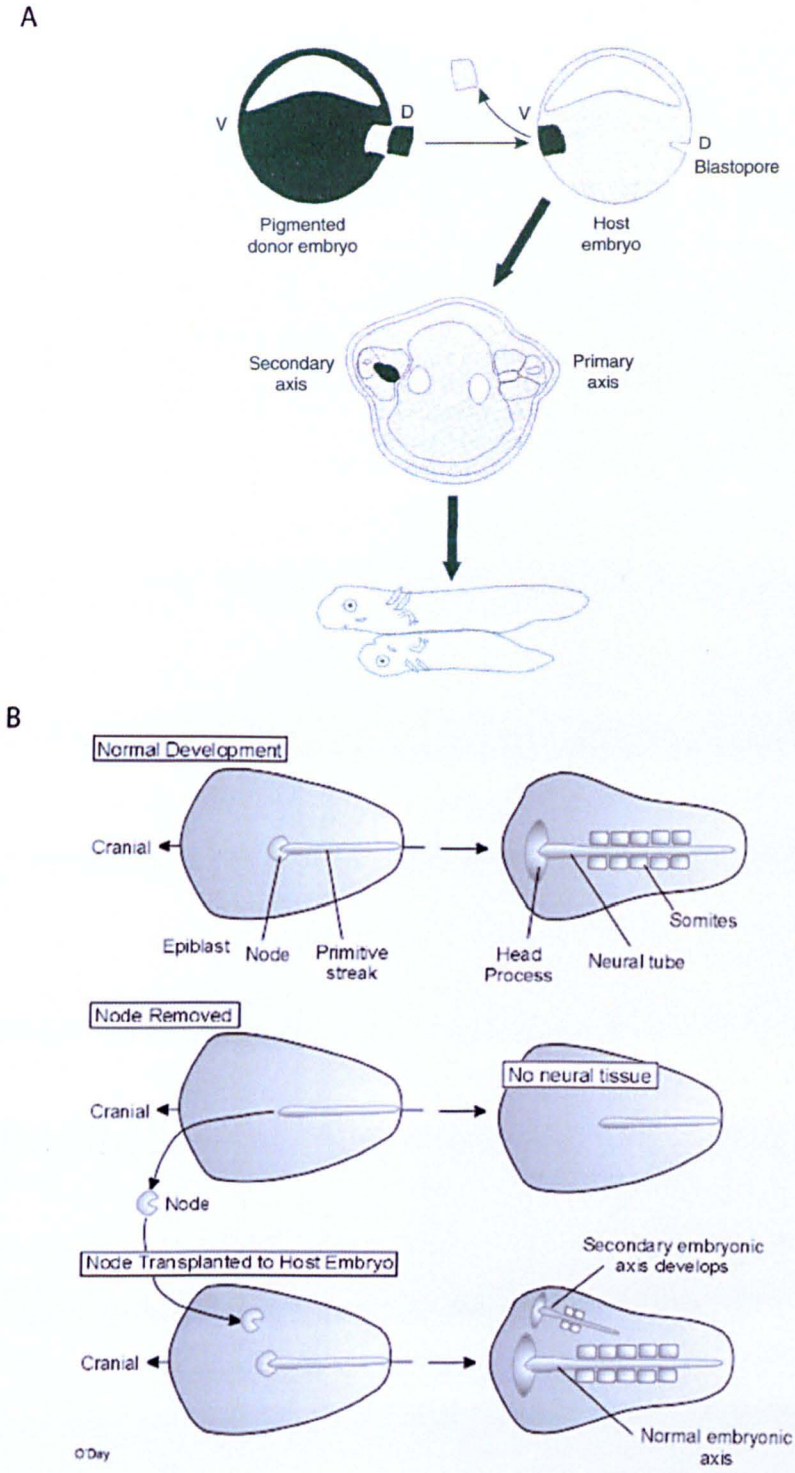

Figure 3: The organisers of neural induction in the frog and chick. (A) The Spemann's organiser in the frog's neural induction process. Grafting experiments performed by Spemann and Mangold showed an induction of a secondary CNS neuroaxis by the donor notochord derived from the grafted dorsal blastopore in the host embryo. (B) Similar experiments performed in the chick led to the finding that the Hensen's node is the functional equivalent of the organiser.

Image sources:
i) Image A was obtained from [151]
ii)Image B was obtained from [152]

In primary neurulation the neural folds come into contact and fuse to form the neural tube, as described above. In contrast, secondary neurulation occurs when a coalescence of multiple cavities appears in a preformed solid cord of posterior-most neural cells, which resembles a rudiment form of the neural tube. Thus both processes occur in the embryo but are spatially segregated: primary neurulation occurs in the anterior neural tube and secondary neurulation in the posterior neural tube. The tubes from both primary and secondary neurulation form the complete neural tube.

In the zebrafish however, as in all teleosts, the neural tube forms through a different neurulation process. The neural tube of the zebrafish forms through convergence-extension movements that cause ectodermal cells to accumulate along the midline and protrude ventrally. This give rise to a structure called the neural keel, which later produces a rod-like structure called the neural rod. A cavity then forms along the centre of the neural rod to produce the neural tube (Figure 4). This process is somewhat similar to the secondary neurulation process described above.

1.2.3 Regionalisation of the neural tube

The CNS in vertebrates is organized along two main axes, AP and DV, that underlie future distinct anatomical and functional structures. Signals operate early in embryogenesis to pattern the neural tube along the AP and DV axes, so that the anterior neural tube forms the brain and the posterior neural tube gives rise to the future spinal cord. Regionalisation along the D-V axis occurs through signals that derive, dorsally from the ectoderm, and ventrally from the notochord and prechordal mesoderm, specialized structures that differentiate from the organiser.

Regionalisation of the neural tube, along both the A-P and D-V axes, occurs through the action of long-range signalling molecules that can transmit signals from one cell to another and can trigger a response in the recipient cell. Cells that primarily produce these signals serve as the 'signalling source' or the 'signalling center' for a particular tissue. Well- characterized signalling molecules in embryonic development include Shh, BMP, Nodal, Fgf and Retinoic Acid. These molecules

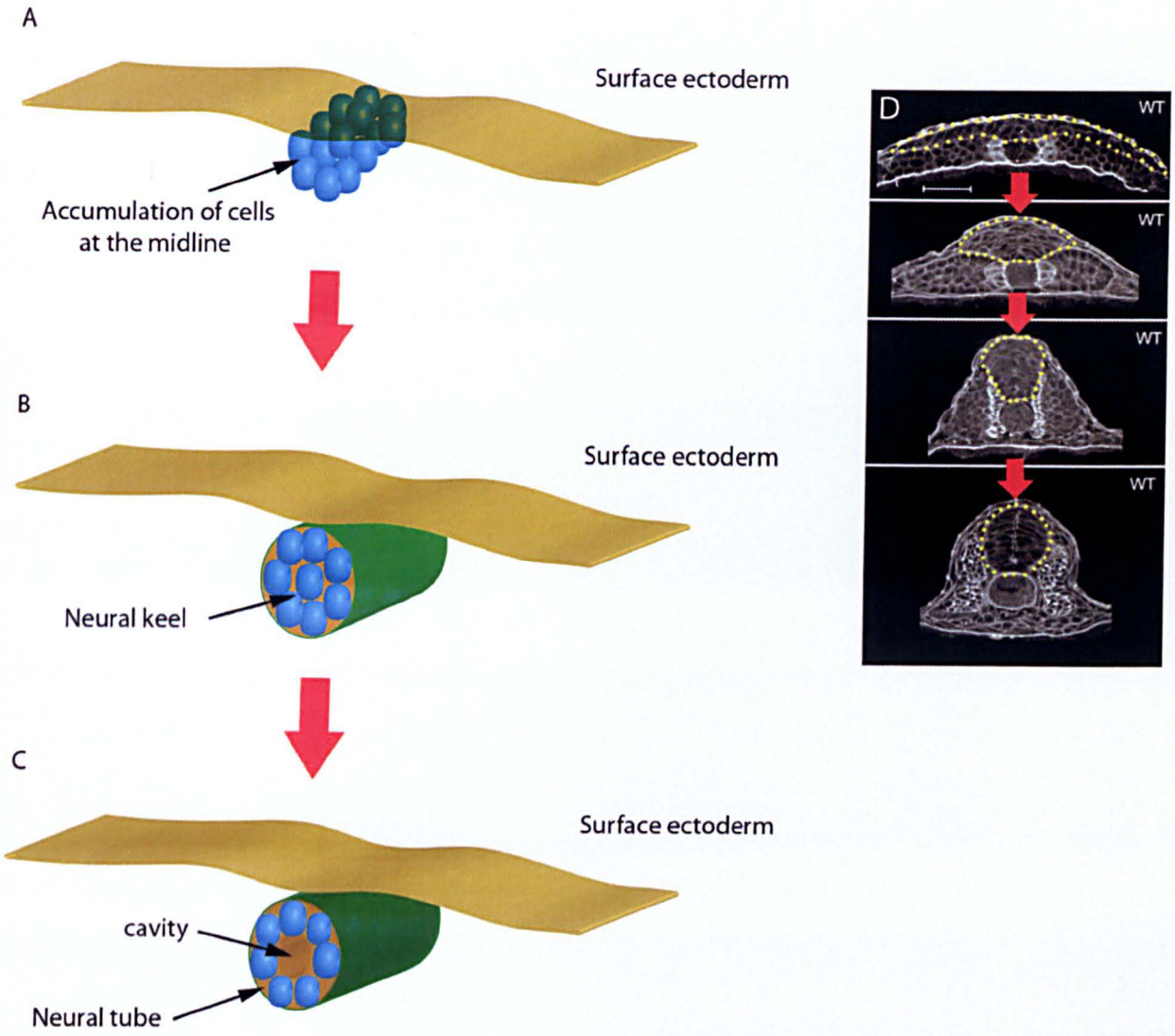

Figure 4 : Schematic representation of neural tube development in the zebrafish. (A) Cells accumulate and pile up at the midline of the surface ectoderm through convergence-extension movements. (B) The cells bulge ventrally creating a rod-like structure called the neural keel. (C) The neural keel later cavitates to form the neural tube. (D) Confocal micrographs of transverse sections through rhodamine-phalloidin-stained zebrafish embryo showing the formation of neural tube.

Image source:
i) Image D is obtained from [154].

execute their function by regulating transcription factors in responding cells. A number of lines of evidence show that signalling molecules, especially Shh, function as morphogens[5], molecules that govern the patterning of a tissue by establishing a concentration gradient across the tissue. This gradient elicits different responses in recipient cells in the tissue, according to the threshold concentration. In other words, initially similar cells are differentially patterned based on the amount of morphogens they received. The morphogen concept is best described using the 'French flag' model first suggested by Lewis Wolpert in the 1960s. The signalling molecules-transcription factor interaction gives rise to a highly organised topology of the neural tube where disctinct neuronal subtypes are generated in a characteristic order (see Figure 5 for example of this in the D-V axis of the neural tube)[6]. Recently emerging evidence suggests that signalling molecules (i.e. Shh)-transcription factors operate in a dynamic feedback loop to establish compartmentalised response within the ventral neural tube during early patterning[7].

As a result of these patterning events, distinct domains are established in the early neural tube. Additionally, cross-talk between early regions establishes further subdivions, particularly well-characterised along the A-P axis. Thus, in the early embryo the rudimentary brain can be separated into three distinct anatomical compartments, the prosencephalon (forebrain), mesencephalon (midbrain) and rhombencephalon (hindbrain). Further subdivisions arise from these: the telencephalon and diencephalon forming from the prosencephalon and the metencephalon and myelencephalon from the rhombencephalon. The diencephalon occupies relatively ventral regions of the brain, and gives rise to a variety of ventral forebrain structures, including the epithalamus, dorsal thalamus, ventral thalamus and the hypothalamus. The orders of these structures are evolutionarily conserved throughout vertebrates.

1.3 Development and patterning of the hypothalamus

The integrated patterning and development of A-P and D-V regions of the neural tube means that anterior-most floor plate cells extend into the forming diencephalon. A number of recent studies, in fact, show that anterior-most floor

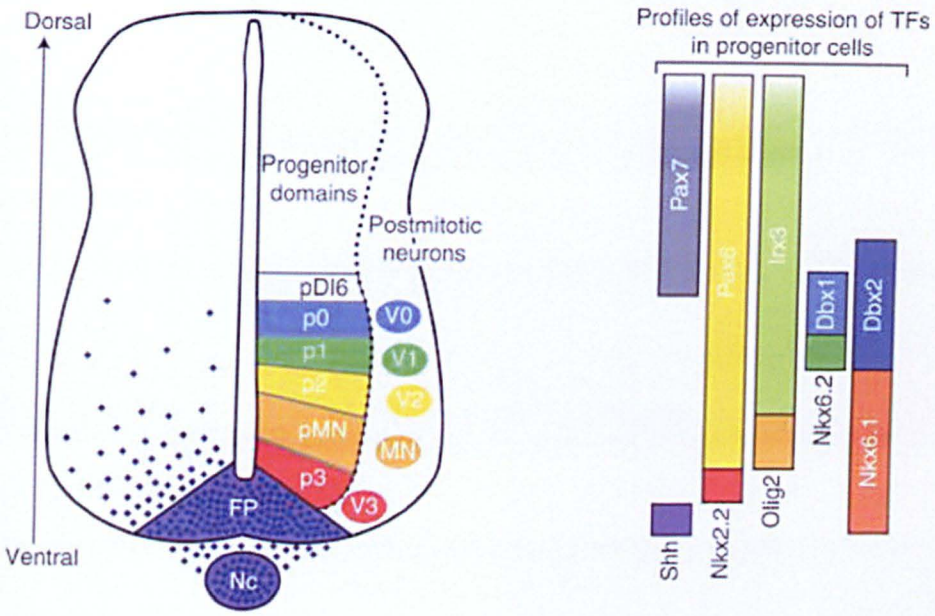

Figure 5: Graded SHH concentration along the D-V axis of the posterior neural tube (spinal cord anlage) and the responsive trancription factors (TFs). Different progenitor cell domains (p0-p3) form in response to the graded SHH (blue) emanating from the floor plate (FP). The graded signal elicits different responsive transcription factor that give rise to the specific and compartmentalised progenitor domains.

Image source:

Images were obtained from [7].

plate cells give rise to ventral-most regions of the forming hypothalamus, through a series of signalling event orchestrated by secreted molecules emanating from the adjacent prechordal mesoderm (PM).

1.3.1 Formation of the floor plate

The notochord and prechordal mesoderm underlie the neural tube and signal to it along the entire A-P axis. Ventral midline regions of the neural tube that lie immediately adjacent to the notochord and floor plate will ultimately form a specialised group of cells, termed floor plate cells (Figure 6). The floor plate is a highly conserved morphological structure in vertebrates, and serves as a signalling source for adjacent cells in the neural tube. Thus the floor plate, along with the notochord/prechordal mesoderm, and its complementary dorsal organizer, the roof plate, plays a key role in the determination and specification of cell fate along the neural tube.

The mechanisms underlying floor plate determination have been fiercely-debated and as a result, two models were proposed: a) inductive model and b) allocation model[8]. The first model suggests that underlying mesoderm (notochord or prechordal mesoderm) induce ventral midline neural tube cells to differentiate into floor plate fate via secretion of Shh from the notochord, or Nodal (or, in the chick, a combination of Nodal and Shh) from the prechordal mesoderm[9]. Support for this interpretation derives from experiments showing that naive and uninduced epiblast precursor cells isolated from the ectoderm immediately anterior to the Hensen's node, or lateral neural plate cells, differentiate to floor plate cells when exposed to recombinant Shh. In the presence of recombinant Nodal, a lower concentration of Shh is required to achieve a similar induction of floor plate. Conversely, removal of the notochord, or genetic ablation of Shh, prevents floor plate formation in the posterior neuraxis; similarly, removal of the prechordal mesoderm, or genetic ablation of Nodal or Nodal signalling, prevent floor plate formation in the anterior neuroaxis[9].

The second model proposes a common origin of precursor floor plate cells with axial mesoderm. Fate mapping experiments in the chick and quail hypothesize that

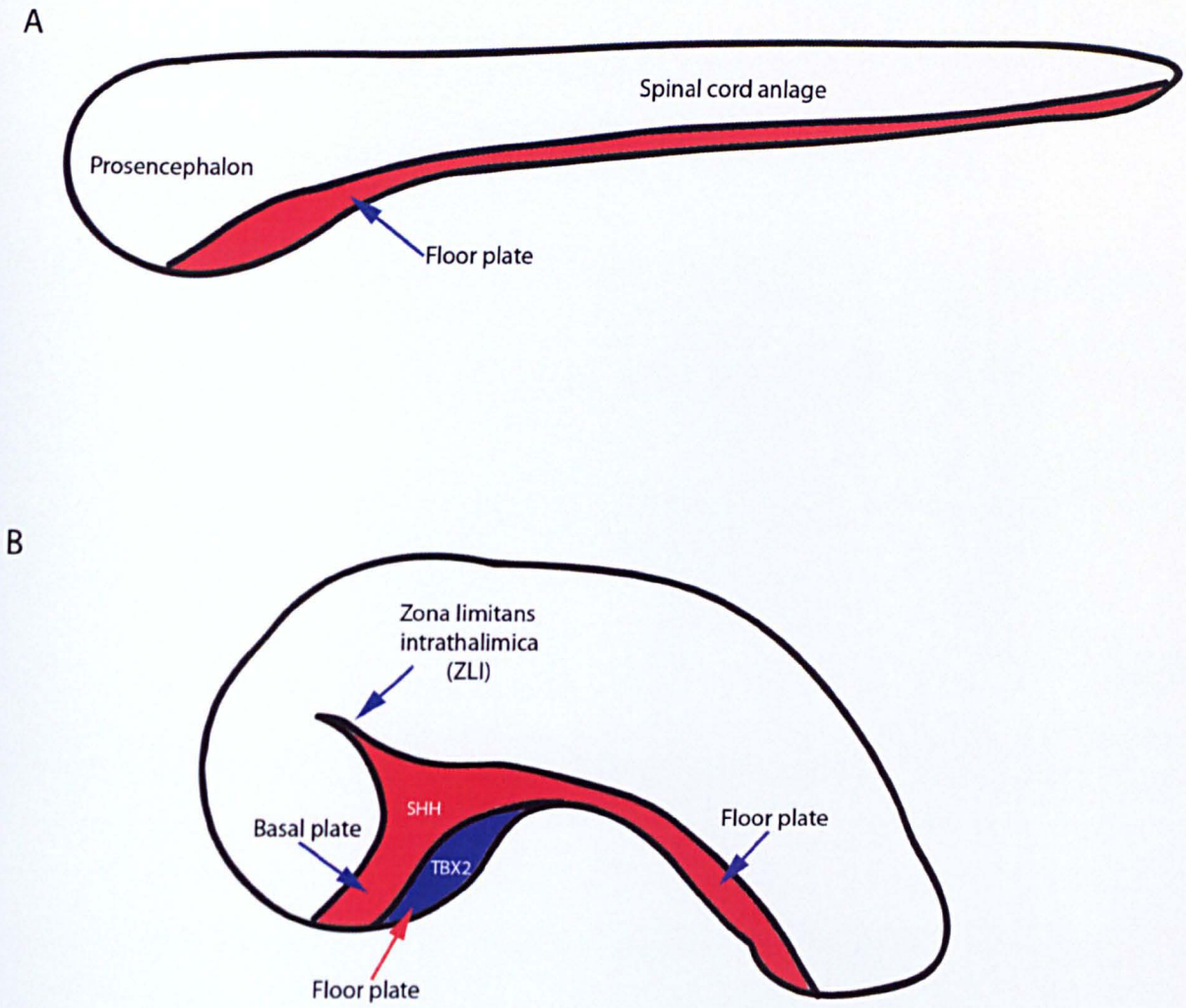

Figure 6 : Development of the hypothalamus. (A) SHH is expressed in the floor plate at the ventral neural tube of the early developing embryo. The floor plate spans the entire anterior-posterior neuraxis. (B) The hypothalamus is specified when SHH is induced in the anterior basal plate. Simultaneously, signals (BMP/WNT) from the underlying prechordal mesoderm activate the expression of TBX2 in the anterior floor plate. TBX2 inhibits the expression of SHH in the anterior floor plate. The TBX2 positive domain subsequently undergoes further patterning into different discrete domains along the anterior-posterior axis of the hypothalamus. (A,B) SHH is represented in red; TBX2 in blue. Anterior to the left; dorsal to the top.

the floor plate and notochord are derived from a common cell pool located in the Hensen's node[4]. Mutant analysis in the zebrafish support this idea[10]. These findings led to the proposal that Shh is required as a trophic factor for the survival and maintenance of the floor plate cells rather than an inducing factor. The two models are not mutually exclusive, and recent evidence suggest that the two models operate at different positions of the floor plate, induction required for anterior-most floor plate cells, and maintained trophic support for more posteriorly-located floor plate cells[8].

1.3.2 Hypothalamus identity: induction of the anterior floor plate

As outlined above, Shh and Nodal are secreted from prechordal mesoderm and induce anterior-most Shh positive floor plate cells. As in posterior regions of the neuraxis, such Shh positive floor plate cells have been proposed to then homeogenetically induce Shh in the ventro-lateral forebrain[11-13], resulting in Shh expression in cells of the basal plate. Together, the anterior floor plate cells and Shh positive basal plate cells comprise the anlage of much of the future hypothalamus (Figure 6). Almost immediately, anterior-most floor plate cells undergo a further differentiation to 'hypothalamic floor plate-like' cells, losing Shh expression and instead expressing hypothalamic markers. Shh expression is downregulated through the action of BMP (Bone Morphogenetic Protein) secreted from the PM. Analyses in the chick demonstrate that BMP mediated expression of the T-box transcriptional repressor, TBX2, is sufficient to repress SHH expression and promote hypothalamic floor differentiation, and suggest that BMP promotes the upregulation of TBX2 by reducing the levels of WNT activity in anterior floor plate cells[14]. This mechanism is likely to operate in other species: in the mouse, deletion of a TBX binding site upstream of the *Shh* gene results in prolonged expression of SHH in the hypothalamic floor[15]. In the zebrafish, Tbx2b is expressed in a similar fashion to that shown in the chick[16], and Axin, a Wnt antagonist, is required for the differentiation of floor plate cells into hypothalamic cells[17]. The reduction in Shh expression in anterior floor plate cells leads also to a loss of Shh signalling components. Experimentally prolonging Shh signalling in anterior floor plate cells prevents their differentiation towards a hypothalamic floor fate. Normally, the homeodomain transcription factor, Emx2 is upregulated in the

posterior hypothalamic floor, and the signalling ligands, FGF10 and FGF3 are upregulated in and adjacent to the medial hypothalamic floor. When Shh signalling is prolonged, such markers fail to be upregulated[14]. However, expression of both Shh and Shh signalling components are maintained in the immediately adjacent basal plate through late stages of embryogenesis (Figure 6).

In the published literature, a different nomenclature has been used to define regions of the forming hypothalamus in the chick and the zebrafish. In the zebrafish, no study has examined early stages of zebrafish development (10-15 hpf), when Shh might be expressed in the anterior floor plate. However, examination of 26-30 hpf embryos reveals a similar profile in gene expression: cells in a midline region defined as the 'posterior ventral hypothalamus' (PVH) express FGF3, FGF8, Tbx2b and Emx2. This suggests they are the homologous cells to chick 'hypothalamic floor'. In support of this interpretation, Nodal signalling has been shown to be required for the specification of the PVH. In the 26-30 hpf embryo, PVH cells are surrounded, anteriorly and dorsally, by Shh positive 'anterior dorsal hypothalamic' (ADH) cells[13]. These appear to be homologous to the Shh positive basal plate cells that are in a similar position in the chick embryo (see Figure 1.9 in result chapter 1). In the zebrafish, hypothalamic cells at the ADH express the transcription factor *rx3* (retinal homeobox transcription factor 3). In this thesis, I retain the use of the term PVH; however, I refer to the ADH and the basal plate as distinct structures.

The conservation of signalling molecules and transcription factors in both amniotes and anamniotes suggests a conserved mechanism for formation and patterning of the hypothalamus. Some of these mechanisms in which transcription factors operate in the hypothalamus are even found to be conserved in invertebrates[18]. Despite this, little is known about the function of such highly conserved transcription factors. In this thesis, I am going to focus on one such factor, the *rx3* or *rx/Rax* gene.

2. The retinal progenitor homeobox 3 (*rx3*)

The retinal progenitor homeobox gene (*rx*) or its mammalian homologue the 'retina and anterior neural fold homeobox' gene (*RAX*) belong to the homeobox gene family of transcription factors and play a pivotal role in the development of the optic vesicles and the eyes. In the early mouse embryo, *RAX* is expressed in the anterior neural fold, a group of cells at the anterior pole of the neural plate that constitute a secondary signalling centre, responsible for the localised patterning of the anterior forebrain including areas that will give rise to the forebrain and optic vesicles[19]. An early study[19], demonstrated *Rax* expression in the anterior neural fold of embryonic day 7.5 (E7.5) mouse embryos, a restricted expression in the optic vesicles, optic stalk and ventral diencephalon at E9.5, and maintained expression in the retina. These observations suggested a function for the *Rax* gene in development of the optic vesicles/eyes, and led to further investigations into the function of *Rax/rx* gene, the majority which describe how mutations in the *Rax/rx* gene result in severe eye malformations as discussed in the following sections.

2.1 Conservation of *rx/Rax* gene and protein sequences

The *rx/Rax* gene is highly conserved amongst vertebrates and *Drosophila* as well. The *rx* gene belongs the family of homeobox genes and has, in its sequence, conserved octapeptide and Rx homeobox domains as well as a conserved OAR domain at the C- and N-terminals of the peptide respectively. The homeobox domain is approximately 180 base pairs long and encodes a protein that binds to DNA, thus allowing the gene to perform its role as a developmental transcription factor in all eukaryotes[20].

The *Rax* gene shares a high nucleotide sequence similarity with a range of 93-99% sequence identity within primates including humans and 65-91% within mammals compared to humans. The zebrafish orthologue *rx3* gene shares a 57% sequence similarity to the human *RAX* gene, whilst *rx1* shares 54% and *rx2* shares 53% respectively. According to gene annotations in Ensembl[21], the zebrafish *rx3* gene is the true orthologue of the human *RAX* gene. It is also syntenically homologous to the human *RAX* gene on chromosome 18 compared to *rx1* and *rx2*, although in the

zebrafish, *rx3* gene is located on chromosome 21. This is consistent with its similarity in both expressions and functions attributed to the mouse *Rax* gene as previously described.

2.2 Phylogeny of the *Rax/rx* genes

The phylogenetic tree in Box1 describes the evolution of the RAX/Rx gene across selected vertebrates. The tree is generated through ClustalX2.0[22] and TreeView X[23] based on the multiple sequence alignment (MSA) of the RAX/Rx proteins of the respective organisms, analysed using ClustalX2.0 as well (Figure 7). The tree in Box1 shows a high similarity of the RAX proteins in higher vertebrates with the mouse (Mus musculus) and the rat (Rattus norvegicus) sharing the closest similarity. Although the zebrafish Rx3 does not share the same clade or branch as the human, mouse and rat, it does share a high protein sequence similarity with the RAX proteins of human, mouse and rat (see Figure 7). The OAR and homeobox domains are highly conserved as shown in the MSA data.

2.3 *rx* (*Rax*) in vertebrate eye development

As mentioned above, the *rx* gene has been shown to be critical in vertebrate eye development. Mutations in the *RAX* gene in human cause anophthalmia, a condition where either both eyes (or one eye) are missing[24]. Micropthalmia, a less severe form of anopthalmia, where eyes are formed smaller than the usual size, also arises from mutations in the *RAX* gene. These defects can also be observed in the mouse, xenopus and zebrafish where perturbation of the *rx/Rax* gene function results in the development of small or absent eyes[25-27]. The genomes of the teleosts (including the zebrafish) and amphibians contain three *rx* genes of which *rx3* gene is expressed the earliest in the presumptive eye field. The *rx3* gene in the zebrafish is 1260 base pairs (bp) in length or 292 amino acids (aa). In the zebrafish, mutation in the *rx3* gene (*chokh* mutant) disrupts the formation of the presumptive eye field and subsequently prevents the morphogenesis of the optic vesicles, which fail to evaginate from the presumptive forebrain region[26]. In this mutant, only the surface ectoderm-derived eye lenses remain. This consequently leads to the failure of eye formation. The mechanism by which *rx3* specifies the eyes is partly

BOX 1

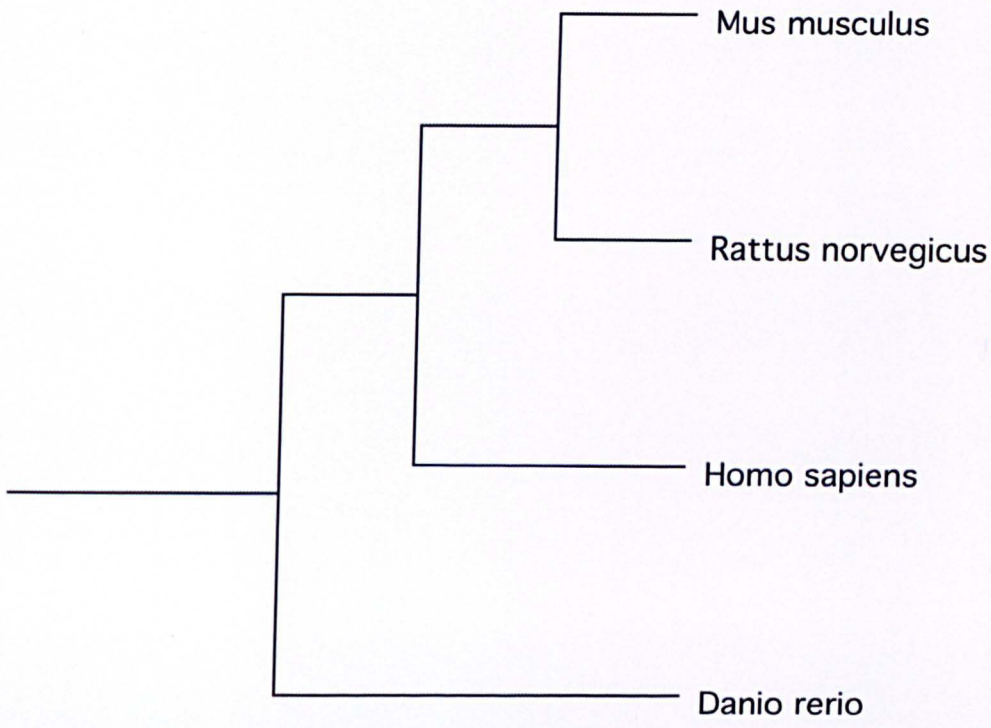

Phylogenetic tree representing the degree of similarities between the RAX proteins of the mouse (*Mus musculus*), rat (*Rattus norvegicus*) and human (*Homo sapiens*), with the Rx3 protein of the zebrafish (*Danio rerio*). The mouse and rat share the same clade indicating the closest similarities of the protein among all four vertebrates.

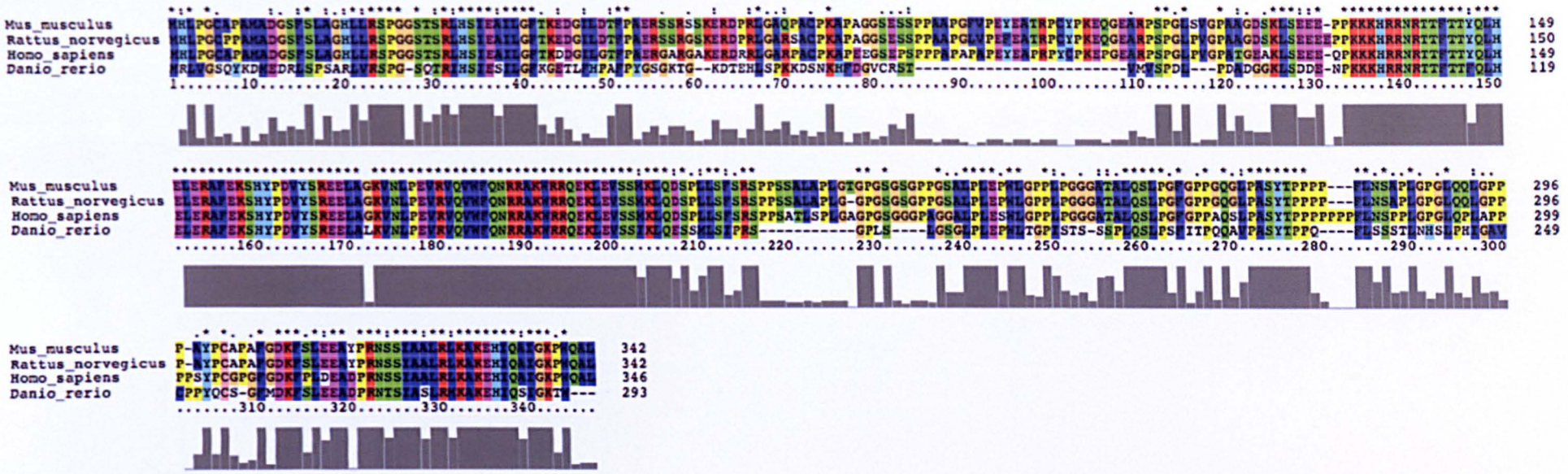

Figure 7: Multiple sequence alignment (MSA) of RAX/Rax protein sequences from selected vertebrates including the zebrafish (*D.rerio*). Conserved sequences are indicated.

understood: in the *chokh* mutants, retinal progenitor cells are specified, but remained trapped in the lateral wall of the diencephalon, failing to undergo morphogenesis to form the optic vesicles [26, 28, 29].

2.4 Rx/Rax expression in the hypothalamus

In contrast to the many studies that have analysed the role of Rax/rx gene in eye development, fewer studies have analysed its function in the hypothalamus. The *Rax* null mice exhibit defects, not only in the eyes, but also patterning defects in the hypothalamus[30]. In early embryonic development, the optic cup (the outer layer of the optic vesicles) maps to an adjacent region to the hypothalamus in the anterior neural plate. Together, these observations have led to the proposal that the two tissues may have common origins that require *rx* gene for specification. An additional study has demonstrated that *Rx* function is cell autonomously required for the formation of the neurohypophysis (posterior pituitary) in the mouse[31].

Of all three *rx* genes in the zebrafish, only *rx3* is expressed in the hypothalamus: expression is first detected in embryogenesis, but maintained in the hypothalamus of adult zebrafish[32]. However, our current knowledge and understanding of the role of *Rax/rx3* gene in the development of the hypothalamus is still in its infancy. Previous studies have begun to analyse the function of Rx3 in the hypothalamus, and have demonstrated a reduction in the number of propiomelanocorticotropin (pomc)[33] and vasotocin-neurophysin (vtn)[18] hypothalamic neurosecretory neurons, in both *chokh* (*rx3*) mutants and *rx3* morphants, indicating a requirement for *rx3* in the formation and (or) differentiation of these neurons. However, the mechanism by which *rx3* governs the formation for these neurosecretory neurons are unclear. In result chapters 1 to 4 of this thesis, I will focus and investigate the mechanism that underlies the role of *rx3* for the formation of the Pomc neurons in the arcuate nucleus of the hypothalamus of the embryonic zebrafish.

In this thesis, I have also investigated the maintenance of signalling factors in the adult zebrafish hypothalamus independently from investigating the function of *rx3* in the embryonic hypothalamus. As will be seen and discussed through result chapter 5, the signalling molecules are hypothesized to govern the behaviour of

neural progenitor cells in the medial hypothalamic region of the adult zebrafish. Section 3 below hence serves as the overall Introduction to result chapter 5.

3. Adult neural stem cells and neurogenesis

3.1 Overview of stem cells

Studies in invertebrates and vertebrates, including humans, have shown the existence of stem cells that have the capability to self-renew and give rise to cells of different fates through the process of differentiation. They are the origin of all cells in an organism. The great pathologist Rudolph Virchow (1821-1902) once stated, "All cells come from cells" reflecting the nature of stem cells which were yet to be discovered at that point in time. Stem cells are pluripotent or multipotent and have the ability to self-renew and repopulate the niche in which they reside. Pluripotency refers to the ability of stem cells to repopulate each and every cell type in an organism, a key property that is attributed to embryonic stem cells[34]. Multipotency refers to the ability to differentiate and give rise to cells within an organ or tissue and it is used, for instance, to characterise tissue-specific, or adult stem cells, including neural stem cells (Figure 8). Recent research indicates the maintenance of stem cell niches in many areas of the adult, including the brain. These findings demonstrate the persistent nature of stem cell maintenance in the adult through self-renewal, and suggest they could serve as potential sources for new cell birth to replenish dead or damaged cells.

However, the adult stem cell field, though advancing rapidly, is still clouded with scientific altercation on a proper guideline that can be used to identify and classify a 'stem cell'. The general opinion of what a stem cell should constitute in the adult system mainly stems from researches into adult haematopoietic stem cells, since it was in this system that adult stem cells were first identified[35]. Thus a rigorous definition: adult stem cells, like embryonic stem cells, must demonstrate the capacity to self-renew either *in vivo* or *in vitro* in artificial culture conditions and must also demonstrate multipotency i.e. retaining the ability to differentiate to different (albeit limited) cell lineages. A number of cellular markers are used to define both the stem cell and the niche, but none is strictly specific. Another

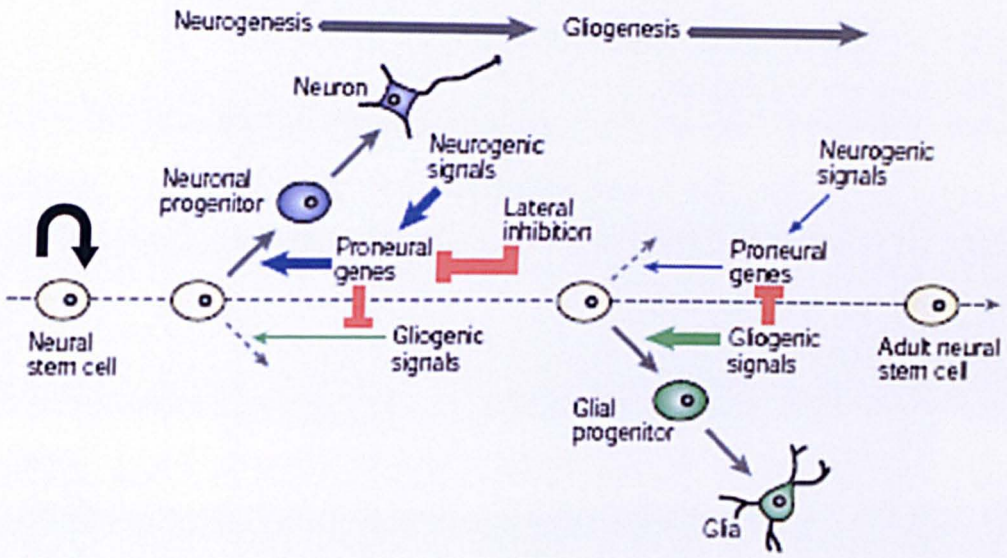

Figure 8: Schematic representation of neural stem cell differentiation process. Neural stem cells are multipotent and can undergo neurogenesis and gliogenesis to produce all neural cell types in the CNS. Gliogenesis generally takes place after neurogenesis and both of these processes mutually inhibit each other. Neural stem cells are also capable of undergoing self-renewal.

Image source:
Modified from [154].

emerging opinion but not yet a requirement for defining a stem cell is the observation of asymmetric cell division to produce a 'stem' daughter cell and a lineage-determined daughter cell.

3.2 The stem cell niche concept

Stem cells are believed to exist in niches where they are maintained as a group of cells or population instead of randomly distributed individual cells. A stem cell niche can be defined as a specialized microenvironment in which stem cells reside[36]. The stem cell niche concept originated from studies in the mouse haematopoetic system and mouse gonads[36]. Their molecular control has been particularly well-studied through analyses of the gonadal niches in invertebrates[37]. The precise nature of stem cells has been a fiercely-debated topic, and will be discussed further in the context of the adult brain in the proceeding sub-chapters.

3.3 Adult neural stem cells in the mammalian and non-mammalian central nervous system

3.3.1 Neural stem cells and neural progenitor cell identification

In the developing central nervous system (CNS) of the vertebrate embryo, a myriad of neuronal, glial and ependymal cells are produced in a spatio-temporally defined order [38]. These cells originate from neural stem cells (NSCs), which are the multipotent stem cells, found in the nervous system. NSCs appear to be maintained in the adult CNS as well, where they can continue to serve as multipotent stem cells with the capability of producing new neurons and glia cells via intermediary neural progenitor cells (NPCs). Despite our relatively advanced understanding of the biology and function of adult stem cells, the detection of NSCs in the adult CNS has been extremely difficult. This is mainly due to the intricacies of identifying a *bona fide* NSC, as distinct from a neural progenitor cell. Molecular markers, such as those listed in Table 3, cannot easily distinguish between NSCs and NPCs. Proliferation is frequently used in attempts to distinguish NSCs from NPCs: the latter can be readily detected using cell proliferation markers, since they are actively dividing. PCNA, which marks for S-phase, MCM5, which marks for cells in G1, and BrdU,

which marks S-phase cells, are frequently used to assess the presence of NPCs and potential NSCs.

Molecular markers	Functional classification
SoxB1 (including sox2 and sox3)	Transcription factor
Nestin	Structural protein
GFAP	Structural protein
BLBP	Lipid binding protein
Vimentin	Structural protein
S100- beta	Calcium binding protein

Table 3: Established neural stem cell/progenitor markers in the CNS and their functional effects.

3.3.2 NSC niches in the adult vertebrate brain

In the CNS of adult mammals, dividing NPCs are most commonly detected in the subventricular zone (SVZ) of the lateral ventricles and subgranular zone (SGZ) of the dentate gyrus, both in the telencephalon, with some detected additionally in the central canal of the spinal cord[39,40]. The seminal works of Joseph Altman (1965, 1969) showed that cells near the site of a induced-lesion rat brain could form new neurons, glias and neuroblasts (precursor neuronal cells) to repair and replenish the damaged site. We now know that the NSCs that contribute to these cells in the adult rat or mouse brain mainly reside in the SVZ and SGZ. In the mouse, NSCs from the SVZ of the lateral ventricles undergo neurogenesis under normal conditions, migrating tangentially to the olfactory bulb where they reconstitute the neuronal component of the olfactory epithelium. This migratory route is referred to as the rostral migratory stream. There is no evidence as yet to suggest a similar migratory event in humans and other higher primates, although proliferation and neurogenesis have been detected within the olfactory bulb of adult humans[41]. This may be attributed to the fact that the sense of smell in humans is underused, relative to rodents that are highly dependent on their sense of smell to navigate for food and escape from predators. Multipotent NSCs can also be found in the innermost subgranular cell layer of the adult hippocampus. Newly

hippocampus. Newly born neuroblasts migrate to the dentate gyrus where they become incorporated as granule neurons in the granular cell layer. These cells are thought to contribute to the formation of new memories in adult vertebrates.

Apart from the well-defined niches of the SVZ and SGZ, NSC niches have also been detected in several other brain regions, including the neocortex[42, 43], substantia nigra in the midbrain[44], cerebellum[45] and hypothalamus[46] (Figure 9). Active research is currently being carried out to further validate the extent of neurogenicity of the NSCs at these sites.

Whilst the mammalian system, especially the mouse, has been at the forefront of neural stem cell research in adults, non-mammalian systems (teleosts) such as the zebrafish are fast gaining popularity as an alternative model for stem cell research. (The zebrafish as a model system for my work will be discussed further in the proceeding section). It has been reported in many studies that areas of active proliferation can be detected throughout the rostro-caudal brain axis of teleosts, including the zebrafish. Unlike mammals, in the zebrafish, neurogenesis (i.e. the birth of neurons) naturally occurs at an active rate to replenish the neuronal network in the adult zebrafish central nervous system. This makes the zebrafish attractive as a model for the study of adult neural stem cells and neurogenesis especially since neurogenesis occurs at a much less-frequent rate in the mammalian system including humans. It is thought that the neurogenic niches in the zebrafish may suggest a function that has been 'lost' in higher vertebrates. Progenitor cells from several so-called 'non-neurogenic' mammalian NSC niches regions have been isolated and successfully differentiated *in vitro* into neurons[47], suggesting that they are normally 'suppressed' in their ability to regenerate *in vivo*. Research by Michael Brand's group in 2006 showed the existence of constitutively proliferating cells in 16 different positions along the rostro-caudal axis of the ventricles in the adult zebrafish brain[48]. Cells from these areas undergo neurogenesis to give rise to new-born functional neurons in the adult zebrafish brain[48].

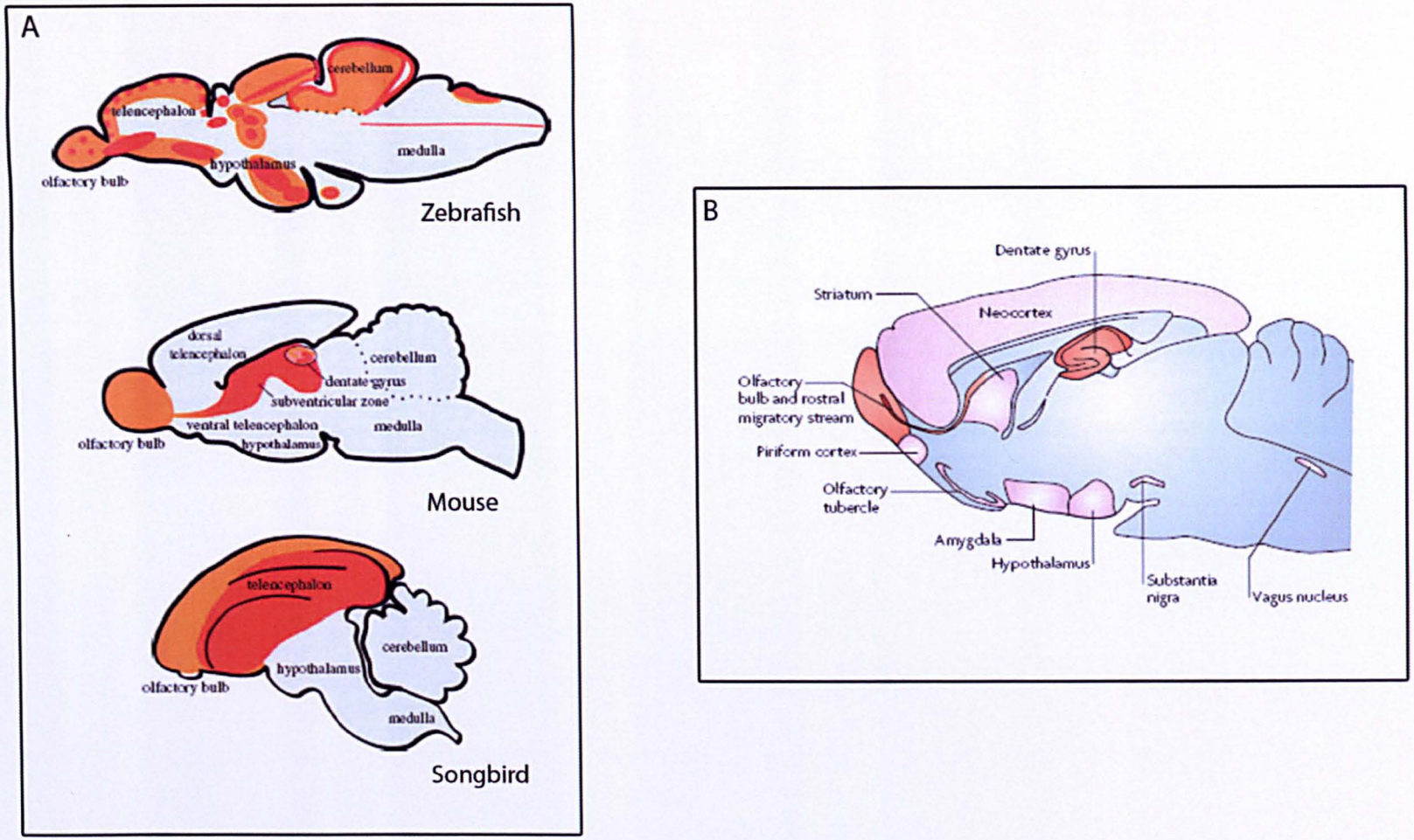

Figure 9: Neurogenic regions identified in different regions of the vertebrate brain. (A) Comparative regions of different areas acting as neurogenic niche and regions of constitutive proliferation as identified in the brains of the zebrafish, mouse and songbird. Regions with constitutive proliferation are shown in red and neurogenic regions are shown in orange. (B) Regions in the adult mouse brain where existing (red) and emerging (pink) neural stem cell niches can be found.

Image source:

i) Image A is obtained from [47].

ii) Image B is obtained from [155].

3.3.3 Neural stem cells and neurogenesis in the adult hypothalamus

Neurogenesis in the adult mammalian hypothalamus was first reported Xu et. al. (2005) in the rat model system. It was shown through this work that a specialized subset of radial glial-like ependymal cells termed tanycytes, which line the third ventricle in the hypothalamus, may function as neural progenitor cells. Lineage tracing experiments showed that tanycytes give rise to neurons that migrate along tanycyte processes, into the parenchymal region of the hypothalamus, where they integrate into the neuronal network and form functional synapses. In 2005, research in Jeffery Flier's lab showed that ciliary neurotrophic brain factor (CNTF) can induce neurogenesis in the arcuate nucleus of the adult mouse hypothalamus[49]. CNTF-induced differentiated cells partake in the regulation of energy balance through the generation of cells involved in feeding behaviour (i.e. propiomelanocorticotropin or pomc; neuropeptide Y or NPY)[49]. In another study by the same group, proliferating NPCs detected and labelled via BrdU co-expressed Hu or doublecortin, both of which are prominent markers for immature or early born neurons[50]. BrdU labeling is a basic yet very powerful technique to fate map proliferating cells since BrdU (a synthetic nucleotide) is incorporated into the replicating DNA strand during cell division. BrdU is retained in the cells even after the cessation of proliferation and hence cells that are BrdU and Hu or doublecortin positive provide evidence that the immature neurons originate from proliferating neural progenitor cells. Actively dividing cells which are BrdU positive were localized mainly to ventricular regions of the ventricle supporting the idea that NPCs are generated from a NSC population in these regions. More recently in 2010, research by Pierce et. al. demonstrated the potential plasticity of neurons in the arcuate nucleus in the hypothalamus of the adult mouse[51]. They show that de novo neurogenesis in the arcuate nucleus can occur without any induction when functional agouti-related peptide (AgRP) neurons (similar to the NPY neurons) are loss through progressive neuro-degeneration. These newly born AgRP positive cells replace the lost cells and integrate into the feeding regulatory network[51]. These findings provide evidence for functionally-important de novo neurogenesis, and suggest that a local neural stem cell niche may be present in the adult vertebrate hypothalamus.

Evidence from our lab[52] provides substantial new support for this idea. Unpublished data from our lab, showed that Nestin and Vimentin double positive tanycytes largely occupy the medial portion of the hypothalamus, and are found lining the median eminence, and the ventral third of the 3rd ventricle suggesting that they may function as neural stem or progenitor cell. Intriguingly, the analyses of the adult mouse hypothalamus suggest that endogenous FGFs may govern hypothalamic tanycytes NSC/NPC proliferation. *Fgf-10* and *Fgf-18* are expressed specifically within tanycyte subpopulations and FGF signalling elements are detected in tanycytes.

The combination of all the above works arguably provides ample evidence for the existence of a NSC niche in the adult hypothalamus. However, two main factors mean it is difficult to analyse the behaviour of NSCs/NPCs in the adult mouse hypothalamus. First, although there is evidence that hypothalamic NSCs/NPCs undergo proliferation, this appears to occur at extremely low levels. Thus, it has proved difficult to detect the proliferation of NSCs/NPCs, far more so than in the SVZ of the lateral ventricles or the subgranular zone (SVZ) of the dentate gyrus. Such low-level proliferation can be attributed to the usually quiescent nature of the NSCs in the hypothalamus of adult rodents. Second, the in vivo manipulation of factors that may be involved in governing the behaviour of the NSCs/NPCs is technically challenging. Given the difficulties involved in having to study the NSCs of the adult rodent hypothalamus *in vivo*, there is a real need for a complementary model system. It is now widely accepted that NSCs exist in the adult zebrafish hypothalamus as well and that they are more actively re-entering the cell cycle to proliferate compared to their rodent counterparts[48]. Hence investigating NSCs in the hypothalamus of the adult zebrafish will provide valuable insights into the regulation and behaviour of the NSCs, complementing analyses of rodent models.

4. The zebrafish as a model system to study development and adult neurogenesis

The zebrafish (*Danio rerio*) originates from the tropical freshwaters of India and is a well-established vertebrate model for scientific research especially in developmental biology. Although the rodent models (i.e. rat and mouse) are for

many, the ideal vertebrate model to study human development, given their closer evolutionary relationship with humans, the zebrafish has proved to be a powerful system for genetic manipulations, embryology studies and in vivo imaging, all of which are indispensable tools for the study of developmental biology. Moreover, the zebrafish has certain advantages over the rodent models that make it a more viable model system for many experiments. Its embryos are transparent and large enough for their development to be easily observed under a dissecting light microscope. During the first 24 hours of development, the embryos are pigment-free and completely transparent. These features allow for a clear visualization of developing organs and tissues, including the hypothalamic anlage. There are also pigmentation-free mutant lines that prevent pigments from forming throughout the lifespan of the embryos. Pigment-free lines that remain pigmentless in the adults have also been developed and made available to researchers (i.e. *golden*[53] and *casper* lines[54]). Zebrafish embryos develop at a very fast rate and most of the anlage can be easily identified after two days of fertilization, including a compartmentalized brain[55]. Also, the high fecundity of the zebrafish allows for a high number of embryos to be collected for experiments. This is especially useful for studies involving mutant or transgenic line screening, sorting and analysis.

Adult zebrafish have also proved to be a useful tool for wide-ranging studies, from cell regeneration to environment toxicology. The adult zebrafish can be maintained in large numbers that require less space compared to a housing facility for rodent models. They are easier and less-costly to maintain compared to rodent models. In the study of NSCs and neurogenesis, the adult zebrafish provides an extremely crucial and exciting link to study the factor/s that allow NSCs in the adult brain to naturally replenish the neuronal circuitry with new neurons, a feature that is thus far limiting in higher vertebrates including rodents. It is thought that neurogenic niches in the higher vertebrates have been 'suppressed' in their ability to regenerate *in vivo* since progenitor cells from several so-called non-neurogenic regions have been isolated and successfully differentiated *in vitro* into neurons[47]. Like the mouse, the availability of adult viable mutant and transgenic lines allows for gene functional studies to be performed in the adult zebrafish. Research studies, including mine, are actively seeking out the gene or genes that regulate the active cell cycle of the NSCs and NPCs in the adult zebrafish brain. This knowledge

active cell cycle of the NSCs and NPCs in the adult zebrafish brain. This knowledge can then be transferred to the mouse model to investigate if the same genes can be manipulated to increase the re-entry of the NSCs into active cell cycle in the adult mouse brain.

5. Thesis hypotheses

In this thesis, I aimed to complement ongoing studies in the lab, by investigating some outstanding and pertinent questions in both early hypothalamic development and the adult hypothalamus, using zebrafish as the preferred model system, as follows:

A) Role for *rx3* in the embryonic hypothalamus (Chapters 1 to 4)

As described in section 2, the highly-conserved *rx/Rax* gene is required for the development of the eyes, and many studies have focused on the role of *rx/Rax* in vertebrate eye development. However, *rx/Rax* is expressed in the anterior hypothalamus. The effects of *rx3* gene knockdown in the hypothalamus have been only very briefly described in the literature, where brief studies have suggested a role in the differentiation of *pomc* positive neurons. No study has yet examined the mechanisms by which *rx3* may mediate these effects. I therefore set out to investigate the expression, role and function of *rx3* in the hypothalamus of the zebrafish embryos by investigating:

i. Region/s in which *rx3* is expressed in the embryonic hypothalamus.
ii. Effect of *rx3* loss of function on hypothalamic markers, including signalling ligands and pomc. In particular, I wished to test the hypothesis that rx3 functions cell-autonomously to govern *pomc* neuronal differentiation.
iii. The regulation of *rx3* expression in the hypothalamus

B) Maintenance of signalling factors and the regulation of NSCs in the adult zebrafish hypothalamus (Chapter 5)

The existence of NSCs/NPCs at the ventricular layer of the 3rd ventricle in the adult vertebrate hypothalamus, including the zebrafish, has been described in many studies. Nevertheless, the NSC niche in the adult hypothalamus has yet to gain acceptance as an established and functional NSC niche since most of the studies involved either introduction of inductive/mitogenic factors, unnatural ablation of existing cells or artificial in vitro cultures; all of which were performed in adult rodent models. Moreover, little is understood of the molecular control of NSCs/NPCs in the hypothalamic niche. As discussed in section 3, there are limitations to the study of hypothalamic NSCs/NPCs in the adult rodent models. These limitations can be complemented through the use of the zebrafish model system. I therefore set out to address the existence of NSCs/NPCs in the adult zebrafish hypothalamus and investigate their potential regulation by signalling factors that are expressed within the same region (i.e. the ventricular zone of the 3rd ventricle) of the NSCs. The adult zebrafish is ideal based on the reasons I have described in sections 3 and 4. In particular, I investigated the following questions/hypotheses:

i. Can I find evidence for a NSC niche in the adult zebrafish hypothalamus that harbours cells similar to those detected in the mouse hypothalamic NSC niche
ii. Is the NSC niche located in a similar region to that described in adult rodent models (i.e. the medial hypothalamus)
iii. Do local signalling ligands regulate NSC/NPC cell proliferation in the adult zebrafish hypothalamic niche.

Materials & Methods

Materials and Methods

1) Zebrafish storage and housekeeping

All wildtype zebrafish used in this thesis are LWT (London wild type) strain. The *nestin::GFP* transgenic embryos were kindly provided by Dr. Uwe Strahle (Karlsruhe Institute of Technology, Germany). The *chokh* mutant embryo used in chapter 2 was kindly provided by Dr. Breandan Kennedy (University College Dublin, Ireland). All zebrafish lines are kept in a controlled and regulated environment at the Aquaria Facility, University of Sheffield. The zebrafish were kept at constant water temperature of 28.5°C with a daily light-dark cycle of 14 hours light and 10 hours dark. All lines are maintained and embryos obtained through natural mating. Embryos for experiments were obtained through 'marbling' technique where marbles are placed in an inner container with a wire-grid base that holds the fish and an outer container where the eggs will collect. Embryos collected for experiments are kept in E3 medium prepared according to the Zebrafish handbook[55] and are maintained at 28.5°C throughout experimental procedures.

2) Zebrafish staging

All embryonic zebrafish were staged according to Kimmel's staging guide[56]. All adult fish used in this thesis were of one year of staged through birthdates record.

3) Plasmid cloning

All of the in situ hybridisation probe constructs (plasmids) used in this thesis were either obtained directly from the source (i.e. maker) or through secondary sources, except for *pomc,* which I have made and produced. Please see probe list for details. In this section, I will first describe how the *pomc* probe construct was made and then proceed to outline the general steps that are involved in the processing of the constructs for probe synthesis.

i) PCR (polymerase chain reaction) primer design

PCR Primers targeting the 3' region excluding the 3' UTR (untranslated region) from nucleotide number 699 to 1216 of the *pomc* gene (sequence obtained from ENSEMBL Genome Browser[21]) were designed using Invitrogen Primer Design programme[57], which is available online. Following is the *pomc* gene region as described above, which was used as the input (Box1) for the primer design programme and the corresponding primers designed to target this region (Box2):

Box 1

>*pomc* 3' region (excl. 3' UTR) (BLAST confirmed)

CGCTTCCGGCAGAGATGAGACGCGAGCTGGCAAATAACGAGGTCGACTATCCGCAAGAAG
AGATGCCTTTAAACCCACTGGGGAAGAAGGACCCCCCCTACAAAATGACCCATTTCCGCT
GGAGCGTCCCGCCGGCTAGCAAGCGCTATGGAGGCTTCATGAAGTCCTGGGACGAGCGTG
CTCAGAAACCACTGCTCACACTCTTCAAAAACGTAATGCATAAAGACCAACCGAGGAAGG
ATGAGTGAGTGGCTTTAAGGGGGAGAGGTTGTTATAGGGGGATGTTTTGAATATACTTTC
TTCCCAGCAAACTTCTGGATGAGAGGTTCTTATCATGCATAGAAACGAAGGTGGGCAATG
TTAACAATAGCACTTAAATCTTGATGAGTTTATTCACACTGTATTCAACAATAAATTCTG
AATTCTGTATATAGAAATGCTGTGGTGATTAAATACCAGCTTAGAGGCTAAAACAGCATT
TTTAGAATATTTATTGAACATGTATTATACTGTACATTTTGAAAATGTGACATAAAATGA
TGTTTCAAGCAGAAGAGAACACAA

Box 2

Primers:

Forward (5'-3')	AGGTCGACTATCCGCAAGAA
Reverse (5'-3')	TTGTGTTCTCTTCTGCTTGAAA

ii) RNA extraction and cDNA library synthesis

RNA was extracted from a clutch of 40-50 embryos at stage 40 hpf collected in a 2.5 ml microcentrifuge (Eppendorf) tube. The embryos were first anaesthetized using Tricaine according to the prescribed procedure and was culled by freezing in dry ice minus E3 buffer for 15 minutes. Trizol solution was then added into the tube and the embryos were then passaged through 25G needles attached onto syringe multiple times until fully sheared to homogeneity. Chloroform was then added to the tube, mixed and centrifuged at 4°C. The aqueous phase was then

aliquoted into a new and clean tube, isopropanol added and mixed. The mix was then centrifuged at 4°C. The supernatant was aliquoted and disposed, and the RNA pellet was left to air dry before resuspending in DEPC water. cDNA synthesis was performed using the Superscript First-Strand Synthesis System (Invitrogen).

iii) PCR parameters and validation

PCR for the *pomc* gene fragment (as in Box 1) from the cDNA library was performed using the following protocol and parameters:

PCR reaction volume = 50 μl; reaction components as follows:

- cDNA template
- Forward primer
- Reverse primer
- Taq polymerase
- Taq polymerase buffer
- dH2O

The PCR reaction was performed on the MJ Thermocycler using the following cycle parameters:

I.	Denaturation	92°C (for 30 seconds)
II.	Annealing	50°C (for 30 seconds)
III.	Elongation	72°C (for 45 seconds)

The above steps were repeated for 30 cycles. The size of the resulting PCR product was then verified using agarose gel electrophoresis to match the expected *pomc* gene fragment band size of 564 base pairs (bp) or roughly at 500 bp measured against the 1000 bp DNA ladder (Promega).

iv) TOPO-TA cloning

The *pomc* PCR product (gene insert) was cloned into the TOPO-TA cloning vector (Invitrogen), following the instructions provided by the manufacturer.

v) Bacteria subcloning and Plasmid Extraction

The resulting *pomc* (TOPO) was subcloned into the bacteria *E.coli* (DH5 alpha strain) through standard transformation protocol and the bacteria was propagated in *Luria Bertani* (LB) culture medium (Invitrogen) as described in Molecular Cloning: A laboratory manual[58]. The amplified *pomc* (TOPO) plasmid was extracted from the bacteria culture, purified and concentrated using the Maxi-prep Plasmid Extraction Kit (Qiagen).

vi) DNA sequencing and sequence verification

A minute amount of the purified pomc (TOPO) concentrated stock was sent to the DNA Sequencing Facility (University of Sheffield) to validate if the gene insert matches that of *pomc* as well as to investigate the gene insert direction (orientation) in the Multiple Cloning Site of the TOPO vector. The DNA Sequencing Facility employs the use of BigDye Terminator (ABI) and the ABI Sequencer. The sequencing was performed only in one direction using the T7 primer. The sequence was verified against the genome database using BLAST (NCBI)[59] to ascertain if the *pomc* identity of the insert gene and its sequence direction or orientation within the TOPO vector. The BLAST result showed a strong match of the gene insert with the zebrafish *pomc* gene in the database (i.e. 99% identity) and orientation is in the sense direction (5'-3') in tandem with the vector. The map of the *pomc* (TOPO) construct is provided in Box 3.

vii) Determination of RNA polymerases and the corresponding restriction sites

Based on the map provided in Box3, the SP6 RNA polymerase site would serve to synthesize the anti-sense probe (true probe) and the T7 RNA polymerase site for

Box 3

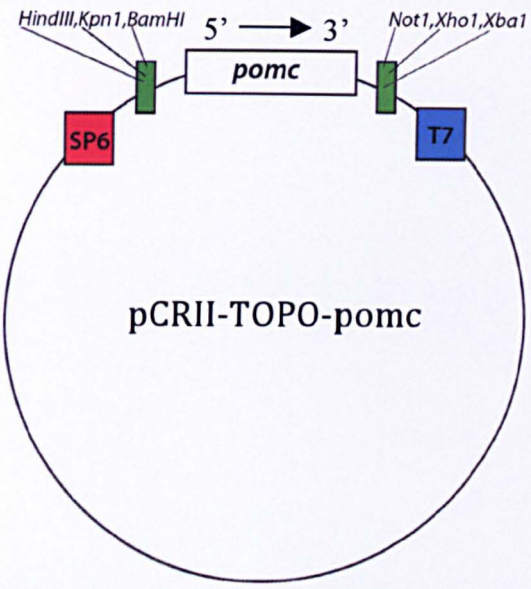

Map of *pomc*-TOPO construct.

the synthesis of the sense probe (control probe). Their corresponding restriction digestion sites for the construct linearisation (as discussed in the following section), was determined based on the map as well. The RNA polymerase / restriction site combination is as follows:

- sense probe
  Polymerase: T7; Compatible restriction sites: *HindIII, Kpn1, BamH1*
- antisense probe
  Polymerase: SP6; Compatible restriction sites: *Not1, Xho1, Xba1*

To ensure that these restriction sites do not cut or digest the *pomc* gene insert internally, I used the NEBcutter (by New England Biolabs)[60] programme which is available online. The result shows that all six of the above restriction enzymes do not have restriction sites within the *pomc* gene insert.

viii) Linearisation of construct

The *pomc* (TOPO) construct was linearised at both directions to make the sense and antisense probes. The restriction enzymes used were *HindIII* for sense direction and *NotI* for antisense direction. The linearisation protocol follows the standard single restriction digestion protocol as provided by the enzymes manufacturer (Promega).

N.B. Processing steps of all other constructs obtained from contributed sources were performed similar to steps v, vi and viii described above. Step vii was not necessary since the contributed constructs came with full instructions on the polymerases and their corresponding restriction sites for linearisation. The full list of probe constructs can be found in Table 1.

Probe	Restriction site	Polymerase	Source
shh	*HindIII*	T7	Ingham Lab (CDBG, Sheffield)
fgf3	*SalI*	T3	Dr. William Norton (CNRS, Paris)

fgf8	*NotI*	T7	Roehl Lab (CDBG, Sheffield)
fgf10	*HindIII*	T7	Roehl Lab (CDBG, Sheffield)
sox2	*EcoRI*	T7	Cunliffe Lab (CDBG, Sheffield)
sox3	*EcoRI*	SP6	Dr.Richard Dorsky (Utah, U.S.A)
pea3	*Not1*	T7	Roehl Lab (CDBG, Sheffield)
ptc1	*XbaI*	T7	Whitfield Lab (CDBG, Sheffield)
ptc2	*EcoRI*	T7	Whitfield Lab (CDBG, Sheffield)
rx3	*XbaI*	T7	Dr. William Norton (CNRS, Paris)
emx2	*XhoI*	T7	Dr. William Norton (CNRS, Paris)
pomc	*NotI, XhoI, XbaI*	SP6	Self made
tbx2a	*BamHI*	T7	Whitfield Lab (CDBG, Sheffield)
tbx2b	*BamHI*	T7	Whitfield Lab (CDBG, Sheffield)
gli2	*BamHI*	T7	Whitfield Lab (CDBG, Sheffield)
pax6	*SmaI*	T7	Cunliffe Lab (CDBG, Sheffield)
isl1	*XbaI*	T3	Dr.Richard Dorsky (Utah, U.S.A)
th	*XhoI*	T7	Cunliffe Lab (CDBG, Sheffield)
zic2a	*EcoRI*	SP6	Dr. Yevgenya Grinblat (Wisconsin, U.S.A)
zash1a	*EcoRI*	T7	Cunliffe Lab (CDBG, Sheffield)

Table 1: Restriction enzyme site used for construct linearization in the process of making antisense probes for *in situ* hybridisation experiments.

4) ISH probe synthesis (DIG and Flr labelled)

The in situ hybridisation probes were synthesised using either DIG labelled or Flourescein labelled haptens with the following protocol:

The following reaction was prepared:

- Linearised vector
- RNA polymerase (i.e. SP6, T7 or T3 from Promega)
- 5x transcription buffer (Promega)
- DIG – or Flourescein – labelled haptens (Roche)
- RNase inhibitor (Promega)
- dH_2O

and incubated at 37°C for 2 hours. DNase (RNase free) (Promega) was added to the reaction above and was incubated at 37°C for an additional 15 minutes. This step is vital to digest the linearised vector. Lithium chloride (4M) and ice-cold ethanol was then added to the reaction and gently mixed by tapping on tube. This was kept at -25°C overnight to allow the precipitation of the synthesised RNA probe. On the following day, the reaction was centrifuged at 13,000 rpm in 4°C. The RNA probe pellet was identified through eyes. The supernatant was aspirated and replaced with 70% ethanol. The tube was gently tapped to allow rinsing of the pellet. The tube was the centrifuged again at 13,000 rpm in 4°C. The supernatant was aspirated and the RNA (probe) pellet was allowed to air dry at room temperature. Finally, the pellet was resuspended in a formamide and dH_20 solution (1:1 volume ratio). The formamide is important to maintain the probe in RNase free environment. The probe is then examined on agarose gel electrophoresis to validate their expected band size and was stored in -25°C.

5) Embryonic zebrafish protocols

i) Embryonic zebrafish processing for experiment

A) Eradicating pigmentation on embryos

Like all other model organism, the zebrafish has it own processing procedure to mainly to facilitate visualization and image acquisition. All embryos analysed in this thesis are processed either before or after fixation with chemicals that are able to eradicate their pigmentation. The development of pigmentation in the zebrafish embryos begins to take place at around 32 hpf and can be a major hindrance during image acquisition. Its dark shade prevents viewing accessibility to the signals during microscopy defeating the translucent feature of the embryo. There are two ways of circumventing this problem; a) using PTU, b) bleaching. PTU (1-phenyl-2-thiourea) is specialised chemical that targets the development of melanophores/cytes in the embryo that are responsible for the pigmentation. It works by addition into the embryo-containing E3 medium directly before 24 hpf of development. It is recognisably a pre-fixation method, which would normally have no side effect on the embryos although the development of oedema in the heart have been reported in PTU treated embryos at late stage of embryonic development. Nevertheless, very few or no pigmentation exists in the embryos after PTU treatment making it still widely used technique in most labs. Another technique is the use of bleach solution, which is made up of Formamide (%), and Hydrogen peroxide (%) in dH2O. This is a post-fixation as well as a post-hybridisation technique aimed eradicating the pigments once the in situ hybridisation signals have been fully developed. Since this technique is performed post-fixation, there is no effect at all to the development of the embryos. The only disadvantage of this technique is the appearance of remnant pigments that although less darker in shade, can still sometimes hinder the full and proper visualization of signals. The protocols used for both above are follows:

a) PTU

Stock solution of PTU was made up to 100x concentration and stored in toxic cabinet at room temperature. Solution was warmed-up to 70°C before use to dissolve crystals that might form. The PTU solution was added directly into the embryo-containing E3 medium to 1x concentration. This was done at approximately 90% epiboly or early tail-bud stage and left to incubate at 28.5°C overnight (approximately 12-15 hours). The E3 medium was replaced after this time period and embryos were allowed to develop to the desired stages before fixation.

b) Bleaching procedure

Bleaching solution was made fresh before use as described above. Solution was added directly onto post-hyridisation fixed embryos in 4-well dishes and allowed to mix on orbital shaker at low speed. The embryos were monitored consistently every 5-10 minutes to gauge levels of pigment dissipation. The reaction was stopped as soon as pigmentation dissipates to satisfaction, by replacing the bleaching solution with PTW. The embryos were rinsed 3x in PTW before placing in glycerol solution as described below.

B) Glycerol mounting

After fixation, the embryos were rinsed 3x with PTW. They were then transferred through a series of glycerol solution at different concentration starting from the lowest (i.e. 30%) followed with 50%, 70%, and finally, 90% solution. Embryos were visualised and imaged in 90% glycerol solution. Embryos were also kept in the same solution at 4°C for long-term storage.

ii) In situ hybridisation

In situ hybridisation was performed on fixed embryos using desired probes based on the protocol as follows:

Day 1

Embryos kept in 100% methanol, were rehydrated following a series of diluted methanol solution (i.e 75%, 50% and 25%) before fully rehydrated in PTW solution in which the embryos were rinsed for 3x ; 5 minutes each time. The embryos were then treated with Proteinase K in PTW solution for 10 minutes for younger staged embryos (10 – 30 hpf) and 20 minutes for older staged embryos (55 hpf), both at room temperature. After Prot K treatment, the embryos were then briefly rinsed once with PTW and re-fixed with 4% PFA for 20 minutes at room temperature. This step is vital to fix and kill the activity of any left over Prot K since these can degrade the antibodies that will be used at a later step in this protocol. After the re-fixation step, the embryos were rinsed in PTW for 3x, at 5 minutes each time. The embryos were then incubated with hybridisation solution (minus probe) for 1 to 2 hours at 68°C. The probes were diluted in the hybridisation solution according to their optimised concentration and were pre-warmed at 68°C before adding to the embryos for the hybridisation to take place for an overnight period.

Day 2

On day 2 of the protocol, the embryos were succumbed to a series of 68°C and room temperature washes. All washing steps were either performed in incubator-shakers or on orbital shakers. All washing buffers used at 68°C were pre-warmed to this temperature before use. The probe solution was aspirated off the embryos and replaced with a buffer comprising the hybridisation solution and 2xSSC at 1:1 ratio. The embryos were incubated in this buffer for 20 minutes at 68°C. This buffer is then replaced with 2xSSC buffer and continued incubating at for 20 minutes at 68°C. The 2xSSC buffer was then replaced with 0.2xSSC buffer and the incubation continued at 68°C for 30 minutes. This step was repeated twice. The embryos were then allowed to cool down to room temperature before replacing the 0.2xSSC buffer with a buffer comprising a mix of PTW and 0.2xSSC (1:1 ratio). The embryos were washed in this buffer on an orbital shaker for 20 minutes at room temperature. The embryos were then washed with PTW for 3x; 5 minutes each time before being placed into Blocking Buffer for 1 to 2 hours at room

temperature. The blocking buffer is then replaced with the same buffer that contains either an anti-DIG (4000x dilution) or anti-Flourescein antibody (3000x dilution) and allowed to incubate overnight at 4°C.

Day 3

The antibody-containing buffer was aspirated and the embryos were washed in PTW for 3 to 4 hours. The PTW solution was replaced every half-hour within this time frame. The embryos then rinsed 3x with alkaline phosphate buffer and allowed to stand in this for 1 hour at room temperature. The developing solution according was prepared as described and the embryos were transferred into this to allow the signal development to take place. The development of the signal was monitored and stopped by post-fixation with 4% PFA for 1 hour at room temperature. The embryos were rinsed with PTW for 3x and were processed for pigmentation eradication and stored in glycerol as described in sections 1A and 1B.

iii) Double in situ hybridisation

This protocol describes the steps that were performed to achieve double *in situ* labelling to simultaneously detect two different gene expression using two different probes. Steps on Day 1 are the same as described above except both probes were added simultaneously at the overnight incubation step. The steps on Day 2 and Day 3 are generally the same as above. However, the secondary antibodies were added and detected sequentially. The choice for which should be detected first is arbitrary but the one which shows the stronger signal among the two would usually be detected first. Also the stronger signal would be detected using Fast Red and the weaker one is detected using NBT/BCIP. If both signals have similar intensities, then the gene with a wider area of expression would be detected using NBT/BCIP for the reason that Fast Red would quite often produce background staining more easily compared to NBT/BCIP.

iv) Immunohistochemistry

Immunohistochemistry was performed on whole mount embryos as described in this thesis. Similar to the in situ hybridisation protocol, embryos kept in 100% methanol were rehydrated to PTW. The embryos were then permeabilised with Trypsin (0.025%) at 37°C for 20 minutes. After permeabilisation, the embryos were rinsed 3x with PTW; 5 minutes each time. The embryos were then incubated in Blocking Buffer at room temperature for at least 1 hour. The blocking buffer is then replaced with the primary antibody (diluted in Blocking Buffer) and incubated at 4°C overnight on an orbital shaker. On the following day, the embryos were washed with PTW for 2 hours with PTW changes every half hour. After washing, the embryos were incubated in blocking buffer that contains the secondary antibody to detect and label the corresponding primary antibody. This step was done for 45 minutes to 1 hour at room temperature on an orbital shaker. This and all the following steps were performed in the dark. The embryos were then washed in PTW for 1 hour with PTW changes every 15 minutes. The embryos were then very quickly visualised under a fluorescence-equipped stereomicroscope to check if the labelling worked before actual imaging.

Primary antibody	Concentration	Source
BrdU	1:200	Abcam
MCM5	1:1000	Kind gift from Dr. Soojin Ryu (MPI, Heidelberg)
Vimentin	1:100	Milipore
HuC/D	1:1000	Milipore
GFP	1:500	Abcam

Table 2 : List of primary antibodies used in this thesis and their corresponding concentration and sources.

Secondary antibody	Concentration	Source
FITC	1:200	Jackson Immunolabs
Cy3	1:200	Sigma
Alexa Flour-488	1:500	Invitrogen
Alexa Flour-563	1:500	Invitrogen

Table 3 : List of secondary antibodies used in this thesis.

v) Chemical treatment of zebrafish embryo

The section describes the chemical treatment used in the attenuation of *shh* and *fgf* signalling pathways that forms the core of result chapters 3 and 4 of this thesis. Details pertaining to the nature of the chemicals used are described in the above two chapters.

A) Cyclopamine

Cyclopamine (Merck) was prepared in ethanol according to instructions to make 5 mM stock concentration and stored in dark at – 25°C. The preparation was performed in the dark as instructed in the datasheet and all safety procedures including personal safety procedure were strictly obeyed. Cyclopamine is added directly onto the embryos in E3 medium to the desired working concentration (in this thesis, the concentration is optimised at 100 uM), in the dark. Prior to this, the 30 hpf embryos were dechorionated and placed in 6-well plates; approximately 15-20 embryos per well. Dechorionation was not necessary for the younger stage embryos and was not performed. The plates were kept in the dark by wrapping with aluminium foil and incubated at 28.5°C for the duration of time as described in the result chapter 3. Cyclopamine medium was disposed according to regulations.

B) SU5402

SU5402 (Merck) was prepared in DMSO to make 20 mM stock concentration according to instructions and was stored in dark at -25°C. The preparation was

performed in the dark as instructed in the datasheet and all safety procedures including personal safety procedure were strictly obeyed. Treatment of embryos with SU5402 was performed in the same way as the cyclopamine treatment according to the duration of time as described result chapter 4, except that a 5 μM concentration was used. Disposal of SU5402 was performed in accordance to the regulations.

vi) Morpholino

Morpholinos were used in this thesis as detailed in result chapter 2 to investigate the loss of *rx3* gene function. There were two morpholinos used against the *rx3* mRNA; i) rx3MO ATG which is designed to inhibit the translation start site and preventing the translation process of the *rx3* mRNA from occurring, ii) rx3MO splice that targets specific splice sites within the *rx3* mRNA preventing the functional processed form of *rx3* mRNA from being produced. Both morpholinos were purchased from Gene Tools, LLC. The sequences of the morpholinos are as follows (5'-3'):

i) rx3ATG MO
Sequence: GAGATCCAACAAGCCTCATTGAACG

ii) rx3E212 MO splice
Sequence: GTGTCTCTCACCTGTACTCGGACTT

iii) Control morpholino
Sequence: CCTCTTACCTCAgTTACAATTTATA

In this thesis, a cocktail of both *rx3* morpholinos was used as described in result chapter 2. The working concentrations; rx3 MOATG: 0.25 mM and rx3MO splice: 0.15 mM. The morpholinos were prepared according to the instructions supplied by Genetools Inc. The morpholinos were prepared the night before their use and diluted up to the respective working concentrations as above using dH2O. A small amount of phenol red was added to the solution. This works as a marker-indicator

during the microinjection process. The prepared morpholinos were kept in 4°C overnight until ready for use the next morning.

vii) Microinjection

Microinjection needles (Harvard apparatus) were prepared through the needle-puller. The microinjection process was conducted using the microinjector (Nirashige) and the morpholino injection was performed on embryos at the 1-cell stage using standard procedures[55]. The morpholinos were injected into the yolk close to the cell. The injected embryos were then collected and kept in 28.5°C to resume normal growth up to the desired stages. The microinjection efficacy was validated through the loss-of-eyes and enlarged telencephalon phenotypes that characterized the *rx3* morphant embryos as described in result chapter 2. The morphant embryos were segregrated based on the strength of their phenotype i.e. *absent* (complete loss of both eyes), *reduced* (reduction in the size of both eyes) and *normal* (normal eyes observed). Only the absent phenotype was used for this thesis as it mimics the phenotype seen in *rx3* mutant or *chokh* as described in result chapter 2.

viii) Heat shock procedure

This procedure was used in result chapter 5 to upregulate *fgf3* expression in the heat-shock promoter-driven *fgf3* gene expression (*hsp::fgf3*) mutant embryos. This mutant line also contains a cardiac specific GFP expression cassette in the same heat-shock construct that allows for the segregation of the mutant embryos (GFP expressed in the heart anlage) from the normal siblings (no GFP expression). To upregulate fgf3 signalling, the mutant embryos (GFP positive) and normal siblings (GFP negative) were first segregated as described above and put in different 50 ml test tubes (Falcon) filled with E3 buffer up to 30 ml. The tubes were then kept in water bath at 38°C for 45 minutes before cooling down to 28.5°C. The E3 buffer was replaced and the embryos were maintained in 28.5°C for at least 2 hours prior to the desired stage of interest.

6) Adult zebrafish protocols

i) Culling and Fixing

All adult zebrafish analysed in this thesis are males at 1 year of age. The adult fish were culled according to Schedule 1 of the UK Home Office regulations. The brains were dissected out in the fix solution and were placed in fresh fix solution overnight at 4°C for fixation. The brains were washed with PTW 3x; 5 minutes each time on the next day before storing them in 100% MeOH at -25°C similar to that performed for the embryos.

ii) Sectioning through cryostat or vibratome

A) Cryostat

The brains were rehydrated to PTW as described for the embryos and were kept submerged in 30% sucrose solution overnight at 4°C. The brains were then embedded in O.C.T (VWR) on a plastic mould for cryostat sectioning. Prior to the embedding process, the brains were first put into a series of 30% sucrose:O.C.T solution at ascending concentrations of O.C.T (v/v) (i.e. 2:1 , 1:1 and 1:2) and finally into 100% O.C.T. Once the brains are put into the mould and orientated to the right position, the mould is quickly placed in dry ice for snap freezing. The block of O.C.T that contains the brain is removed from the mould and place onto specialised cryostat holders or 'chuck'. The chuck is then placed into the cryostat (Bright) for sectioning. The sections in this thesis were cut at 30 μm in thickness and collected on Superfrost slides (Thermo Scientific). The sections were then allowed to airdry for 1-2 hours before processing for experiments.

B) Vibratome

For thicker hypothalamic sections, the vibratome was used instead of the cryostat. The brains were similarly rehydrated to PTW after storage in 100% methanol. The brains were then embedded in 4% agarose. The agarose is then carefully trimmed to the right orientation of the embedded brain and glued onto the vibratome

holder. The holder is then placed in the vibratome (V-vibratome) and the brains were sectioned at 50 μm.

iii) Intraperitoneal injection of adult

In this section, I will describe the intraperitoneal injection (IP) technique that I have used to introduce cyclopamine and BrdU into the adult zebrafish system including the hypothalamus. Whilst IP injection of BrdU has been done before, IP injection of cyclopamine and its regime is novel and was innovated through this thesis.

A) General technique

One-year-old adult zebrafish (wild type) were kept separately and individually into smaller tanks a day before the procedure to enable accustomization to isolation. On the day of procedure, the fish were anaesthesised in tricaine through submerging and was immediately placed into the groove of the specially prepared agar plate in a ventrally-upwards position. The fish were then very quickly injected intraperitoneally (IP) through the stomach and placed back into the tanks for recovery (see Figure 1). A tiny amount (2 μl) of methylene blue was added into the injected solution to serve as an indicator to ensure the solution was injected properly.

B) IP injection of cyclopamine

Using the above procedure, cyclopamine was injected into the adult zebrafish as discussed in chapter 5. The cyclopamine stock was prepared similar to that described for the embryos, but was used at a working concentration of 1 mg/ml or 2.4 mM. The zebrafish were injected at 1 μg/0.1 g of body weight. The fish were injected with cyclopamine once everyday for seven consecutive days and were injected with BrdU (3.3 mg/ml) on the eight day. The zebrafish were BrdU-chased for 4 hours before culling according to Schedule 1 of Home Office procedure and fixed as described previously.

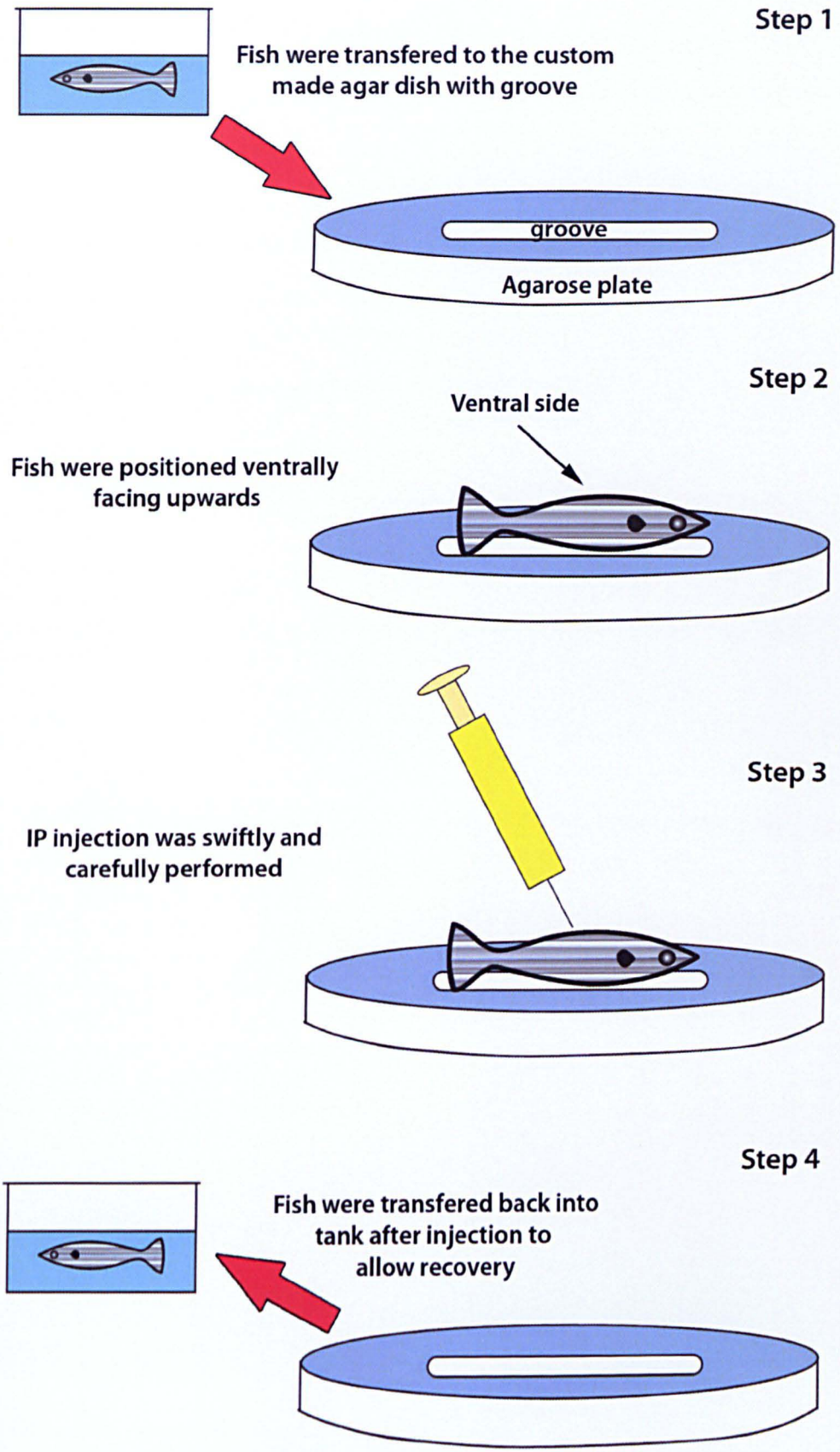

Figure 1: Illustration of the IP injection technique performed on the adult zebrafish

7) Image acquisition

Standard DIC images were obtained using an Olympus BX60 with SPOT Programme (Diagnostic Instruments Inc). Wholemount fluorescence images of embryos were acquired using a Zeiss Confocal microscope. Optically sectioned DIC and fluorescent images were obtained using a Zeiss Axioimager equipped with Apotome and Axiovision Programme (Zeiss). Processing of data images were performed using Adobe Photoshop CS3. Models and illustrative images were constructed using either Adobe Illustrator CS or Microsoft Powerpoint 2004.

8) Statistical method

All statistical analyses in this thesis were performed using Prism 5 (for Mac OS X) software. Unpaired t test were performed to determine if mean differences were statistically significant. SEM (standard error of mean) were analysed and plotted in the columns of each graphs. Each data value sampled, were tested for Gaussian distribution prior to t test by performing baseline subtraction of the two data sets and analysed through *D'Agostino and Pearson omnibus* normality test as recommended by the programme.

Results

Chapter 1

Chapter 1: Molecular profile of the embryonic zebrafish hypothalamus

1.1 Introduction

As outlined in the Introduction, a number of studies suggest that the early developmental signalling processes and patterning events that establish the embryonic hypothalamus appear to be largely conserved between the zebrafish and higher vertebrates. However, to confirm this and to seek a clear understanding of the anatomical division of the zebrafish hypothalamus, as well as examine differences between the zebrafish and chick embryonic hypothalamus, I first set out to identify the different divisions of the embryonic zebrafish hypothalamus using defined published molecular markers. These studies act as the basis for my investigations into the role, and potential mechanism of action, of the transcription factor *rx3* in the embryonic hypothalamus (Chapters 2-4). I focused on the markers *shh*, *fgfs* and the transcription factors *rx3*, *emx2* and *tbx2a/b*. Additionally, to test if the signalling pathways of *shh* and *fgfs* operate in the embryonic zebrafish hypothalamus, I examined well-characterised molecular read-outs for both these pathways. These include *ptc1/ptc2* as molecular read-outs for Shh signalling and *pea3* as a molecular read-out for the Fgf signalling pathway. I also provide reasons for studying these molecules in the context of the transcription factor, *rx3*.

1.2 Results

Expression analyses in the embryonic zebrafish hypothalamus

1.2.1 Expression of *shh* and *ptc1/2*

Shh is a secreted ligand that signals through the transmembrane protein Smoothened (Smo) and the Gli family of transcription factors (known as Cubitus interuptus in the *Drosophila*). In the absence of Shh ligand, Smo is inhibited by the Hh transmembrane receptor protein Patched (Ptc). The pathway is activated when Shh binds to Ptc and releases Smo from the inhibitory process of Ptc. Upon activation, Smo signals to the Gli transcription factors (see Box 1.1 for details on the Shh signalling pathway). The inhibition of Smo by Ptc is still an area of active

Box 1.1

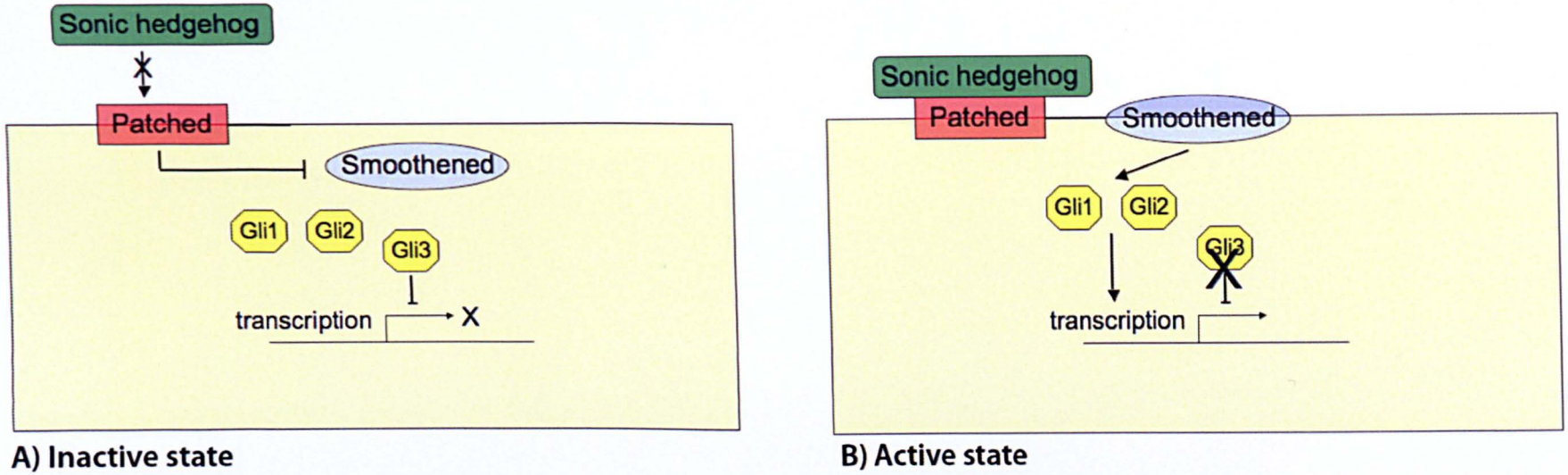

A) Inactive state

B) Active state

SHH signalling is activated when SHH ligand binds to PATCHED (PTC) and prevents it from inhibiting SMOOTHENED (SMO). SMO is a transmembrane protein whose function is inhibited through the action of PTC in the absence of SHH ligand. SMO is found mainly in the cytoplasm of the cell when the pathway is inactive. The signalling cascade is activated when SHH ligand binds to PTC. This binding results in the abrogation of the inhibitory function of PTC. SMO is then released from its inhibition by PTC and becomes hyperphosphorylated. It then accumulates in the plasma membrane in *D. melanogaster*. In vertebrate cells however, SMO accumulates in the cilia following exposure to SHH ligand or the HH ligands, SMO is then activated and functions as the modulator for the GLI transcription factor family (Glioma-associated oncogene homologue) which undergo further processing before activating the transcription machinery.

research, recent evidence suggesting an important role for vitamin D3[61]. The Shh ligand itself undergoes processing before binding to Ptc. The Shh protein is comprised of a C-terminal autoprocessing domain and an N-terminal signalling domain. Processing of the protein produces an N-terminal fully-processed form of the secreted Shh ligand with palmitate and cholesterol moieties attached at its ends (see Box 1.2 for details).

I first examined the expression of *shh* as a marker of the presumptive hypothalamus. Figure 1.1 shows that *shh* is expressed over an extensive period in the diencephalic basal plate, and an adjacent anterior region, termed the anterior-dorsal hypothalamus (ADH). The precise origin of *shh* positive ADH cells in zebrafish, and their relationship to the *shh* positive basal plate is unclear. However, fate-mapping studies in the chick suggest that, in that species, cells that occupy the equivalent region of the ADH are a mixed population of anterior-most floor plate and basal plate cells (Manning et al 2006). A *shh* negative domain is found ventral to the Shh positive territory; as outlined in the Introduction, in keeping with previous literature[13], I term this region the posterior ventral hypothalamus (PVH). In the chick, this region derives from anterior floor plate cells that are intitially induced by Nodal/Shh, and then downregulate Shh[6]. The literature suggests that a parallel mechanism may operate in zebrafish (see Introduction), but as yet, no study has examined whether, in the earliest stages of neurulation, Shh is expressed in the prospective diencephalon. I therefore examined Shh expression in the 10 hpf embryo. My results show faint, but clear *shh* expression in the anterior (diencephalic) floor plate. As in other species[14, 15], this expression is transient, and is downregulated at approximately 25-27 hpf. In contrast, *shh* expression in the basal plate/ADH persists at least until 100 hpf (the latest stage examined),. At 28-30 hpf, *shh* is prominently expressed in the ADH. However, by 55 hpf, and later stages, only weak expression is detected in the ADH (red arrow, Figure 1.1C,D). *shh* is now expressed more strongly at the ventricular region just posterior-ventral to the ADH (white arrow Figure 1.1C,D). It is unclear whether this is a new domain of

BOX 1.2

SHH protein undergoes multiple processing events before attaining its fully processed form (SHH-N) through which signalling is initiated. The full size SHH protein is 45 kDa and consists of an N-terminal signal sequence, N-terminal signalling domain and a C-terminal autoprocessing domain. The full size SHH protein is also referred to as the preproprotein. During translocation into the endoplasmic reticulum (ER), the N-terminal signal sequence is recognized by the signal recognition particle (SRP), which targets the preproprotein to the ER. Upon translocation, the signal sequence is then cleaved by signal peptidase found in the ER. The C-terminal of SHH protein is then removed through autoprocessing. The autoprocessing of SHH protein produces the N-terminal signalling domain or SHH-N (20 kDa). This cleavage is catalysed by a protease located within the C-terminal domain. A cholesterol molecule is added to the C-terminal of the SHH-N during the process. At the N-terminal, palmitate is added, an absolute necessity for efficient signalling. The fully processed and signalling form of

Cartoon source: Peter Znamenskiy (Wikipedia)

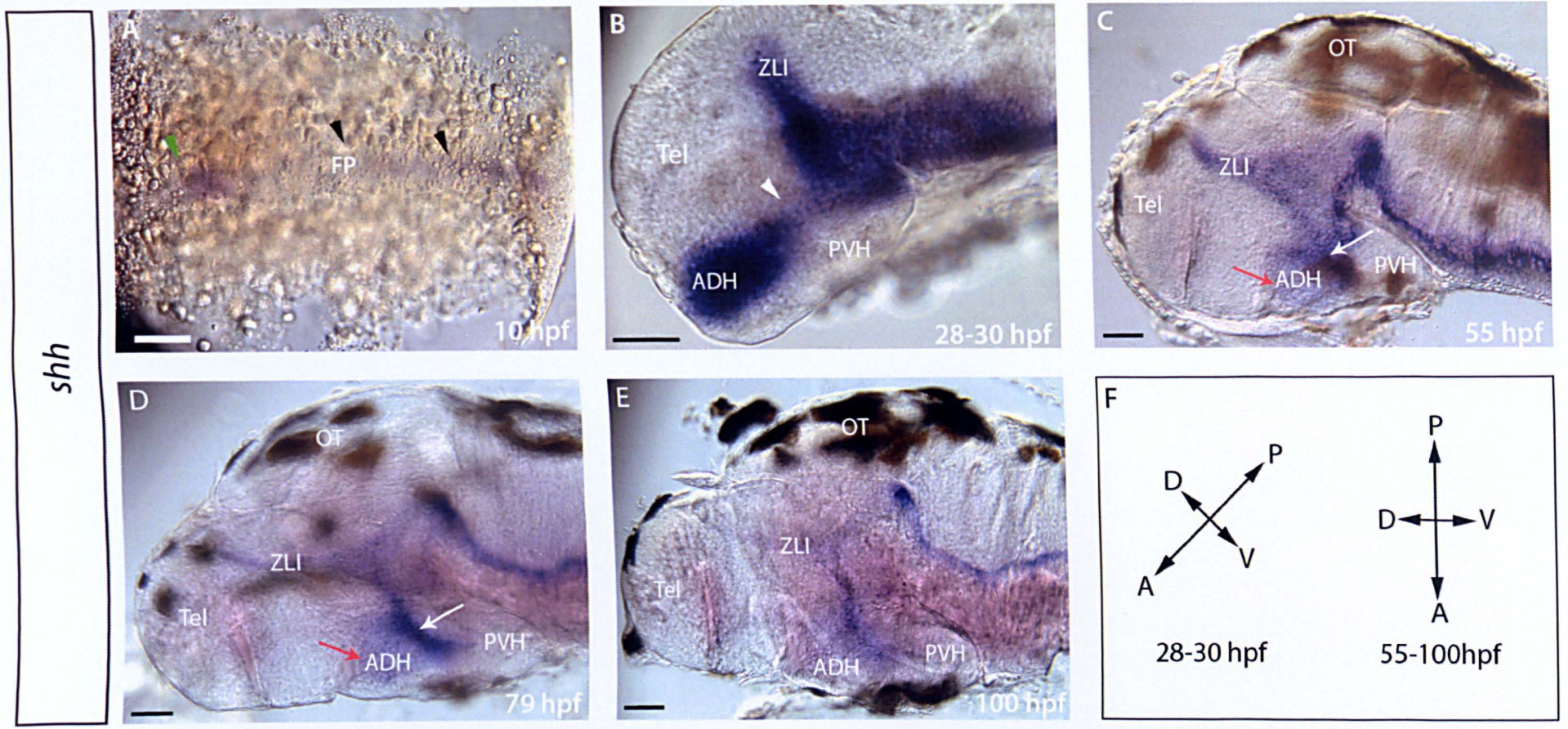

Figure 1.1 : Temporal expression of *shh* in the zebrafish. A-E , In situ hybridization analysis for the expression of *shh* in the zebrafish embryo at various stages of embryonic development. (A) *shh* expression can be detected at the floor plate of a10 hpf embryo (arrowheads; green demarcate expression in anterior). All images are of lateral view of the embryos except (A) which is a ventral view of the embryo. Anterior is to the left for A. Orientation is as described in F for B-E. Abbreviations: ADH (anterior dorsal hypothalamus), PVH (posterior ventral hypothalamus), FP (floor plate), Tel (telencephalon), ZLI (zona limitans intrathalamica), OT (optic tectum) and A,P,D,V (anterior, posterior, dorsal, ventral). Scale bars represents 50 μm.

expression, or whether *shh* is maintained at high levels in posterior-most ADH cells.

As described in the Introduction, *SHH* expression in the hypothalamic floor plate of the chick is downregulated via a molecular cascade, which involves the transcription factor TBX2[14]. The loss of *shh* expression in the zebrafish hypothalamic floor/prospective PVH suggests the possibility for a similar role of the zebrafish *tbx2* gene. To begin to analyze if a similar cascade is likely to operate in the early zebrafish embryonic hypothalamus, I analyzed the expression of *tbx* genes. In zebrafish, two orthologs of *TBX2* have been described, *tbx2a* and *tbx2b*, In situ hybridisation shows that of these, *tbx2b* is confined to the hypothalamic floor (Figure 1.2A,B). Double ISH with *shh* (Figure 1.2B) reveals that *tbx2b* is detected in the hypothalamic floor adjacent to the *shh* expressing basal plate. This expression pattern is remarkably similar to that in the chick, and strongly supports the idea that the region termed the hypothalamic floor in the chick is the homologous region to the PVH of the zebrafish[62]. Further, this finding strongly suggests that the mechanism of regulation of Shh in the hypothalamic floor plate is conserved throughout vertebrates.

Two aspects of *Shh* expression in the basal plate/ADH, however, suggest that these domains may be differentially regulated in zebrafish, compared to chick. First, the expression of *shh* is especially prominent in the ADH, taking the shape of a bulge instead of a more defined rod-like expression observed in the chick. Another observable difference is the lower expression level of *shh* in the basal plate region posterior to the ADH that is not easily observed in the chick (arrowhead in Figure 1.1B and Figure1.2B,E).

As there is no antibody available to detect Shh protein expression in the zebrafish, it is impossible to observe the diffusion of Shh away from the ADH and basal plate, and determine which cells are likely to receive Shh ligand. However, cells that are in receipt of Shh ligand may be active in its pathway. One of the easier and most straightforward ways to identify these cells is to analyse mRNA

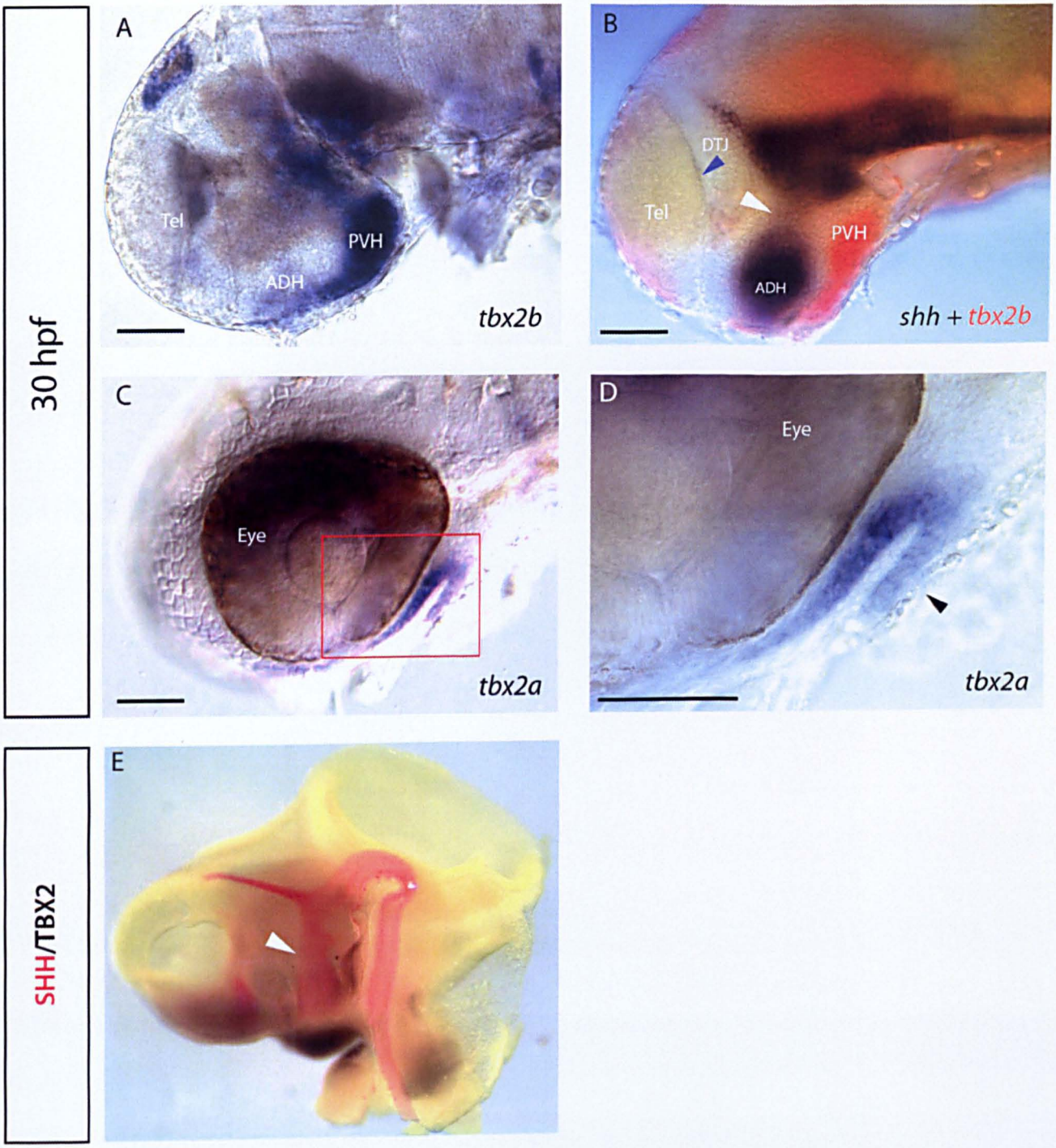

Figure 1.2 : Expression analysis of *tbx2a* and *tbx2b*. A-D, All embryos were analysed at 30 hpf stage of embryonic development. (A) *tbx2b* is expressed at the PVH. It is expressed in a complementary pattern to that of *shh* (B) and together these expression patterns outline much of the hypothalamus. The diencephalic-telencephalic boundary/junction (DTJ) is labelled by the blue arrowhead. (C,D) *tbx2a* is expressed in the Rathke's pouch: the ectodermal component of the pituitary. (E) SHH/TBX2 expression in the chick [14]. Arrowhead labels the basal plate. Scale bars represents 50 μm.

expression of molecular read-outs for the Hedgehog pathway. Positive expression suggests an active pathway. Cells located some distance away from *shh* positive cells that express molecular read-outs reflect non-cell autonomous activation of the pathway through diffusion of Shh protein. The Hedgehog pathway inhibitor *ptc* is commonly used as the molecular read-out of the signalling pathway as it operates in a negative feedback loop to regulate *shh* signalling. To test if *shh* signalling is operating in areas in and around the basal plate and ADH, I performed *ptc1* ISH and found that it is expressed most prominently just dorsal to the ADH and the Shh positive basal plate at 30-55 hpf (Figure 1.3). *ptc1* appears to be expressed in a strip of expression above the *shh* expressing region at the ADH instead of a bulge as described for *shh* expression. At 55 hpf, *ptc1* is detected additionally in the ventricular region, similar to expression of *shh* (Figure 1.1C). *ptc2* is expressed similarly to *ptc1* at 55 hpf but at a much lower level (Figure 1.3). I also analysed the expression of the transcription factor *gli2a* but found no positive expression around the ADH. However, strong expression was detected in cells at the anterior ventral region (arrowhead in Figure 1.3D').

1.2.2 Expression of *fgf* signalling components

Fibroblast growth factors (Fgfs) belong to a family of growth factors that are involved in a variety of developmental processes in the embryo. In total, 22 FGF ligands have been described in human and 24 in the zebrafish. Fgfs signal through Fgf receptors 1-4 (fgfr1-4), found consistently throughout vertebrates, although EST (expressed sequence tags) studies in murine lymph node stromal cells have identified a fifth variant, fgfr5[63]. Each of these receptor variants responds specifically to different sets of Fgf ligands and signal through different pathways that include the Ras/MAP kinase and the phospholipase-C gamma pathways (see Box 1.3 for outline of Fgf signalling pathways)

In the zebrafish, *fgfs* have been shown to be required for the specification of the adenohypophysis (anterior pituitary)[64]. *fgf3* signalling is primarily required for the transcriptional activation of genes regulating the early specification of

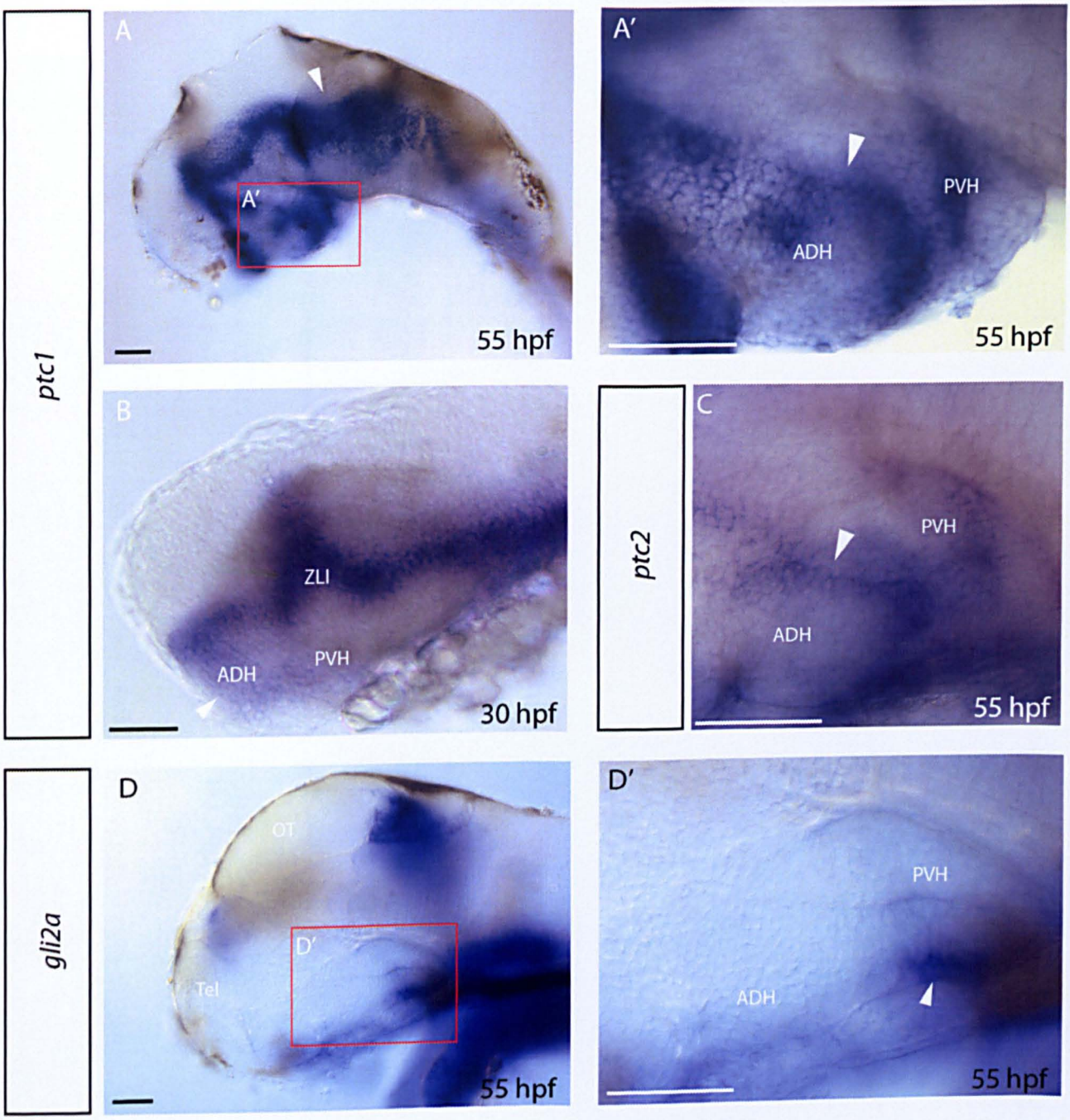

Figure 1.3 : Expression analysis of *ptc1*, *ptc2* and *gli2a*. (A,A') *ptc1* expression at 55 hpf embryos around the ADH and PVH; arrowhead in (A) shows expression in the posterior basal plate region. Arrowhead in (A') is the expression of *ptc1* in the 3rd ventricle. (B) *ptc1* is expressed prominently dorsal to the basal plate and ADH of 30 hpf embryos and very weakly in cells ventral to the basal plate and ADH (arrowhead). (C) *ptc2* expression in a 55 hpf embryo shows similar but much weaker expression to *ptc1*. Arrowhead shows expression in the 3rd ventricle. (D,D') No *gli2a* expression is detected in the ADH of embryos at 55 hpf, but is expressed in cells at the ventral hypothalamus (arrowhead in D'). Scale bars represents 50 μm.

Box 1.3

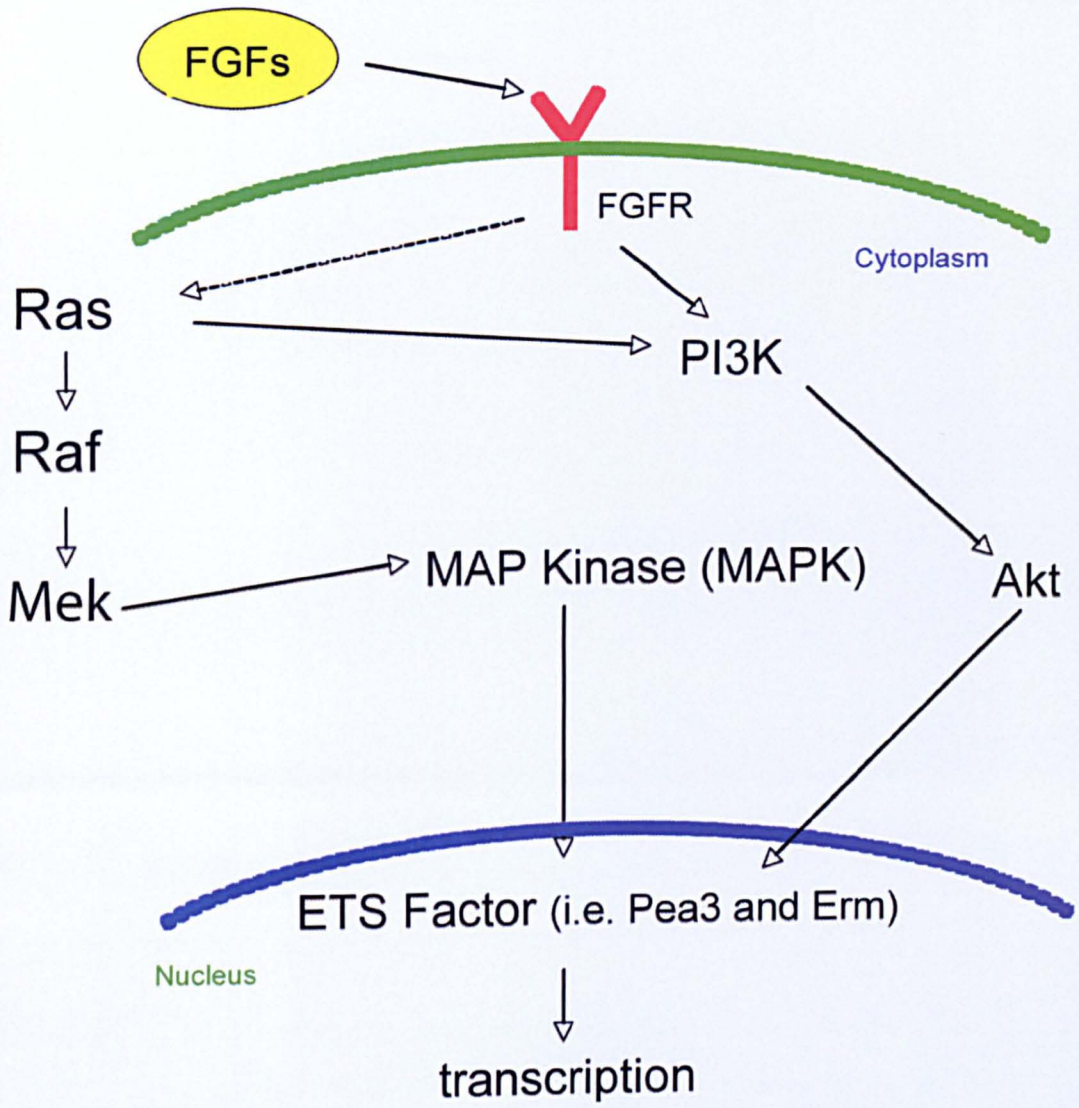

FGF signalling pathway. FGF ligands binds to FGF receptors (FGFR). The signalling cascade is transduced through either Ras-MAPK pathway or PI3K-Akt pathway into the nucleus where the transcription machinery is activated by the ETS transcription factor, Pea3 and Erm. The Ras pathway also feeds into the PI3K-Akt pathway.

Source:
Cartoon is adapted from [93].

adenohypophyseal progenitor cells[64]. However, no study has yet described a role for Fgfs in the embryonic hypothalamus. To begin to investigate a potential role of *fgfs* in the embryonic zebrafish hypothalamus, I examined the expression of *fgf3*, *fgf8* and *fgf10*, since these have been described in the hypothalamus of the zebrafish and other vertebrates[64-66]. As described in Figure 1.4, *fgf3* is expressed in a pattern broadly similar to that of *tbx2b* (compare Figure 1.4A and 1.2A), although expression appears to be slightly broader. Thus, at 26-30 hpf, *fgf3* largely marks the PVH (white arrowheads Figure 1.4A, B). Expression rapidly diminishes, and is markedly less intense at 30 hpf than at 26 hpf. A streak of *fgf3* is also detected in the medio-lateral hypothalamic region (red arrowhead in Figure 1.4B). At 55 hpf, *fgf3* expression can only be detected in posterior-ventral most cells of the PVH (white arrowhead in Figure 1.4C). *fgf8* is expressed only in posterior-ventral-most cells of the PVH at 26 hpf and this expression in maintained to 30 hpf although its expression is only prominent in the ventral most cells at this stage. *fgf8* expression is not observed in the hypothalamus or anywhere else in the diencephalon at 55 hpf; at this stage, expression is detected only at midbrain-hindbrain boundary (MHB) (arrowhead in Figure 1.4F). Analysis of *fgf10* reveals no clear positive expression in the ventral diencephalon including the hypothalamus at all the above stages, although strong expression is detected in the otic-vesicle and the fin-bud (Figure 1.4G').

To test if *fgf* signalling is operating in the hypothalamus, I examined expression of the *ETS-domain transcription factor pea3 (pea3)*, which acts downstream of Fgf and is widely used as a molecular readout for *fgf* signalling. Examination of *pea3* at 30 hpf shows its expression both throughout the PVH, and additionally, some expression in the ADH (Figure 1.5). However, no *pea3* expression is detected in the hypothalamus of a 55 hpf embryo.

1.2.3 Expression of *rx3*, *tbx2a/b* and *emx2*

In addition to analysing the expression of signalling molecules, I also studied the expression of several transcription factors that are known to be expressed in specific domains of the embryonic hypothalamus. As described in section 1.2.1,

Figure 1.4 : Analysis of *fgf* expression in the zebrafish embryonic hypothalamus. (A-I) *In situ* hybridisation of *fgf3*, *fgf8* and *fgf10*. (A) Strong *fgf3* is observed in the PVH at 26 hpf indicated by arrowheads. This expression diminishes by 30 hpf (B) and by 55 hpf is confined to posterior-ventral most regions (C), white arrowhead. *fgf3* is also expressed prominently at the midbrain-hindbrain boundary (MHB) (red arrowhead) at 55 hpf. (D-E) *fgf8* is expressed in PVH at 26 hpf and 30 hpf, but no expression could be detected in the hypothalamus at 55 hpf (E), arrowhead in (F) indicate expression in the MHB. (G-I) *fgf10* expression is not detected in the hypothalamus at all three developmental stages. (G') *fgf10* expression in the otic vesicles and fin-buds of the 26 hpf embryo. Scale bars represent 50 μm.

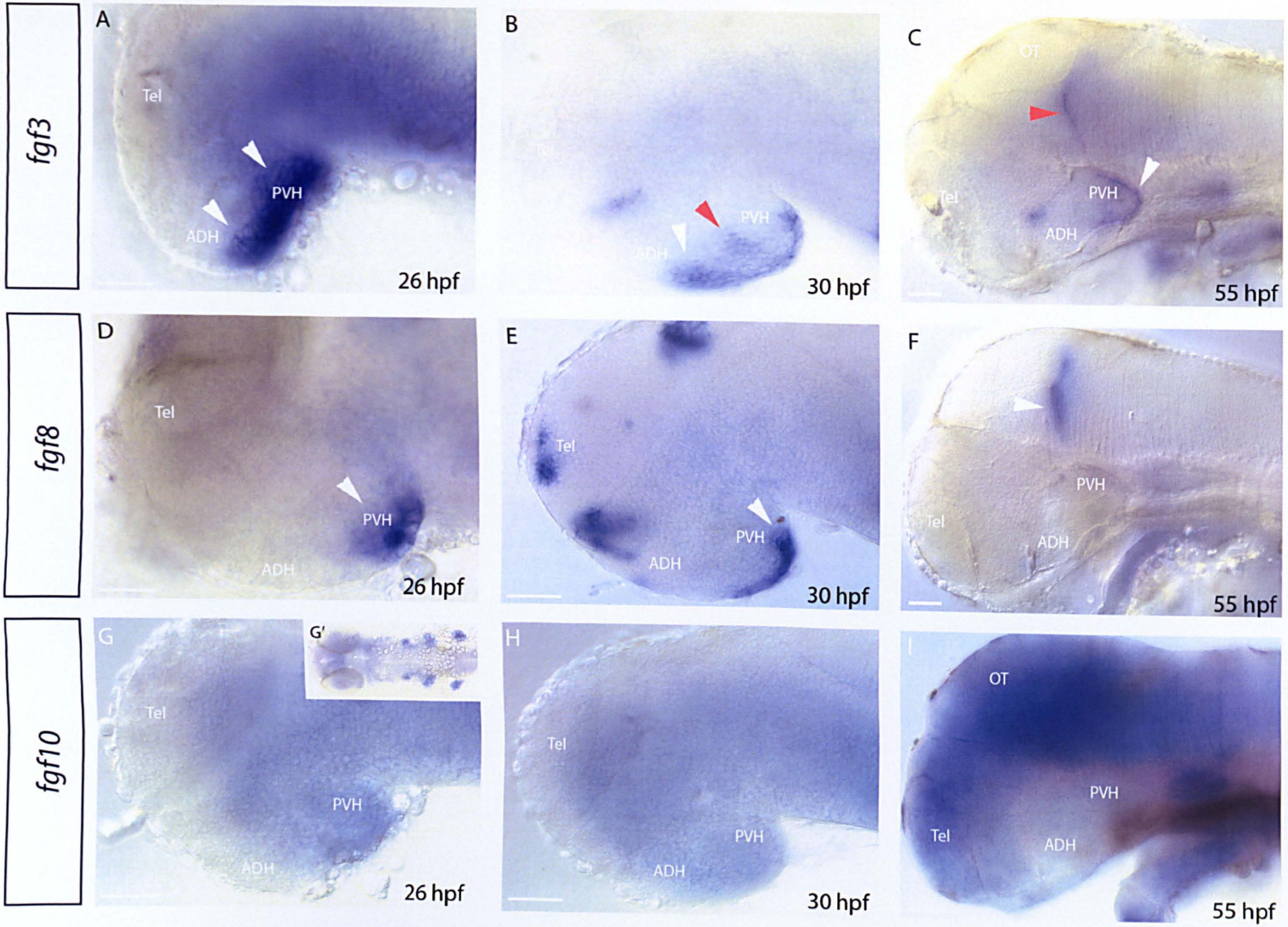
fgf3
fgf8
fgf10
A
B
C
D
E
F
G
G'
H
I
Tel
PVH
ADH
OT
26 hpf
30 hpf
55 hpf

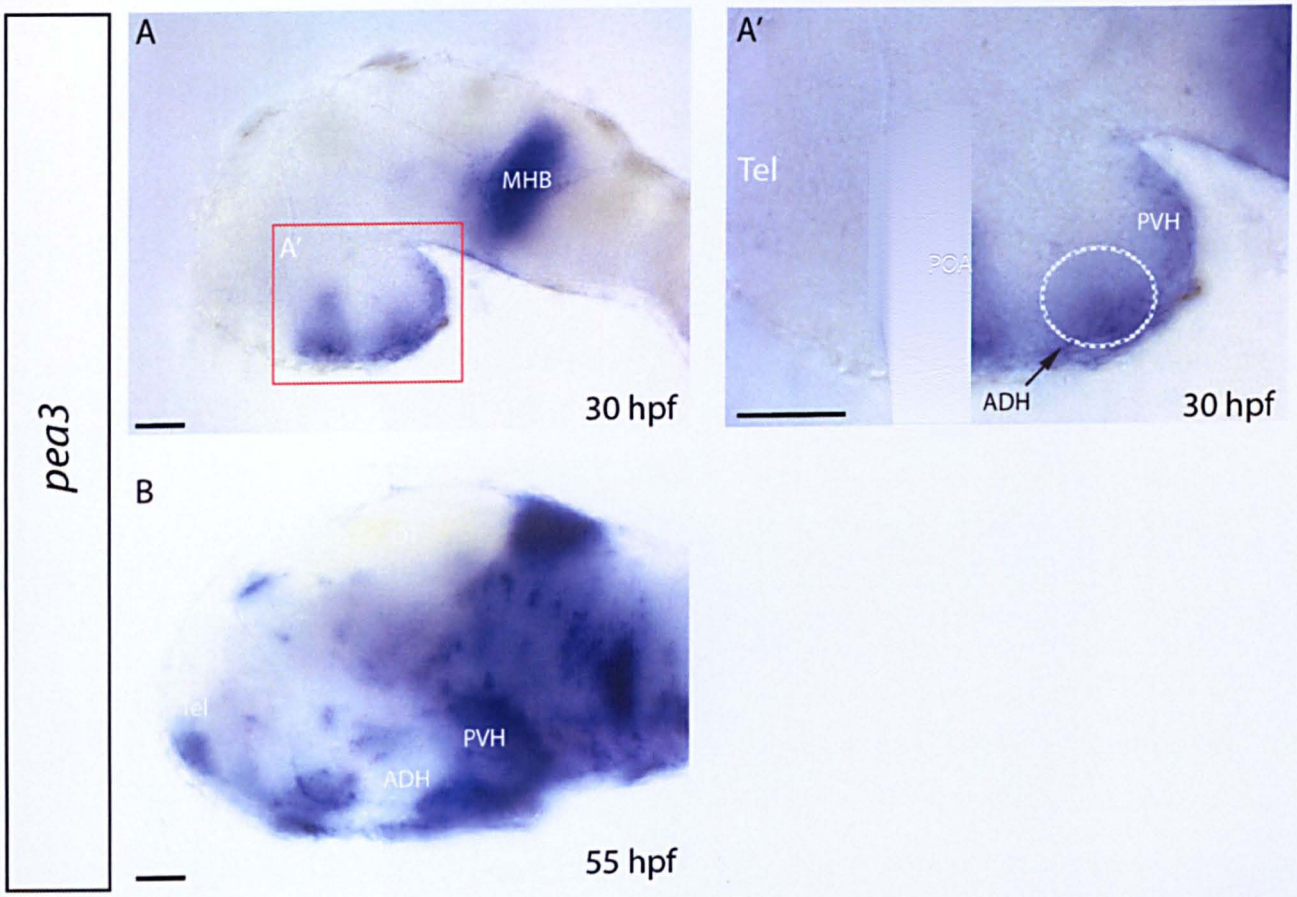

Figure 1.5 : Analysis of *pea3* expression in the embryonic hypothalamus. (A,A') *pea3* is expressed in the ADH and PVH at 30 hpf. It is also strongly expressed in the MHB as well as in the preoptic area (POA). (B) At 55 hpf, *pea3* is not easily detected in the hypothalamus.

tbx2b (homolog of the TBX2 gene in higher vertebrates) is expressed similarly to chick and mouse *tbx2*. However, its paralog *tbx2a* is not found in the neural tube but is expressed in what appears to be the ectodermal component of the adenohypophysis (arrowhead in Figure 1.2D).

In the chick hypothalamus, the homeobox transcription factor *EMX2* is expressed in posterior-most regions of the PVH[14], and studies in zebrafish suggest a similar profile[13]. To confirm that a similar expression pattern is found in the zebrafish embryo, I studied the expression of *emx2* through ISH. My data reveal that in the hypothalamus, *emx2* is expressed exclusively in the posterior PVH at 30 hpf (Figure 1.6D). At 55 hpf however, the expression of *emx2* becomes restricted to only a few cells within the posterior-most boundary of the PVH (arrowhead in Figure 1.6E). It is expressed robustly in the optic tectum (OT) at this stage. Together, these analyses confirm that the zebrafish PVH is likely to be the functional equivalent of the chick hypothalamic floor.

The transcription factor *rx3* is expressed in the ADH of the embryonic zebrafish and has been used as a molecular marker to demarcate the ADH[17]. In order to confirm this, I examined expression of *rx3* at 10 hpf, 30 hpf and 55 hpf. In accordance with previous findings, *rx3* does demarcate the ADH at 30 hpf. At 10 hpf, *rx3* expression can be observed at the precursor optic vesicles (white arrows in Figure 1.6A) and the presumptive hypothalamic field (boxed region in Figure 1.6A). The presumptive hypothalamic field clearly includes midline expression, raising the possibility that, as in chick, early ADH cells may derive in part from anterior-most midline floor plate cells (Manning et al 2006). Examination of *rx3* at 55 hpf however, suggests that *rx3* does not continue to define the ADH. Instead, expression is detected in a group of cells lining and situated adjacent to the presumptive diencephalic ventricle or the 3rd ventricle (3V) of the hypothalamus, reminiscent of the strong *shh* expressing cells detected in this area at 55 hpf (Figure 1.1C white arrow; Figure 1.7C-E). To corroborate this, and examine how expression of *rx3* compares to that of *shh*, I analysed the expressions of *rx3* and *shh* in 30 hpf embryos through double ISH. Both expression domains significantly overlap at the ADH (Figure 1.7A), although a

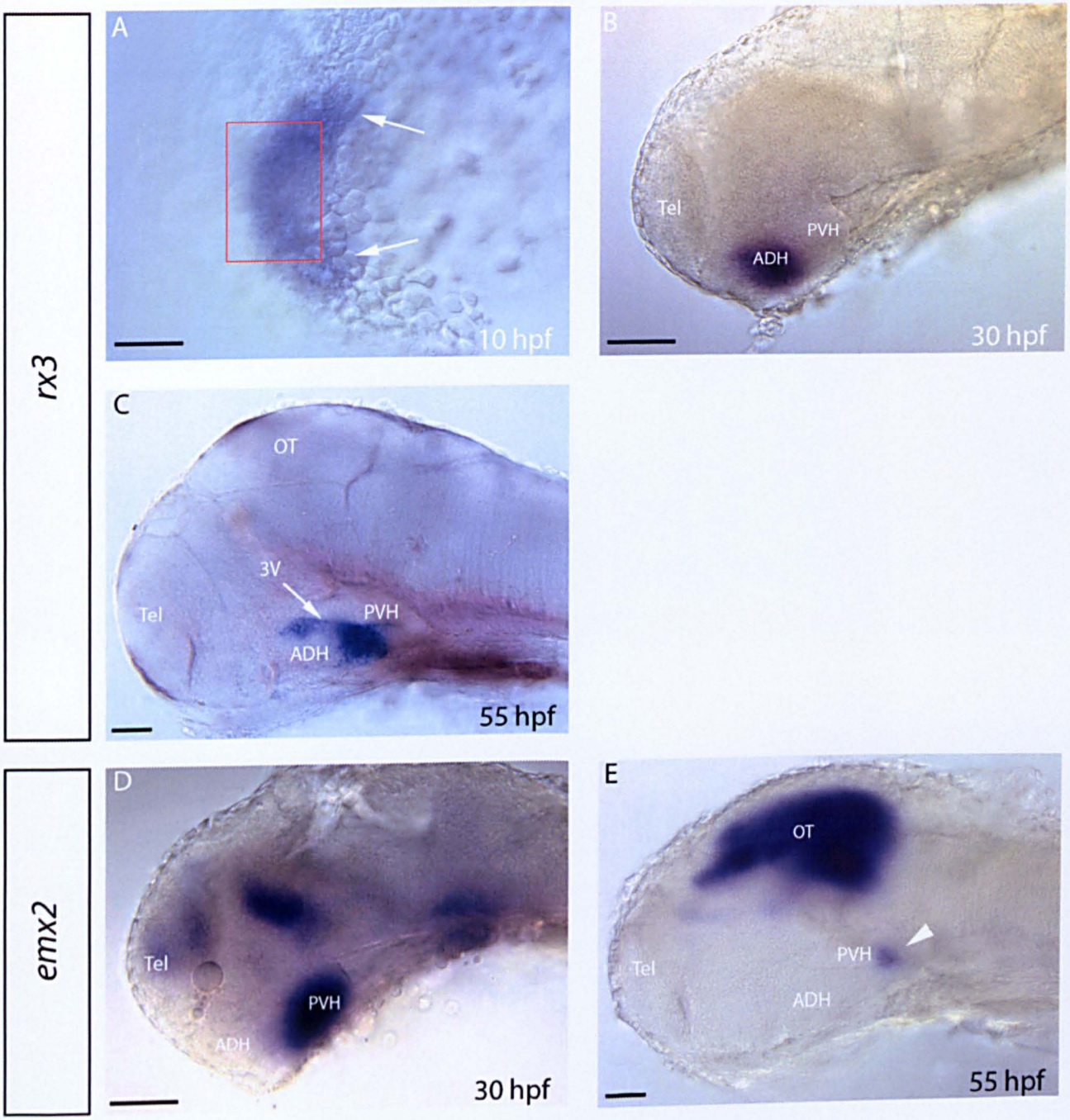

Figure 1.6 : Analysis of hypothalamic regional markers. (A-E), *In situ* hybridisation detection of the transcription factors *rx3* and *emx2*. (A) *rx3* is expressed in the presumptive hypothalamic field (red box) and the precursor optic vesicles (arrows). (B) *rx3* is expressed in the ADH at 30 hpf. However by 55 hpf, a distinct pattern of expression is detected in the areas adjacent to the ADH including the 3rd ventricle (C). (D) *emx2* is expressed in the PVH at 30 hpf and is restricted to posterior-most strip of the PVH cells at 55 hpf (E). Orientation for (A); anterior to the left; embryo viewed dorsally. Scale bars represent 50 μm.

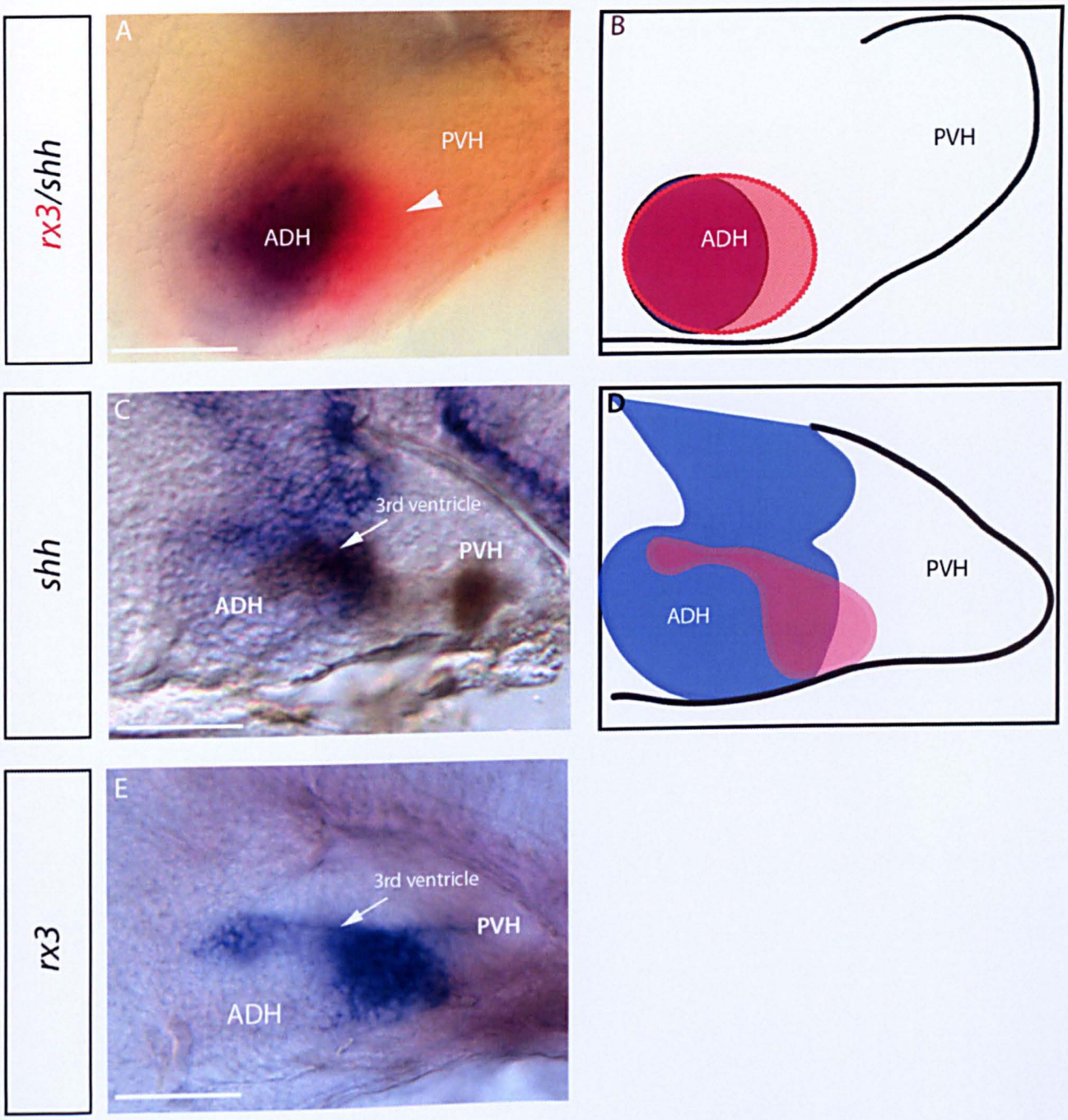

Figure 1.7 : Analysis of *shh* and *rx3* expression at ADH. (A,B) Double in situ hybridisation of *rx3* and *shh* in 30 hpf embryo shows a significant overlap of *rx3* and *shh* signals in the ADH. A small area (arrowhead) of the *rx3* expressing region does not express *shh*. (C,E) The expression of *rx3* and *shh* appears to overlap significantly in the 3rd ventricle (white arrows) with a small non-overlapping region at 55 hpf similar to that in 30 hpf. (D) Cartoon depicting the predicted overlapping expression and non-overlapping expression between *rx3* and *shh*. Scale bars represent 50 μm.

small region of the *rx3* expression domain can be seen slightly ventral/posterior to the *shh* positive ADH (arrowhead in Figure 1.7A). Similarly, at 55 hpf, a significant overlap in expression is detected in cells around the 3rd ventricle (Figure 1.8C). The expression of *rx3* also partially overlaps *pea3* expression in the ADH of 30 hpf embryo suggesting that Fgf signalling is operating in these cells (Figure 1.8D).

1.3 Discussion

1.3.1 Conservation of hypothalamic territories in vertebrates

The data in this chapter clearly demonstrate similarities in the molecular profiles that demarcate the developing hypothalamus in zebrafish to those of the chick and mouse. The downregulation of *shh* expression in the anterior floor plate of the hypothalamus is one of the hallmarks of early hypothalamic patterning event and is observed in all three organisms above, indicating a conserved vertebral feature. Similarly, the division of the hypothalamus into distinct AP domains is also conserved among the three organisms. In the zebrafish, these domains include the anterior hypothalamus or the ADH demarcated by *rx3* and the posterior or PVH that is recognised through its expression of *emx2*. However, in the zebrafish the homologous structure of the medial hypothalamic domain that expresses *FGF10* and is responsible for the morphogenesis of the infundibulum in the chick and mouse does not appear to exist (see Figure 1.9). This is consistent with the non-existence of the infundibulum and median eminence structures in the wider teleost group that includes the zebrafish. Nevertheless the possibility that a different *fgf* is expressed in the medial hypothalamic domain of the zebrafish is potentially worth investigating.

1.3.2 Maintenance of *shh* expression in the ADH

As described in the Introduction, *shh* plays a vital role in the patterning and proliferation of cells in the neural tube. After its downregulation from much of the anterior floor plate, *shh* continues to be expressed in the ADH and basal plate

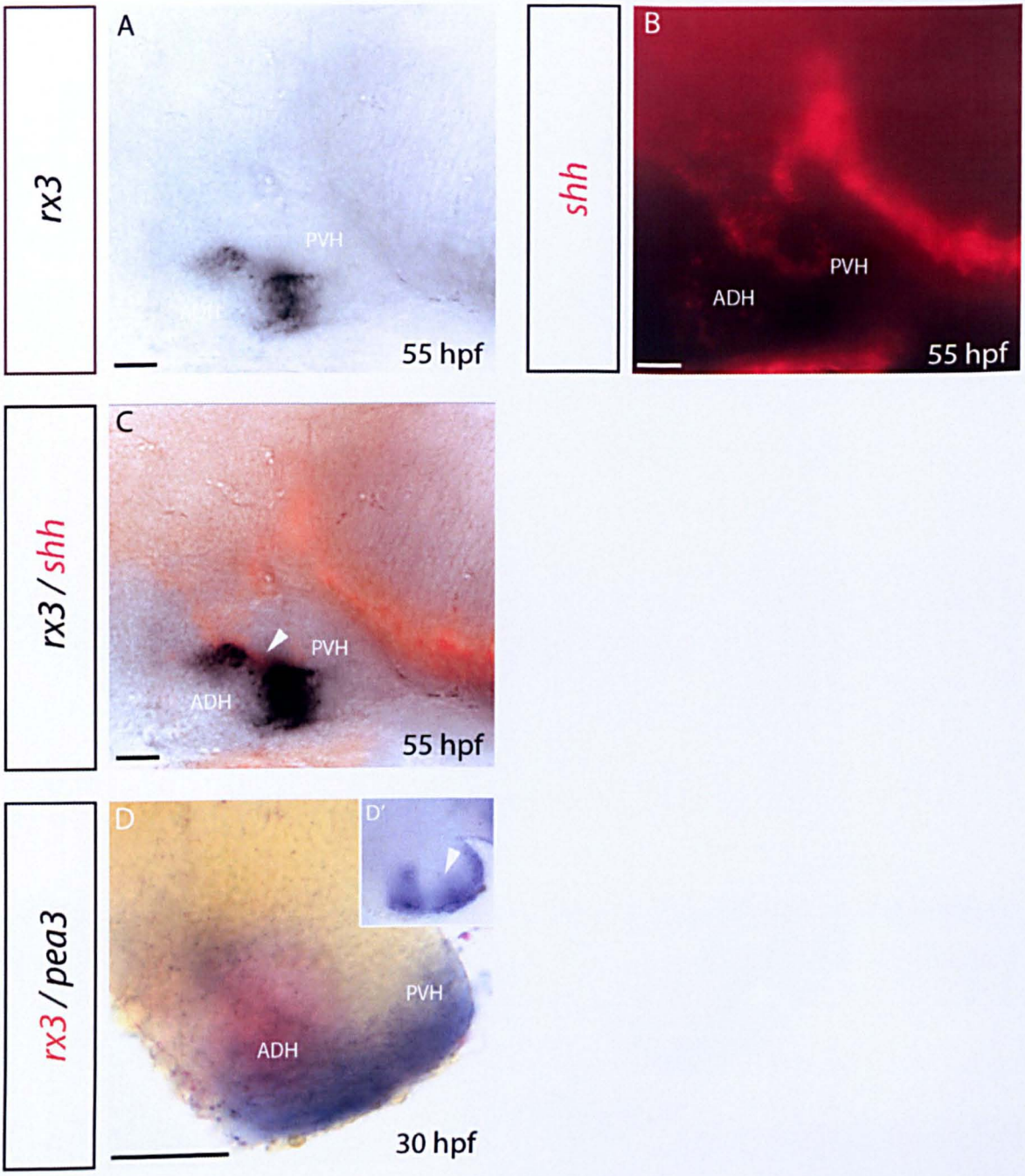

Figure 1.8 : Analysis of *rx3* expression with *shh* and *pea3*. A-D, Double in situ hybridisation of *rx3* with *shh* and *pea3* respectively. (A) *rx3* expression around the 3rd ventricle detected by BCIP/NBT and (B) *shh* expression detected by Fast Red. Merge of both images (C) shows overlapping expressions of *rx3* and *shh* in cells at the 3rd ventricle (arrowhead). (D) overlapping expressions of *rx3* and *pea3* at the ADH of a 30 hpf embryo. (D') *pea3* expression as inset. White arrowhead marks the corresponding ADH region shown in D. Scale bars represent 50 μm.

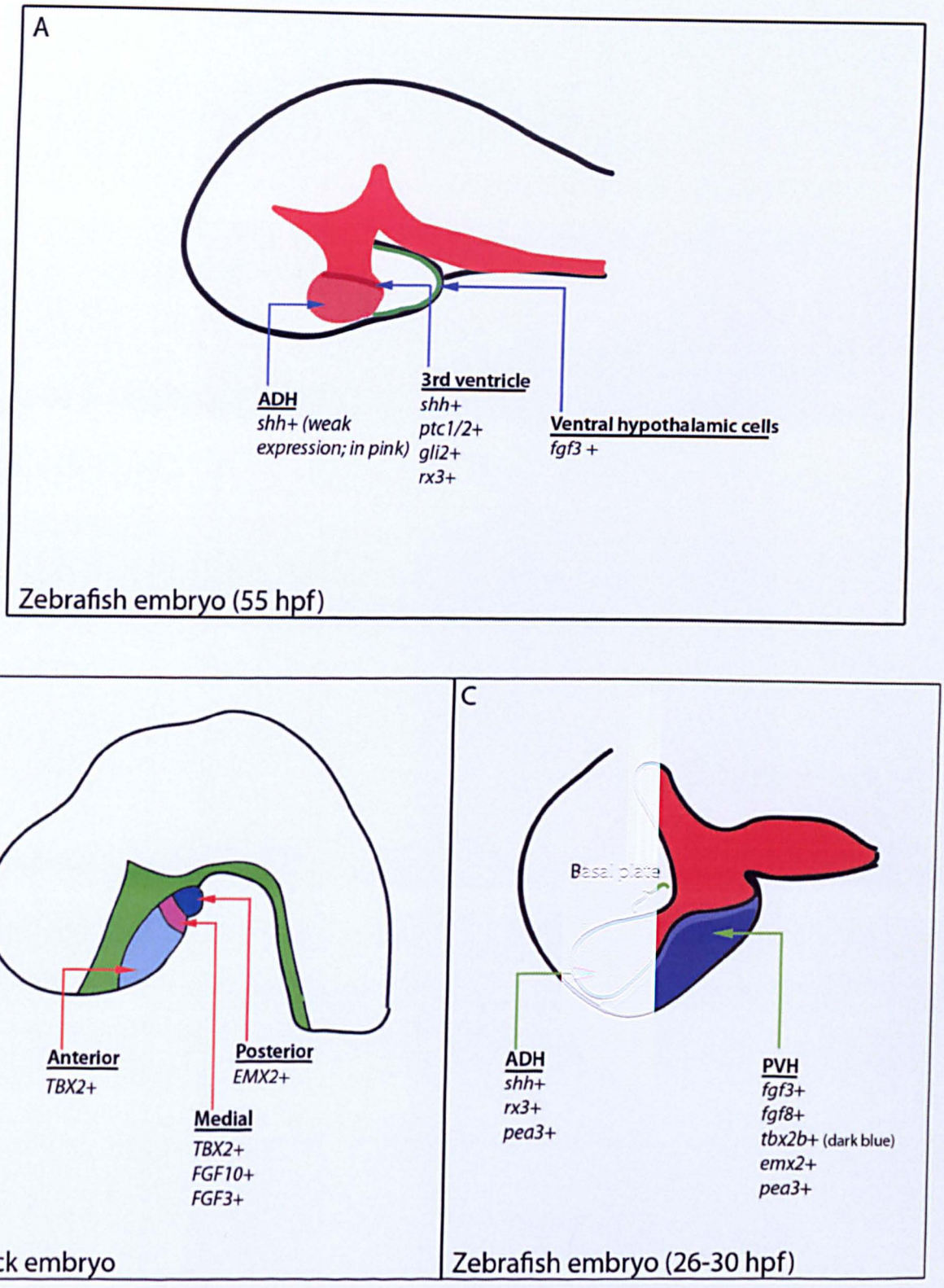

Figure 1.9 : Cartoon summarizing the distribution of signalling factors and transcription factors in the different domains of the developing hypothalamus.(B and C) Comparison of expression profiles between the chick embryo and the zebrafish embryo. The medial hypothalamic domain seen in the chick is non-existent in the zebrafish embryo.
Source : Image B is adapted from [65].

of the hypothalamus. Previous observations in the zebrafish suggest a role for *shh* in the formation of ADH/basal plate, and suggest that Shh from the ADH/basal plate may be required to inhibit Nodal signalling from the PVH[13]. However, no study has yet investigated whether Shh from the ADH/basal plate might play a wider role. My expression analysis shows that *shh* continues to be maintained in the ADH at least through 100 hpf, although beyond 55 hpf, expression is far less prominent than in the 30 hpf embryo..

Whilst a downregulation of *shh* is required for the anterior floor plate of the neural tube to establish the PVH region, the maintenance of *shh* in the basal plate and ADH up to the late stages of embryonic development remains intriguing. This maintenance of expression raises the possibility that *shh*, in the ADH, plays a role in the further development of these regions. It has been reported that *shh* in the ADH is required for the development of the anterior region of the adenohypophysis between 24 and 35 hpf of zebrafish embryonic development[67]. SHH expression in the basal plate has also been linked to the maintenance of the diencephalic-telencephalic junction (DTJ) in the mouse embryo, exerting an effect indirectly through the proper development of the hypothalamus and thalamus[68]. Hence it will be interesting to study the function of the maintained expression of *shh* in the basal plate and ADH in the zebrafish embryo. A notable and interesting feature observed in the data above (Figure 1.1) is the bulge-like appearance of *shh* expression at the ADH of the embryonic zebrafish hypothalamus, which is not observed in the chick and the mouse embryo. This may suggest that the ADH region in the embryonic zebrafish is relatively large, compared to the chick and mouse embryo. In the basal plate, immediately posterior to the ADH, *shh* expression is detected at a lower level compared to its expression in the ADH (arrowhead in Figure 1.1B). This seems to be the similar case for the mouse as well based on a study of molecular markers in the mouse embryo[69], but not the chick.

In the 55 hpf embryo, I detects expression of *shh* in the diencephalic ventricle or the 3rd ventricle of the embryo. Given the wealth of studies that show that neural stem/progenitor cells are located in the ventricular region of the neural tube (CNS), and the reports that Shh can govern the proliferation of neural stem/progenitor cells[70], these observations raise the possibility that *shh* in the 3rd

ventricle may play a role in the maintenance and function of neural stem or progenitor cells found in the 3rd ventricle of the hypothalamus. Cells lining the 3rd ventricle appear to be responding to *shh* signalling, gauged through the expression of *ptc* in these cells (Figure 1.3). As yet, the relationship between the weakly *shh* positive ADH and prominently-expression *shh* in the 3rd ventricle is unclear. It is possible that the expression of *shh* in the ADH and the 3rd ventricle are interdependent or even that the two domains might share a common origin. A site-specific knock-down of *shh* signalling at the ADH or lineage tracing studies would be good experiments to investigate the above.

1.3.3 Potential function of *fgf3* in the ADH

Fgfs play a vital role in the development of the CNS. Addition of basic FGF (bFGF) to ectodermal cells derived from Xenopus gastrula leads to the differentiation of neuronal cell fates[71]. In the zebrafish *fgf8* mutant, the parapineal nucleus fails to migrate from its midline position to the left side the brain[72]. However, the role of Fgfs in the development of the hypothalamus has not been fully described. Studies in the chick suggest a requirement for FGF10 and FGF3 in the medial hypothalamic floor plate, driving formation of the infundibulum and suggest a role for FGFs in promoting cell proliferation in the PVH[65]. In examining the expression of *fgfs* in the zebrafish embryonic hypothalamus, I could not detect any expression of *fgf10*, which is inconsistent with reports in the chick and mouse infundibulum[73]. However, this is not unexpected since the infundibulum is non-existent in teleosts, including the zebrafish. Also, previous studies suggest that the functions of *fgf3* and *fgf10* have partly interchanged in the zebrafish[64]. Hence, although FGF10 does still play a fundamental role in pectoral fin/limb bud development in the zebrafish and mouse, it does not appear to have any developmental role in the zebrafish hypothalamus[64].

In contrast to *fgf10*, *fgf3* and *fgf8* are expressed in the zebrafish embryonic hypothalamus. Close examination reveals that *fgf3* is strongly expressed throughout the nascent PVH at 26 hpf whereas *fgf8* is confined to posterior-ventral most parts of the PVH. Whilst the expression of *fgf3* can still be observed at 55 hpf at the ventral hypothalamus, *fgf8* is no longer being expressed at 55 hpf suggesting

a role for *fgf8* in the early but not the later stages of hypothalamus development. My data indicates that *fgf3* is expressed in the region immediately ventrally-adjacent to the ADH at 26 hpf (Figure 1.4A). Hence, *fgf3* may act non cell-autonomously on cells at the ADH, as double ISH detection of *pea3* and *rx3* shows a slight overlap in expression (Figure 1.8). At this same stage, *fgf8* expression is only observed in posterior-most PVH cells, making it unlikely that *pea3* expression in ADH cells is triggered by the expression of *fgf8*.

1.3.4 Investigating the roles of *shh*, *fgf3* and *rx3* in the ADH/3rd ventricle

As I have shown and discussed, *shh* and *fgf3* are expressed in and adjacent to cells of the ADH and 3rd ventricle. Moreover, downstream components of Shh and FGF signalling pathways are expressed in cells in and around the ADH/3rd ventricle over the period 30-55 hpf, suggesting active signalling. The roles of Shh and FGFs in the ADH/3rd ventricle have not been directly described in any studies thus far. Similarly, the role of the transcription factor *rx3*, a marker for the ADH, remains to be elucidated in the hypothalamus. The overlapping expressions of *rx3* and *shh* at the ADH in 30 hpf embryos hints strongly at a possible interaction between the two (Figure 1.7A). Similarly, investigation into the expression of *rx3* and *shh* at 55 hpf shows a maintained co-expression in cells along the presumptive 3rd ventricle. There is also potentially an interaction between *rx3* and *fgf (fgf3)* based on the overlapping expression of *rx3* with *pea3* in the ADH at 30 hpf.

To investigate these potential interactions, I therefore set out to test in the next chapter if the loss of *rx3* function would have an effect on the development of the ADH and monitor the changes in *shh* and *fgf* expression and their downstream signalling readouts.

Chapter 2

Chapter 2: Loss of *rx3* in the anterior hypothalamus of the embryonic zebrafish

2.1 Introduction

As outlined in the Introduction, *rx3* is an evolutionarily-conserved transcription factor, whose function in the hypothalamus remains poorly addressed. Previous studies have noted expression of *rx3* in the ADH of the hypothalamus, and have demonstrated a reduction in the number of propiomelanocorticotropin (pomc)[18] and vasotocin-neurophysin (vtn)[18] hypothalamic neurosecretory neurons, in *rx3*-null (termed *chokh)* mutants and *rx3* morphants, indicating a requirement for *rx3* in the formation and/or differentiation of these neurons. Pomc is produced in the arcuate nucleus and plays a vital role in the regulation of feeding behaviour. It is a precursor polypeptide that undergoes a variety of post-translational modification through enzymatic cleavage to give rise to different derivatives that execute different functions. These peptides include the melanocyte-stimulating hormone (MSH) and adrenocorticotropic hormone (ACTH). Loss of *pomc* gene function has been implicated with obesity problems. Vtn and its mammalian homolog arginine vasopressin have a wide role in controlling physiological and behavioural responses, for example osmoregulation, stress response and sexual behaviour. In this thesis, I focused on *pomc* positive cells given the successful synthesis (see Materials and Methods) and workability of its probe.

While previous studies show that, under *rx3* loss-of-function conditions, there is a reduction in *pomc* positive neurons in the arcuate nucleus, these studies did not provide any mechanistic details that could explain the loss of these neurons. The arcuate nucleus in which *pomc* neurons are found, is located antero-ventral to the ADH/3rd ventricle region of the 30 hpf embryo. My observations in the last chapter show that *rx3* in expressed in both of these domains, and raise the possibility that expression in both or either domain could normally govern Pomc neuronal differentiation. However, my observations of overlap in expression of *rx3* with *shh*, and *pea3* raises the additional possibility that *rx3* may operate indirectly to govern Pomc neuronal differentiation, through an interaction with either of these signalling pathways. To begin to investigate these possible mechanisms underlying

the regulation of the neurosecretory neurons by *rx3*, I examined *pomc* expression, relative to *rx3* expression in the hypothalamus, and relative to the expression of the signalling factors *shh* and *fgf3*, and their downstream signalling components in wild type embryos and after *rx3* manipulation.

To manipulate *rx3* and examine its regulatory role, I performed *rx3* morpholino injections on one-cell stage zebrafish embryos to produce *rx3* loss-of-function embryos or *rx3* morphants (see Materials and Methods for details on the morpholino technique). At the time of writing this thesis, I was able to perform a single first comparative analysis of morphants with *chokh* mutants (kind gift from Dr. Brandean Kennedy, UCD), but have just received written permission from the UK Home Office to import the *chokh* mutant from University College Dublin, Ireland, and so have not yet had the opportunity to use the *chokh* mutant embryos extensively for the studies described in this thesis. In this chapter, I therefore:

a) test the hypothesis that *rx3* morphant embryos exhibit a similar phenotype to *chokh* mutants, and are a viable loss of function model
b) examine expression of *rx3* relative to pomc
c) test the hypothesis that *rx3* may govern progenitor cell proliferation in the hypothalamus
d) test the hypothesis that *rx3* exerts its effects , by regulating expression of *shh* and *fgf3*

2.2 Results

2.2.1 The *rx3* morphant display similar phenotypes to the *chokh* mutant

To confirm that *rx3* morphants produce embryos of similar phenotype to the mutant *chokh* embryos, I analysed and compared several obvious morphological features attributed to the loss of *rx3* function in *chokh* embryos. The most obvious phenotype observable is the loss of both eyes (Figure 2.1). This phenotype is commonly referred to as the absent eyes phenotype. This is the main phenotype

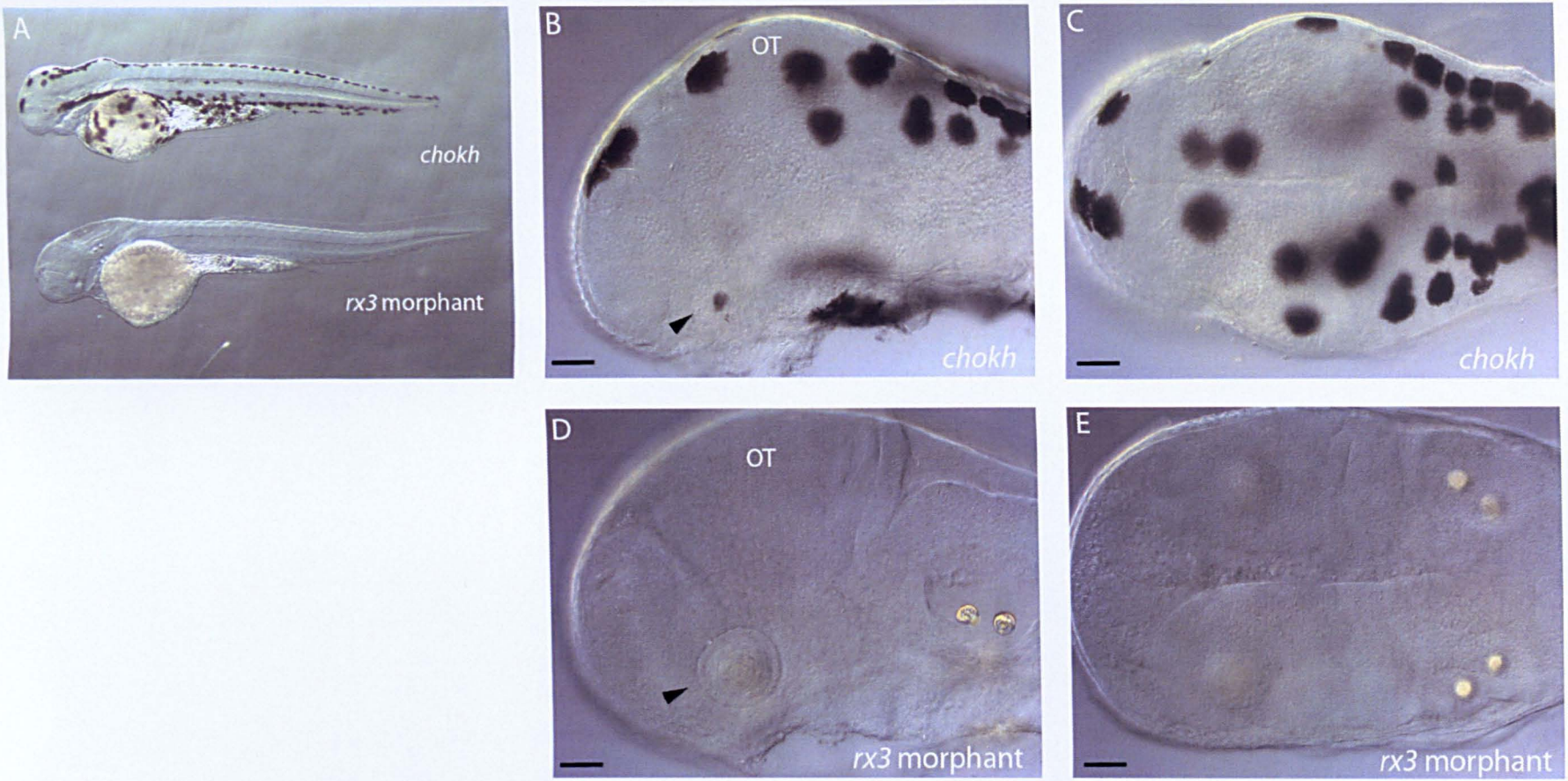

Figure 2.1 : Phenotypic comparison between the *chokh* mutant and *rx3* morphant at 55 hpf. (A) Whole embryo comparison of the *chokh* and *rx3* morphant shows similarity in the overall morphological appearances. In both types of embryos, the eyes failed to develop. (B,D) The non-functional eye lens as observed in the embryos (arrowheads). (A,B,D) Lateral view of the embryos. (C,E) Dorsal view of the embryos. Scale bars represent 50 μm.

observed in a majority of *rx3* morpholino-injected embryos. There are also embryos that display an intermediate, or reduced-eye phenotype. This is consistent with findings reported in a previous study in which both *rx3* morphants and *chokh* embryos were used [18]. In testing the efficacy of the morpholino injection, I found that injecting with a combination of both splice and ATG morpholinos produces a bigger number of embryos with the absent eyes phenotype without any observable non-specific effects in the overall phenotype of the embryo. Hence, all the data in this chapter are produced using *rx3* morphants generated from a cocktail of both morpholinos. This is similar to the method used in the above literature, in which a mixture of both forms of *rx3* morpholinos were used to generate *rx3* morphant embryos[18]. Another noticeable phenotype, which I have used in addition to the absent-eyes phenotype to recognize *rx3* loss-of-function embryos within the pool of *rx3* morphants is the appearance of an enlarged telencephalon (prominent if embryos are viewed dorsally) as reported in Stigloher et.al. (2006)[29] at 30 hpf, although this is not easily observed at 55 hpf. I also performed an overall anatomical survey on the *rx3* morphant embryos, but did not detect noticeable and obvious phenotypic changes apart from those described above.

2.2.2 Reduction of *pomc* cells concomitant with increase in proliferating progenitor cells and early born neurons

Given that the *rx3* morphant embryos appear to mirror *chokh* embryos, I used them to further elucidate the role of *rx3* in the either the formation or maintenance of *pomc* neurons in the arcuate nucleus of the zebrafish embryos. Initially, I determined the temporal and expression profile of *pomc*, relative to *rx3*, to ask whether there is ever an overlap in expression, indicative of an autonomous effect of *rx3* in governing Pomc cell differentiation. My results reveal that I cannot detect an overlap. The earliest *pomc*-expressing cells are found just antero-ventral to the ADH, presumably in the prospective arcuate nucleus, at 30 hpf (Figure 2.2). Soon after, an additional zone of *pomc*-expressing cells is detected in the hypophysis (pituitary). By 55 hpf, *pomc* positive cells are clearly detected in both the arcuate nucleus and hypophysis. The distribution of these cells in the zebrafish is therefore

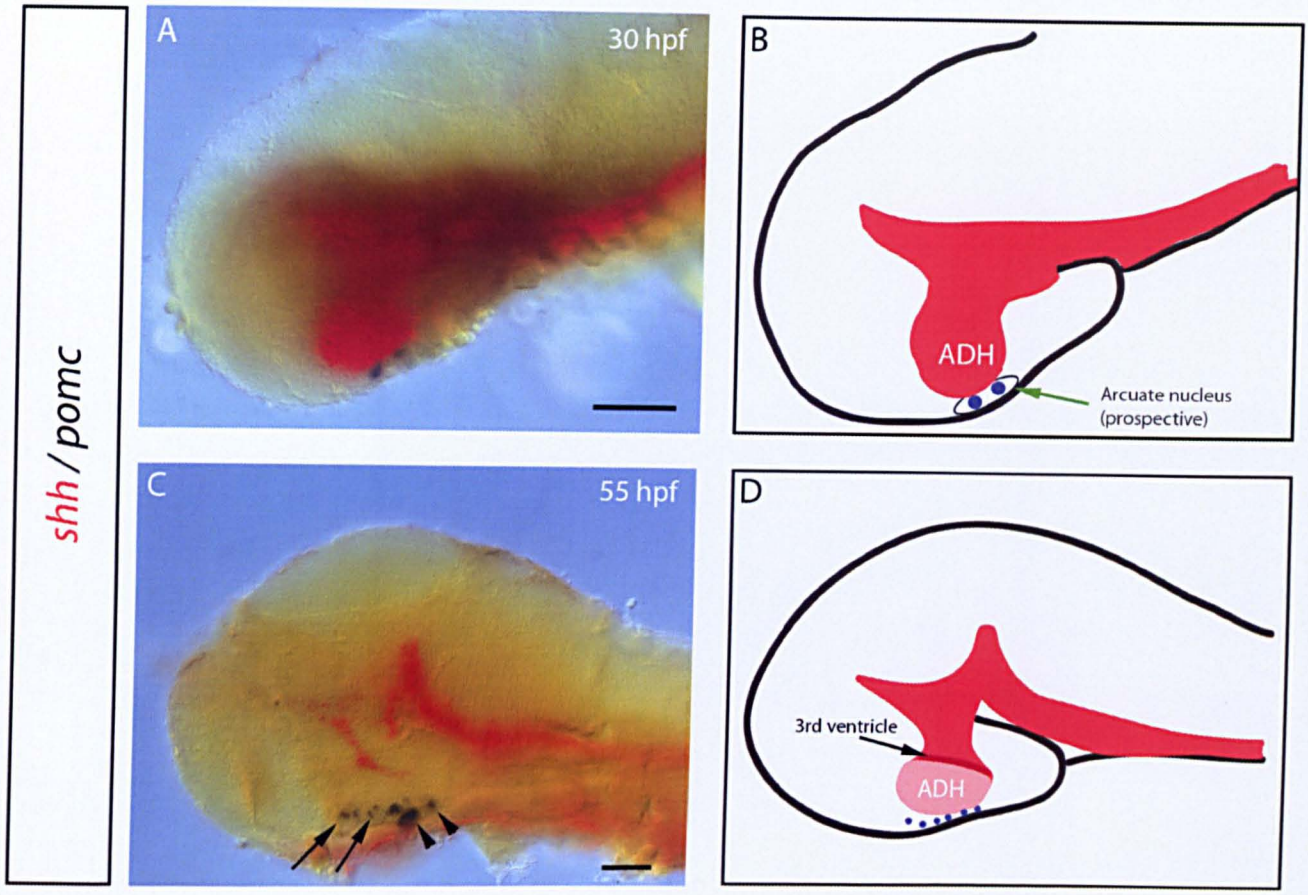

Figure 2.2 : *pomc* (blue) expressing cells are found ventral to the *shh* (red) ADH.
(A) Earliest *pomc* expressing cells are seen in a 30 hpf embryo in the prospective arcuate nucleus. (C) *pomc* positive cells persist in this region at 55 hpf (arrows). In addition, *pomc* positive cells are now seen in the hypophysis as well (arrowheads).
(B,D) Cartoon representing A and C respectively. All embryos are viewed laterally.
Scale bar represents 50 um.

similar to that described in the mouse[69], which suggests similarities in the formation of *pomc* cells in the arcuate nucleus.

The late onset of *pomc* expression relative to *rx3*, and non-overlapping expression, makes it difficult to establish how *rx3* may govern *pomc* cell differentiation. Rx3 may operate autonomously on *rx3* positive progenitor cells, or via a non-autonomous effect. Nonetheless, in an attempt to begin to elucidate the role of *rx3* in the development of *pomc* expressing cells, I first investigated if the number of *pomc* positive cells in the arcuate nucleus of the *rx3* morphant is reduced similarly to the reported reduction in *chokh* mutant embryos. Figure 2.3 shows a clear reduction of *pomc* positive cells in the arcuate nucleus of 55 hpf *rx3* morphant embryos compared to control injected embryos. By contrast, *pomc* positive cells in the hypophysis appear unaffected in the *rx3* morphant embryos at this stage (Figure 2.3B). Quantitative analysis and comparison of the number of *pomc* positive arcuate cells in both control and morphant embryos shows that the reduction is statistically significant (*p* value of 0.008) (Figure 2.3C). Examination of 30 hpf *rx3* morphant embryos reveals, similarly, that *pomc* positive cells are absent from the arcuate nucleus, (*p* value of 0.0029) (Figure 2.3F). At this time point, *pomc* expressing cells are not seen in the hypophysis of the *rx3* morphants, although they appear to expressed and distributed normally at 55 hpf (black arrowheads in Figure 2.3A,B).

To begin to assess whether *rx3* affects the specification of *pomc* positive cells through an effect on hypothalamic neural progenitor cells, I examined expression of phospho-histone 3 (phos-H3) as a marker for actively-dividing cells, through immunolabelling. Phos-H3 is upregulated in cells undergoing the mitotic phase (M-phase) of the cell cycle and hence labels progenitor cells undergoing cell division in the hypothalamus. A combination of *rx3* ISH and phos-H3 immunolabelling on 55 hpf embryos reveals a close correlation in *rx3* expression and actively dividing cells; many positively labelled phos-H3 cells in the domain of *rx3* expressing cells (Figure 2.4A). To test if *rx3* governs progenitor cell division, I analysed the hypothalamus of *rx3* morphant embryos for the expression of phos-H3 alongside the control-injected morphant embryos at 55 hpf. I detected a significant increase

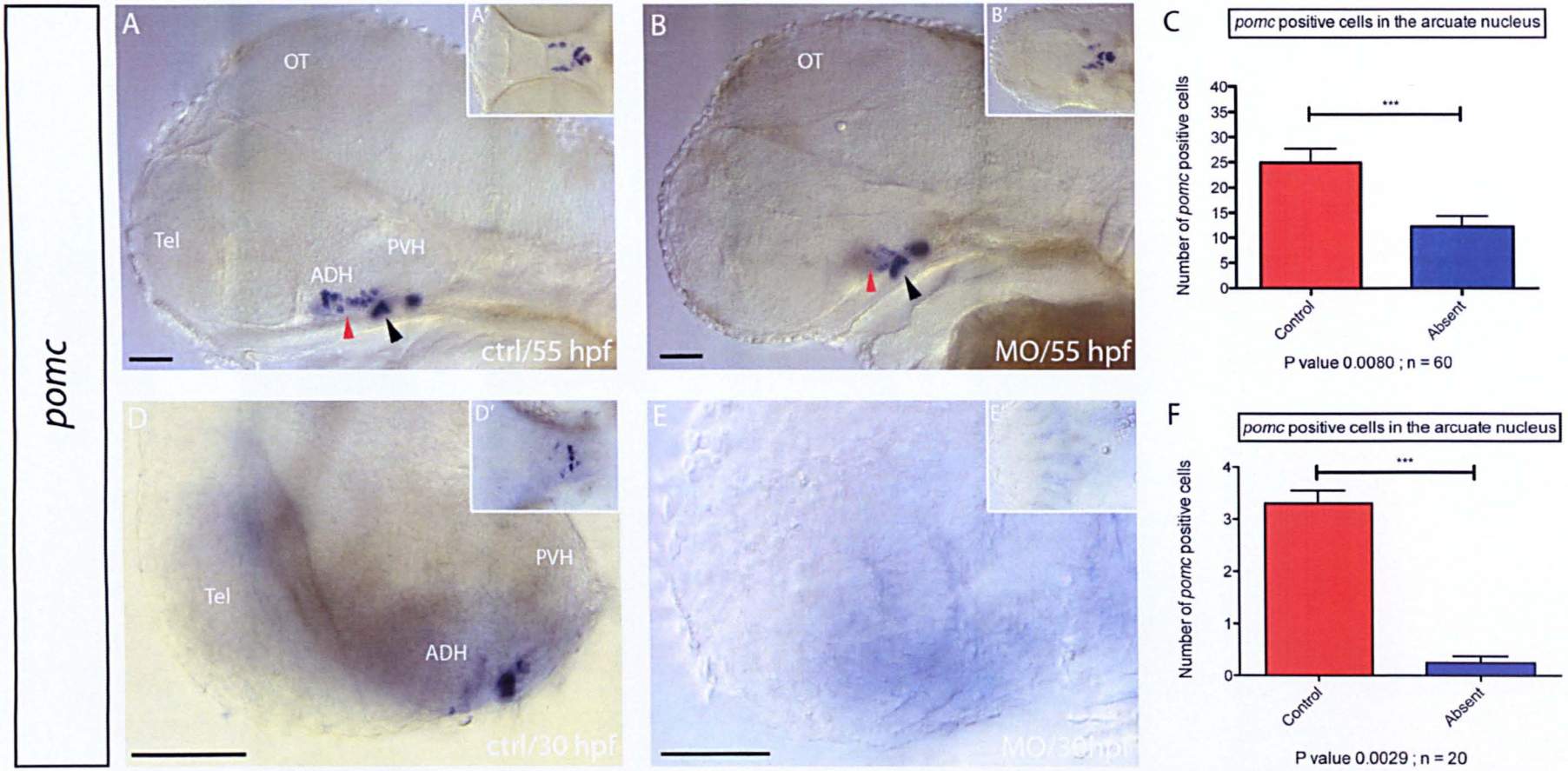

	30 hpf	55 hpf
Control	3	25
Morphant (MO)	0	12

Figure 2.3 : Analysis of *pomc* expression in the arcuate nucleus. (A-C) *pomc* expressing cells are significantly reduced in the arcuate nucleus of the *rx3* morphants (MO) at 55 hpf (red arrowheads), but appear normal in the hypophysis (black arrowheads in A and B). (D-F) A similar observation at 30 hpf except that *pomc* is not seen in the hypophysis as well. (A-E) Lateral view (A'-E') Anterior view. Table represents the average number of *pomc* positive cells in the arcuate nucleus.

Figure 2.4: Examination of proliferation and *rx3* expression in the *rx3* morphant embryos.
(A) *rx3* in situ hybridisation combined with phos-H3 immunohistochemistry shows the distribution of phos-H3 cells in the *rx3* expressing region of the ADH. (C-F) An increase in phos-H3 positive cells is observed in the *rx3* morphants at 55 hpf. (B) graph representing this increase. (G,H) *rx3* is still expressed in the ventricular region of the *rx3* morphant embryos albeit at a higher level. (G'H') Anterior view of the embryos. All images are lateral view of embryos. flr, flourescence; DIC, differential interphase contrast. Scale bars represent 50 μm.

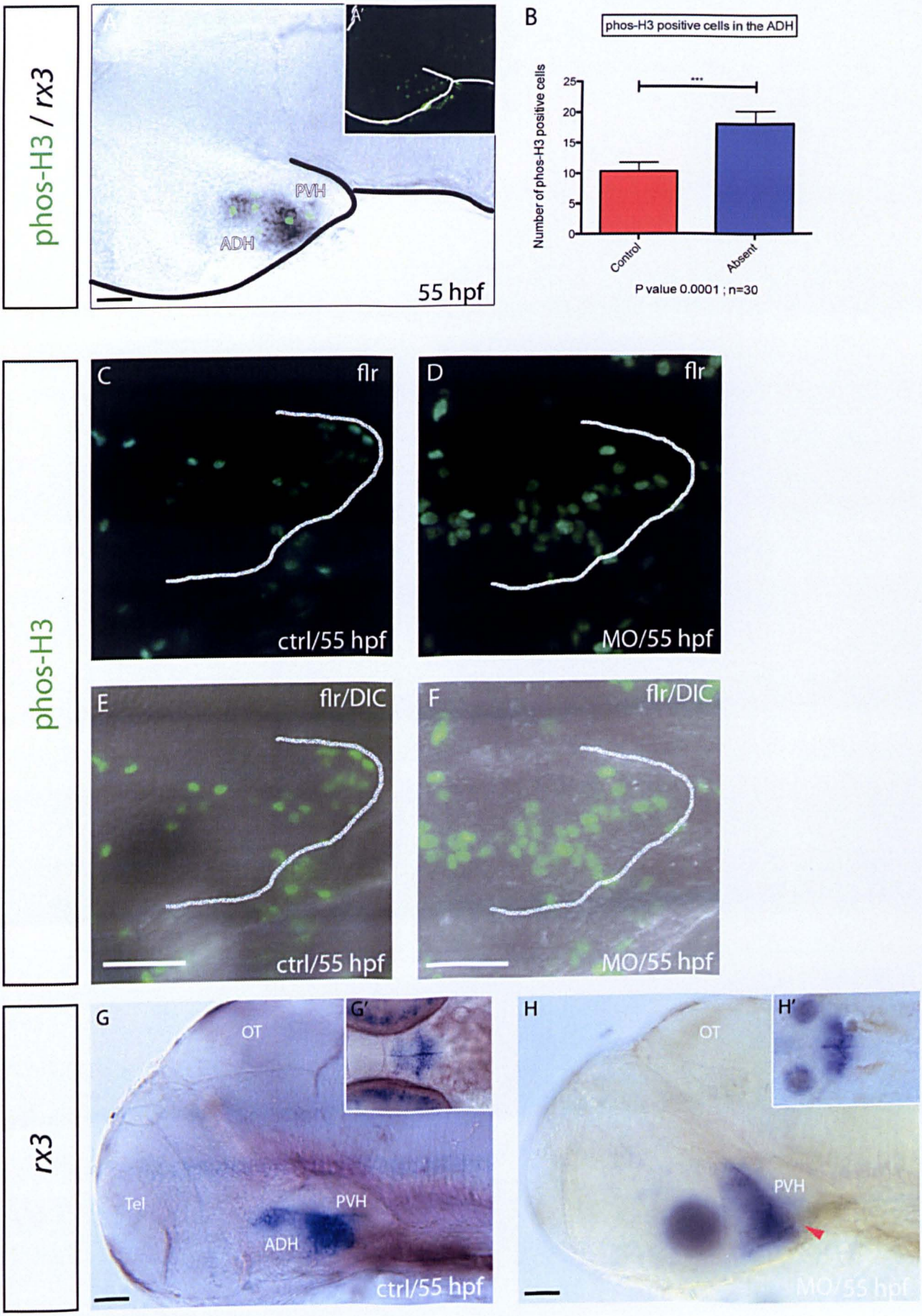
phos-H3 / rx3
A
A'
PVH
ADH
55 hpf
B
phos-H3 positive cells in the ADH
Number of phos-H3 positive cells
25
20
15
10
5
0
***
Control
Absent
P value 0.0001 ; n=30
phos-H3
C
flr
ctrl/55 hpf
D
flr
MO/55 hpf
E
flr/DIC
ctrl/55 hpf
F
flr/DIC
MO/55 hpf
rx3
G
G'
OT
Tel
PVH
ADH
ctrl/55 hpf
H
H'
OT
PVH
MO/55 hpf

in phos-H3 labelled cells in the ADH domain/3rd ventricle of *rx3* morphant embryos compared to control-injected morphants (Figure 2.4 B,D,F). The increase in phos-H3 labelled cells was mainly distributed along the ventricle of the *rx3* morphant at 55 hpf.

To test whether the increase in phos-H3 positive cells affected cells around the 3rd ventricle, I examined *rx3* expression as a marker for the 3rd ventricle at 55 hpf. Unlike antibody staining, mRNA products can still be detected through ISH after morpholino knock down since the morpholinos would only bind to and inhibit the target mRNA (i.e. *rx3* in this case) from being translated and not degrade them (refer to Materials and Methods for details on morpholinos). I performed *rx3* ISH on the *rx3* morphants to examine that the 3rd ventricle is normal. The resulting data show that *rx3* is expressed in the 3rd ventricle, and if anything, appears relatively stronger to controls (Figure 2.4G, H). This, together with the phos-H3 data, raises the possibility that progenitor cells in the 3rd ventricle, including *rx3* positive progenitor cells, are increased in number after *rx3* knockdown.

Together this suggests that *rx3* may act specifically as a negative regulator of hypothalamic progenitor cell proliferation. To examine whether the increase in ventricular progenitors and decrease in *pomc* neurons reflected a general decrease in hypothalamic neurons, I next examined the expression of *isl1*, a LIM/homeodomain transcription factor widely expressed in early developing hypothalamic neurons[11]. In *rx3* morphant embryos, *isl1* expression was generally upregulated around sites of endogenous expression (arrowheads Figure 2.5B). Thus depletion of *rx3* does not lead to a general decrease in neurogenesis. To examine if the loss of *rx3* function affects other regions apart from the hypothalamus, I analysed the expression of *pax6* (homeobox gene) that shows a general upregulation around sites of endogenous expression albeit its absence in the hypothalamus (Figure 2.5D).

Since these effects are non-autonomous to *rx3* expression, this raises the likelihood that reduction in *rx3* may lead to a change in a signalling ligand or signalling pathway, and so cause a widespread change in the patterning of the hypothalamus

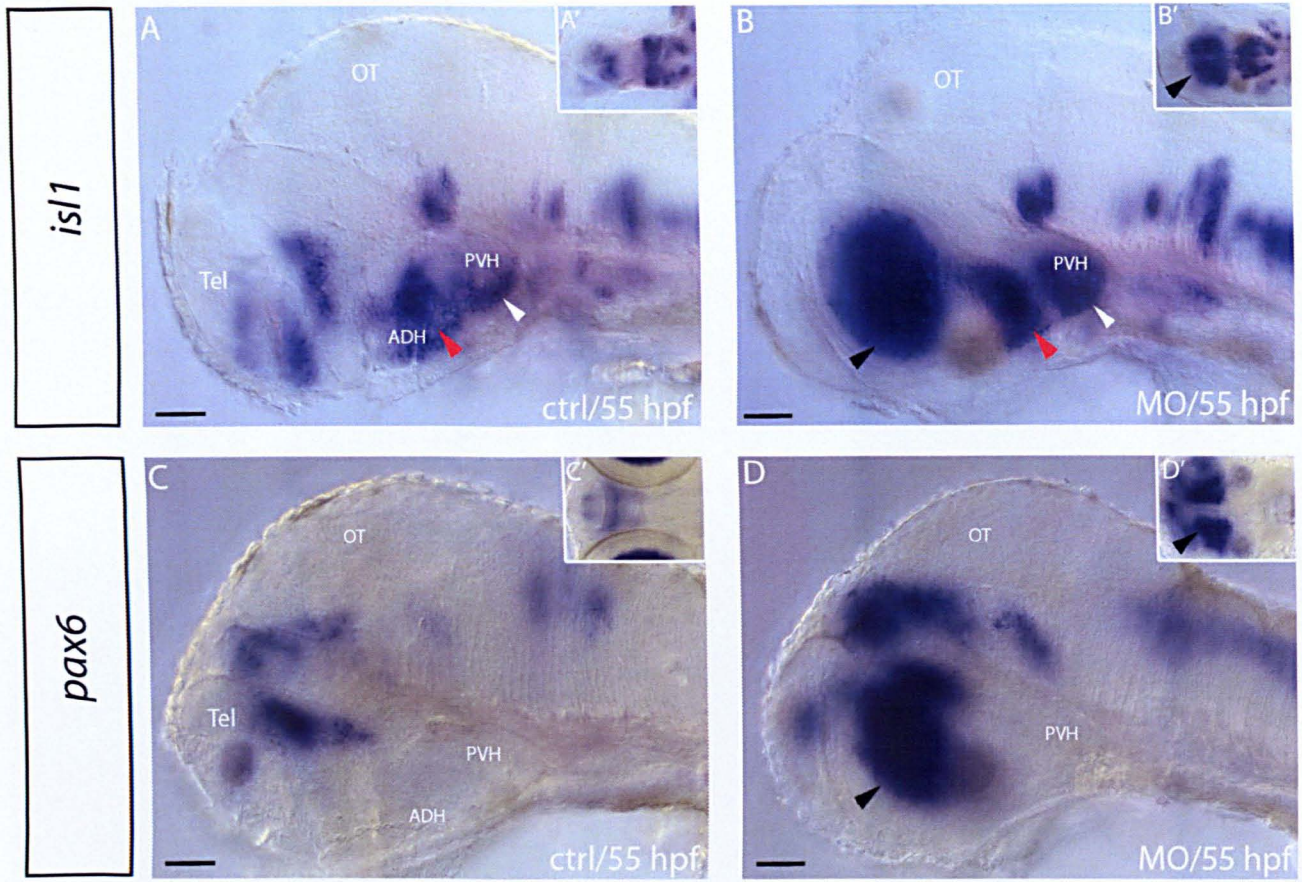

Figure 2.5 : *pax6* and *isl1* expression analyses in *rx3* morphant. (A,B) *isl1* expression is upregulated in the ventricular region (red arrowhead) as well as in the PVH (white arrowhead). It is also vastly upregulated in the dorsal tissue (black arrowhead) as well as in the general CNS. (A',B') Anterior view of the embryos. (C,D) *pax6* is not detected in the hypothalamus of *rx3* morphant as in the control embryo. It is however upregulated in the dorsal tissue similar to *isl1* and is generally upregulated in the CNS of the morphant embryo. Scale bars represent 50 μm.

and its surrounding regions. Based on my observations in result chapter 1 that *rx3* expression overlaps with that of *shh* and *pea3*, I therefore next examined expression of *shh* and *fgfs* in *rx3* morphants.

2.2.3 Changes in *shh* expression domains in *rx3* morphants

The expression of *shh* overlaps with that of *rx3* in the ADH at 26-30 hpf, and in the 3rd ventricle at 55 hpf as detailed in section 1.2.3. To study a possible effect of *rx3* on *Shh*, I investigated *shh* expression in *rx3* morphant embryos. I detected a dramatic change in *shh* expression in 55 hpf *rx3* morphant embryos. *shh* expression around the 3rd ventricle is not diminished upon reduction of *rx3* (red arrowhead, Figure 2.6B). Indeed, *shh* appears to be expressed at higher levels, supporting the idea that there are increased progenitor cells in this region in morphant embryos. By contrast, expression of *shh* in both the ADH and the basal plate (white and green arrowheads in Figure 2.6 A,B) is completely diminished in the morphants. Similarly, expression of *shh* in the telencephalon (in other species, secondarily induced from Shh in the anterior dorsal hypothalamus[12]) is lacking (black arrow, Figure 2.6B). The reduced *shh* expression in the basal plate may be due to a complete loss of this territory. The apparent loss of territory is clearly visible in ventral views (Figure 2.6A', B'), which show a compressed extent of *shh* expression along the dorso-ventral axis. As a result, expression of *shh* around the 3rd ventricle now appears to abut expression in the ZLI.

Together these results show that a loss of *rx3* function through morpholino leads to a loss of *shh* expression in the ADH, and support the notion that a loss of *rx3* function leads to an increase in number progenitor cells in the 3rd ventricle. Thus, I hypothesise that *rx3* exerts two temporally distinct effects on the hypothalamus, the first, an early action mediated through Shh-signalling from the ADH, and the second, a later action, mediated via the control of progenitor cells in the 3rd ventricle.

To test how changes in *shh* signalling in the morphant embryos affect Shh signalling, I examined both *ptc1* and *ptc2* as molecular readouts. Both are

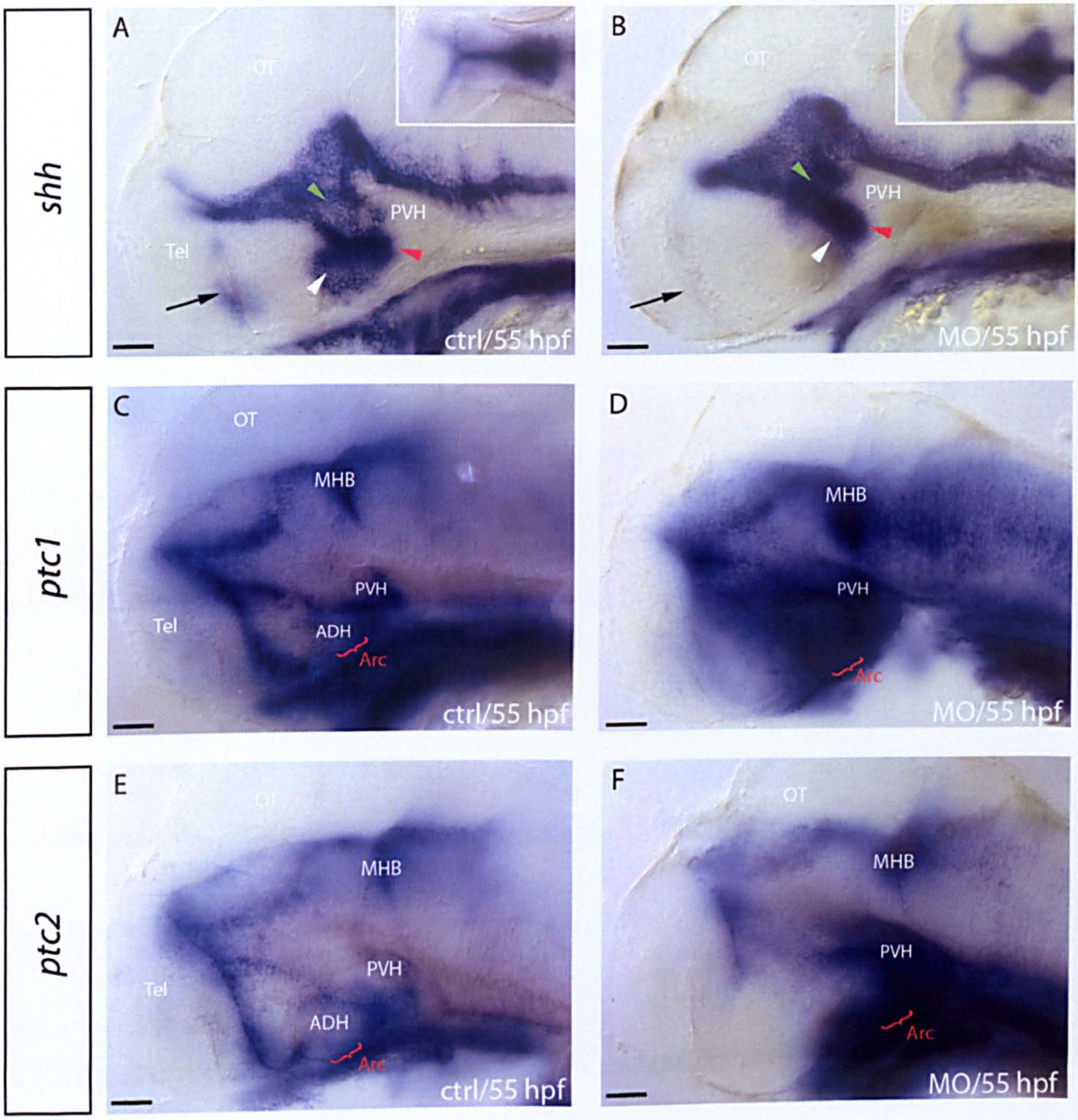

Figure 2.6 : Loss of *shh* expression in the *rx3* morphant embryos. (A,B) *shh* expression is not detected in the ADH region (white arrowheads), the basal plate (green arrowheads) and the telencephalon, but is still expressed in the ventricular region (red arrow-heads). (C,D) Increase in *ptc1* expression is seen generally throughout the embryo including the hypothalamus. (E,F) *ptc2* expression appears to be generally upregulated in the morphant embryos, with the exception of the ADH. (A-H) Embryos are view laterally. (G',H') Embryos are viewed ventrally. Arc; arcuate nucleus. Scale bars represent 50 μm.

dramatically upregulated in morphant embryos in regions that include the arcuate nucleus (Figure 2.4D and F) or its remnant structure. The one exception seems to be *ptc2* expression in the ADH, which does not show a general upregulation; increase in expression is quite specific to the hypothalamus. However, these results together suggest that reduction of *rx3* leads to widespread and general changes in *shh* signalling throughout the hypothalamus and ventral forebrain.

2.2.4 Changes in *fgf* signalling in *rx3* morphants

In section 1.3.3, I described the overlapping expression of *pea3* and *rx3* in the ADH at 30 hpf. I therefore next investigated if *rx3* exerts any influence on the expression of *fgf* ligands, or FGF signalling (as assessed by *pea3*) in the hypothalamus. ISH reveals no change in the territory in which *fgf3* is expressed in *rx3* morphant compared to control embryos. In both cases, *fgf3* is expressed in PVH cells (arrowheads in Figure 2.7A and B). The levels of expression of *fgf3* in the PVH, moreover, appear similar in control and morphant embryos (by contrast, *fgf3* expression is markedly upregulated in the MBH of morphant embryos). Similarly, the Fgf signalling pathway readout, *pea3* shows no change in expression in the hypothalamus (Figure 2.7F), although expression is diminished in the telencephalon and epiphysis of morphants (Figure 2.7F). Although *fgf8* does not overlap with *rx3* in its expression (section 1.3.3), I examined the expression of *fgf8* in the *rx3* morphants and found no change in expression in the hypothalamus, although ectopic expression of *fgf8* was now clearly detected in pseudo-optic tissue (Figure 2.7D). In summary, in *rx3* morphant embryos, *shh* and the Shh signalling pathway show dramatic alterations in cells in and around the hypothalamus, including the ADH, 3rd ventricle, and the region in which *pomc* positive cells differentiate, but Fgfs and *fgf* signalling appear unaffected.

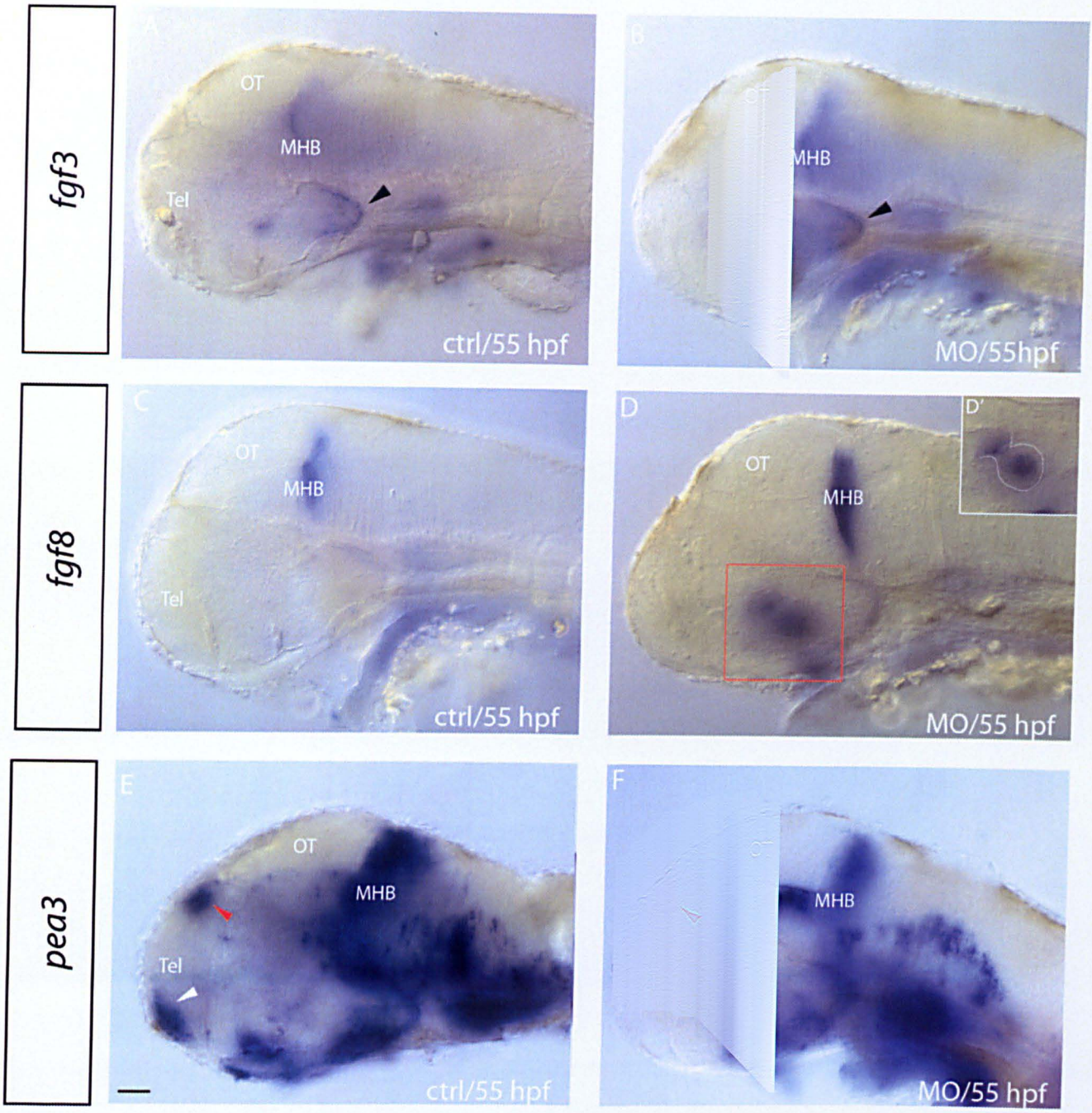

Figure 2.7 : Expressions of *fgfs* show no change in *rx3* morphant embryos. (A-B) *fgf3* expression is maintained in the morphant embryo; expressed at the ventral floor plate region (arrowhead). (C-D) *fgf8* is expressed in the pseudo-optic tissue (boxed) of the morphant embryo; outlined in D'. (E-F) *pea3* remains unexpressed at the ADH and shows no change in expression in the hypothalamus. It is however downregulated in the telencephalon (white arrowhead) and the epiphysis (red arrowhead).
Scale bar represents 50 um.

2.3 Discussion

2.3.1 Requirement for *rx3* in the specification and differentiation of *pomc* positive cells in the arcuate nucleus

The neuropeptide Pomc is the key determinant for the 'starvation' response during active feeding. Hypomorphic mutation in this gene leads to obesity[74, 75]. In the zebrafish embryo as with all other vertebrates, *pomc* expressing neurons are found in the arcuate nucleus of the hypothalamus and the pars distalis and the pars intermedia of the adenohypophysis. As reported in section 2.2.2, *pomc* expressing cells are significantly reduced in the arcuate nucleus of *rx3* morphant embryos. However the number of *pomc* positive cells remains unchanged in the adenohypophysis suggesting that *rx3* function is specific to *pomc* positive cells in the hypothalamus. It also interestingly suggests that the regulation of *pomc* positive cells is different between two tissues that are adjacent to each other. These findings concur with those reported in the *rx3* mutant, *chokh*. Previous study analysing the neuronal genetic enhancers of the pomc gene interestingly shows two different enhancers, each driving the transcription of pomc gene in the arcuate nucleus and the pituitary (adenohypophysis) of the mouse.[76] A similar situation might be operating in the zebrafish and this may just help explain the specific regulation of *rx3* on the Pomc neurons found in the arcuate nucleus and not the adenohypophysis. However no report thus far provides any information on the mechanism by which *rx3* may specify *pomc* expressing cells at the arcuate nucleus. I had set out to examine whether there might be a clear cell-autonomous link between *rx3* and *pomc* positive cells. Instead, my results suggest a complex mode of action of *rx3*. First, I find that *rx3* and *pomc* are not co-expressed: *rx3* is restricted to cells of the ADH and 3rd ventricle, whereas *pomc* positive cells are in the arcuate nucleus and do not appear to overlap with these territories. Second, I find that *rx3* is temporally expressed in two distinct domains, the ADH and the 3rd ventricle, either or both of which could affect differentiation of *pomc* positive cells. Third, I find that loss of *rx3* function leads to profound changes in *shh* and Shh signalling elements (i.e. *ptc1/2*) in and around the ADH, as well as affecting cell proliferation in the 3rd ventricle. These findings suggest that a reduction in *rx3* could elicit changes in patterning, proliferation and specification of the

hypothalamus, including *pomc* positive cells. In result chapter 3, I perform additional experiments to test the hypothesis that Shh signalling governs the differentiation *pomc* positive cells.

2.3.2 *rx3* governs *shh* in the hypothalamus

In this chapter, I show that *shh* expression is downregulated cell-autonomously in the ADH in a non-functional *rx3* environment (i.e. the *rx3* morphant embryos). This observation hints strongly towards the requirement of *rx3* for the normal expression of *shh* in the ADH. In addition, the loss of *rx3* function leads to a loss of *shh* in adjacent regions that do not normally express *rx3* as observed in the basal plate and the telencephalon. In other species, Shh homeogenetically induces Shh. This has been observed both in the posterior floor plate[77] and in the telencephalon, where Shh expression is induced by Shh from the ADH[12]. Thus, the most likely explanation for the loss of *shh* in the basal plate and the telencephalon of the *rx3* mophant is a secondary consequence of the loss of *shh* in the ADH.

Shh is known to induce expression of its own receptor, Ptc1 (Patched1/ptch1)[78]. Thus, the loss of *shh* expression in the ADH of the *rx3* morphants led me to hypothesize that I might detect a loss of its downstream signalling; on the contrary I saw an increase in both *ptc1* and *ptc2* expression. Similarly, although I detected a decrease in *shh* expression in the ADH and basal plate, I detected an increase in *shh* in the 3rd ventricle of *rx3* morphants. The increase in *shh* is concomitant with the increase in the number of proliferating neural progenitor cells labelled by phos-H3, suggesting that there may be more Shh positive proliferating progenitors in the 3rd ventricle of *rx3* morphants. The observation that Shh expression persists in the 3rd ventricle of *rx3* morphants eliminates the possibility that *shh* expression in the 3rd ventricle is induced by its expression in the ADH.

The Fgf signalling pathway appears unperturbed in the hypothalamus of the *rx3* morphant: *fgf3* and *fgf8* and the downstream effector, *pea3*, show similar expression profiles between the morphant and control embryos, although expression levels of *pea3* are diminished in the telencephalon and epiphysis of *rx3* morphant embryos (Figure 2.7 E,F). Neither *fgf3* nor *fgf8* are expressed in these

regions, but possibly, *rx3* could govern the Fgf pathway, or a different *fgf*. Since *rx3* is not expressed in the epiphysis, the loss of *pea3* in this region is most likely due to a loss of a secondary inductive signalling cascade feeding into these regions. The possible link between the loss of Fgf signalling in the telencephalon and the loss of *shh* expression in the telencephalon (which is secondarily induced by Shh from the ADH) is certainly worth investigating.

2.3.3 Patterning defects in the forebrain of *rx3* morphants

rx3 morphants show ectopic expression of *pax6* and *isl1*, markers which are normally expressed in the dorsal hypothalamus, telencephalon and optic vesicle (Figure 2.7)[79, 80]. Through a previous study in the *chokh* mutant, we know that the telencephalon and optic vesicle share a common pool of progenitor cells and that, in the mutant, cells destined for the optic vesicles acquire telencephalic identities instead[29]. The expanded dorsal tissue in Figure 2.7 could therefore be mis-specified telencephalic tissue, which in turn would suggest that *rx3* normally functions in hypothalamic specification. Alternatively, the increase in *pax6* expression in the *rx3* morphant embryos might be a consequence of the loss of *shh* expression in the ventral telencephalon as described. In the neural tube, Shh from the floor plate acts to specify different neuronal fates along the ventro-dorsal axis in a concentration-dependent manner, and inhibits Pax6 expression. Conversely, Pax6 contributes to distinct ventral progenitor cell populations by functioning cell-autonomously to oppose Shh signalling along the gradient[6, 81]. These mechanisms may operate additionally in anterior regions of the neural tube, including the hypothalamus. An intriguing question that needs to be addressed is whether the telencephalon and anterior hypothalamus share the same set of early progenitor cells originating from a common domain in the anterior neural plate.

In summary, my findings demonstrate that *rx3* loss of function results in the loss of *shh* expression in the ADH, but not in the 3rd ventricle as well as the loss of *pomc* positive cells in the arcuate nucleus. A previous study has demonstrated that Shh signalling can act to indirectly induce the expression of Pomc through the Gli activator[82]. This raises the question of why Shh in the 3rd ventricle does not appear to induce *pomc* positive fate. A number of interpretations can be made. First, in

other regions of the CNS, signalling factors operate against the background of competence factors. Early Shh signalling from the ADH could normally be required to establish the correct competence allowing progenitor cells to respond to later Shh signal and acquire *pomc* cell fate. Alternatively, *rx3* itself may provide cell autonomous competence to respond to the late Shh signal, in the process of differentiation to *pomc* cell fate. To begin to examine this, I looked at the loss Shh signalling and study its effects in the next chapter.

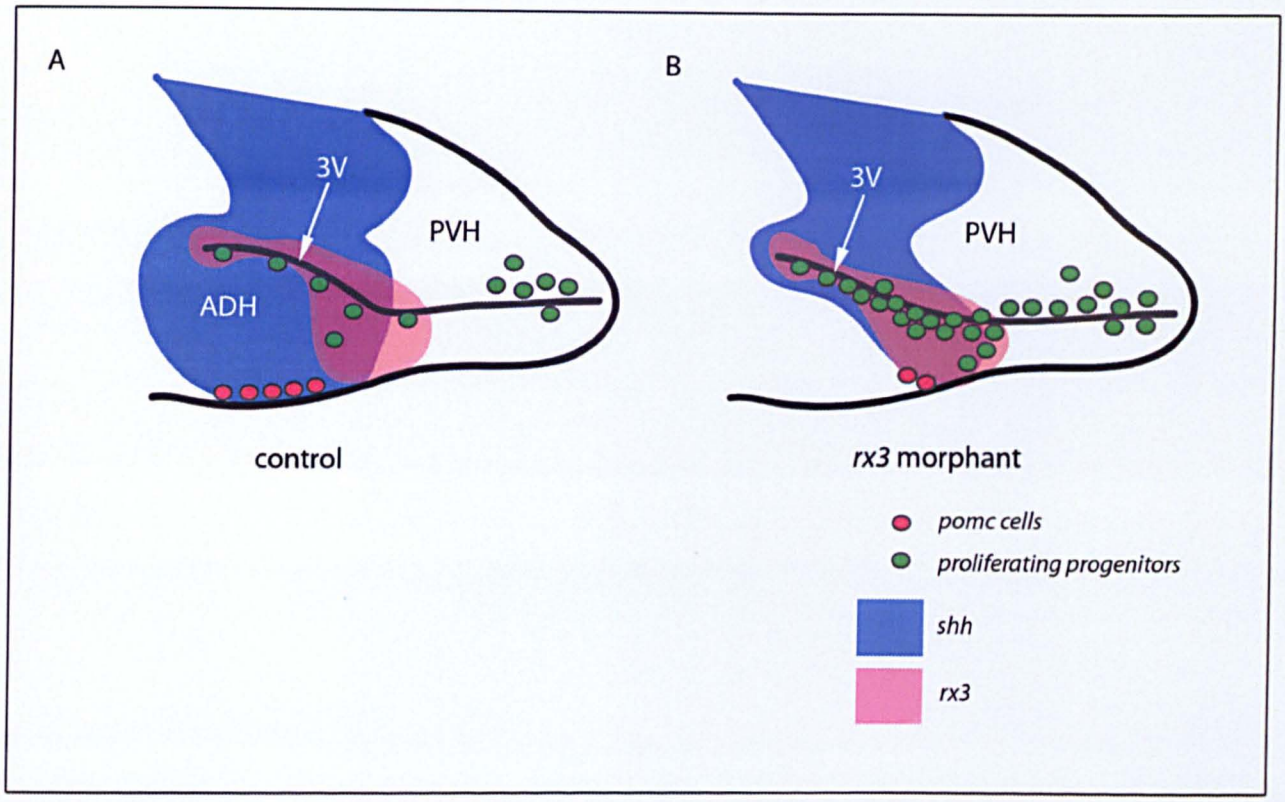

Figure 2.8 : Summary cartoon highlighting the key changes in the *rx3* morphant embryo compared to control embryo at the 55 hpf stage. Loss of *shh* expression in the ADH suggests a loss of this region in the *rx3* morphant. A reduced number of pomc positive cells and increase in proliferating progenitors can be seen in the *rx3* morphant embryo as well.

Chapter 3

Chapter 3: Shh is required for establishment of the ADH and the formation of *pomc* expressing cells

3.1 Introduction

In the preceding chapters, my data demonstrates that *rx3* expression overlaps with that of *shh* in the ADH and the 3rd ventricle and describe that loss of function of *rx3* in morphant embryos results in the loss of *shh* positive cells or downregulation of *shh* in the ADH. At the same time, *pomc* positive cells fail to differentiate in the arcuate nucleus, antero-ventral to the ADH. I therefore set out, in this chapter, to test whether there might be a direct effect of Shh on the specification of ADH cells, and *pomc* positive cells. *shh* continues to be expressed in the ADH, albeit weakly, at least until 100 hpf of zebrafish embryonic development, while *ptc1*is similarly detected in the ADH and forming arcuate nucleus at 30 hpf, supporting an early role for Shh.

Studying the role of Shh in the zebrafish embryo would normally require using established hypermorphic mutant lines in which *shh* signalling is abberant and non-functional. These mutants include *slow-muscle-omitted (smu)*[83], *you-too (yot)*[84] and *sonic-you (syu)*[85]. However, as Shh is integral for induction and patterning of the ventral neural tube, including the prospective hypothalamus, these mutants exhibit severe morphological defects in the diencephalic floor plate and as a result, a malformed ventral diencephalon and the hypothalamus. The embryonic brain of these mutants fails to divide into two lobes and fused optic vesicles can usually be observed, resulting in the cyclops (fused eyes) phenotype. This essentially precludes their analysis for the study of the ADH, or for later-forming cells, such as *pomc* positive cells. At the time of writing this thesis, efforts have been made (including here in the University of Sheffield) to produce mutant lines that would allow conditional-attenuation of Shh signalling in the zebrafish embryo but no report has been made on its progress and viability. An optional and popular way to achieve a similar outcome is to employ the use of a chemical attenuator of Shh signalling, for instance cyclopamine.

The chemical cyclopamine [IUPAC name: (3β, 23*R*)- 17, 23- epoxyveratraman- 3-ol] is a naturally-occurring teratogen found in the corn lily (*Veratrum californicum*) and was first identified through an investigation by the U.S. Department of Agriculture into the cause for one-eyed lambs born to sheep that grazed on these wild lilies. It was eventually discovered that cyclopamine acts to antagonise the Hedgehog signalling pathway[86, 87]. It inhibits the pathway via direct binding and inhibiting the function of the Hh signal transducer, Smoothened[88]

3.2 Results

3.2.1 Loss of *shh* signalling affects *rx3* domains

As described, *shh* is expressed in the ADH, and substantially overlaps with expression of *rx*3; moreover, *shh* appears to be regulated by *rx3,* although, as shown in the previous chapter, it is unclear if this regulation is a direct or indirect effect. To investigate if Shh signalling is necessary for development and maintenance of the ADH, I used *rx3* as a marker of the ADH, and examined its expression after exposing embryos to cyclopamine, to effect a temporal inhibition of Shh signalling. As expression of *shh* begins to take shape in the basal plate/ADH from 27-30 hpf, I initially started the inhibition process of the Shh pathway at this stage. Cyclopamine (100 uM) was added directly onto embryos, which were then incubated in cyclopamine-supplemented E3 for 12 hours (see Materials and Methods for more details on the process). The treated embryos (cyc-t embryos) were analysed for *ptc1* expression to test the efficacy of the treatment. As decribed in Figure 3.1, the expression of *ptc1* was markedly downregulated in cyclopamine treated embryos compared to control treated embryos (55 hpf). Only a minimal remnant of *ptc1* expression could be observed around cells of the 3rd ventricle. To determine whether such ptc1 expression could be entirely eliminated, I exposed embryos to cyclopamine at even earlier stages. This appeared to result in the complete elimination of *ptc1* at 30hpf (Figure 3.1C). Together these data confirm and validate the attenuation of Shh signalling through the use of cyclopamine.

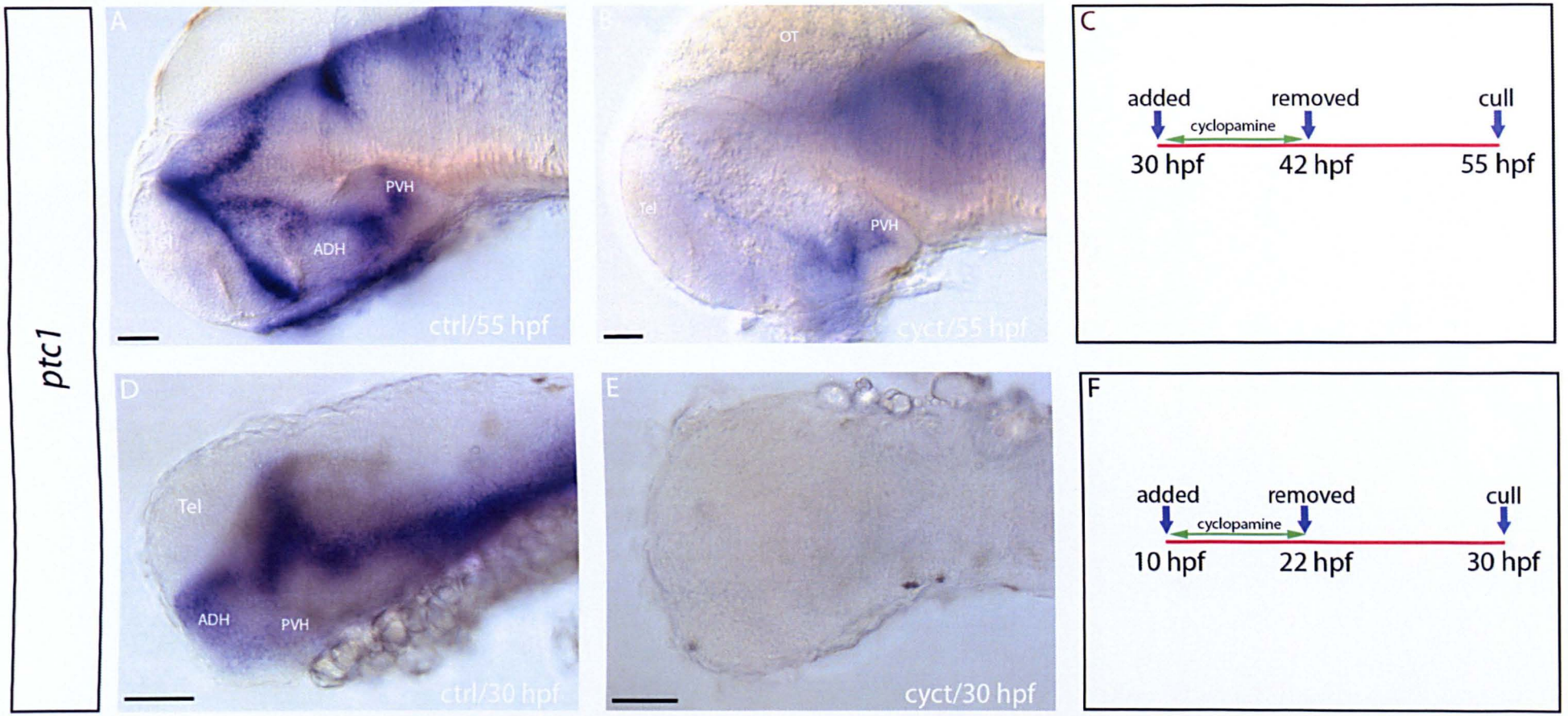

Figure 3.1: Shh signalling is attenuated through the use of cyclopamine, (A,B,D,E) In situ hybridisation analysis of *ptc1* expression in 30 hpf embryos and 55 hpf after treating with cyclopamine following stipulated regimes (C,F) to gauge the loss of Shh signalling. (C) Cyclopamine is added to the embryos at 30 hpf and embryos are fixed at 55 hpf. (F) Cyclopamine is added to the embryos at 10 hpf and embryos are fixed at 30 hpf. (F) All embryos show lateral views. Scale bars represent 50 μm.

To examine if attenuation of Shh signalling would affect the expression of *rx3* in either the ADH or the 3rd ventricle, I examined expression of *rx3* after following both treatment regimes as described above. When the embryos were treated with cyclopamine following the 10 hpf to 30 hpf regime, the expression of *rx3* in the ADH/3rd ventricle was substantially downregulated (Figure 3.2). This indicates that *shh* is required for the expression of *rx3,* either directly, or through an effect on ADH cell specification.

However when early expression of *rx3* was allowed, and Shh signalling only then abolished (i.e. by treating embryos following the 30 hpf to 55 hpf regime), a very different effect was observed. In this case, reduction in Shh signalling appears to result in a marked change in the pattern of expression of *rx3* around the 3rd ventricle. Lateral-views of treated embryos show that *rx3* expression appears to extend more anteriorly than in controls, dipping towards the midline. Ventral views show that normal midline expression for *rx3* is lost (green arrowhead in Figure 3.2C,D). Concomitantly, ventro-lateral expression of *rx3*, which in wild types appears as bilateral diamond-like shapes, appears to be duplicated (compare white arrowheads Figure 3.2C,C' with D,D').

One possible explanation of these two distinct effects is that loss of Shh signalling leads to the loss of anterior hypothalamic tissue, including the ADH, with consequent effects on other tissues, for instance, an expansion of 'posterior-ventral' markers, including the more ventral domain of *rx3* expression. To further test these ideas, I first studied expression of *zic2a*, which is expressed by cells forming the optic chiasm, the crossing of the optic nerves at the junction between the telencephalon and diencephalon (i.e. the DTJ). In cyc-t embryos, the optic chiasm appears not to form in its entirety and only a remnant of this structure can be observed (red arrows in Figure 3.3D). Thus, reduction of Shh signalling may generally cause a loss of anterior-most regions of the hypothalamus. To test whether the reduction in anterior tissue is accompanied by an expansion in posterior hypothalamic tissue, I examined expression of *emx2*, a marker of the PVH. I detected a small but clear upregulation of *emx2* in cyclopamine-treated embryos (Figure 3.2E, F). Together these results suggest that Shh signalling is required at

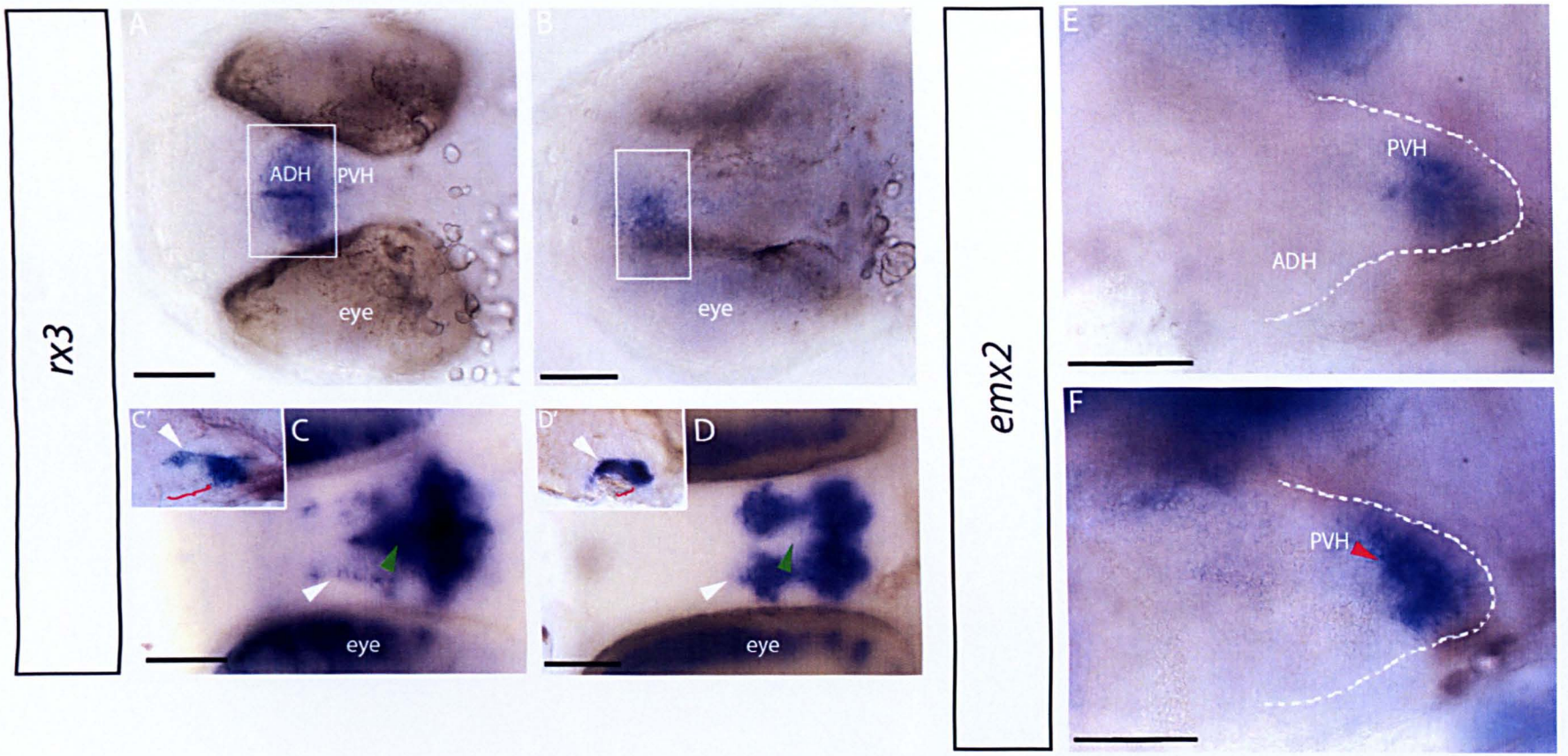

Figure 3.2 : Analysis of *rx3* and *emx2* expression after attenuation of Shh signalling. (A,B) *rx3* expressing domain is at the ADH is greatly reduced when embryos are treated with cyclopamine from 10 hpf. (C,C',D,D') *rx3* expression is markedly changed and forms diamond-like shape dorsally when embryos are treated with cyclopamine from 30 hpf (arrowhead). Lost of *rx3* midline expression is observed in the morphant (green arrowhead). Red bracket in C' and D' marks the anterior expansion of the ventro-medial domain of *rx3* (E,F) *emx2* expression at the PVH (red arrowhead in F) is upregulated in cyclopamine treated embryos (30-55 hpf regime). (A,B,C,D) Ventral view of embryos. (C',D',E,F) Lateral view of embryos. Scale bar represents 50 μm.

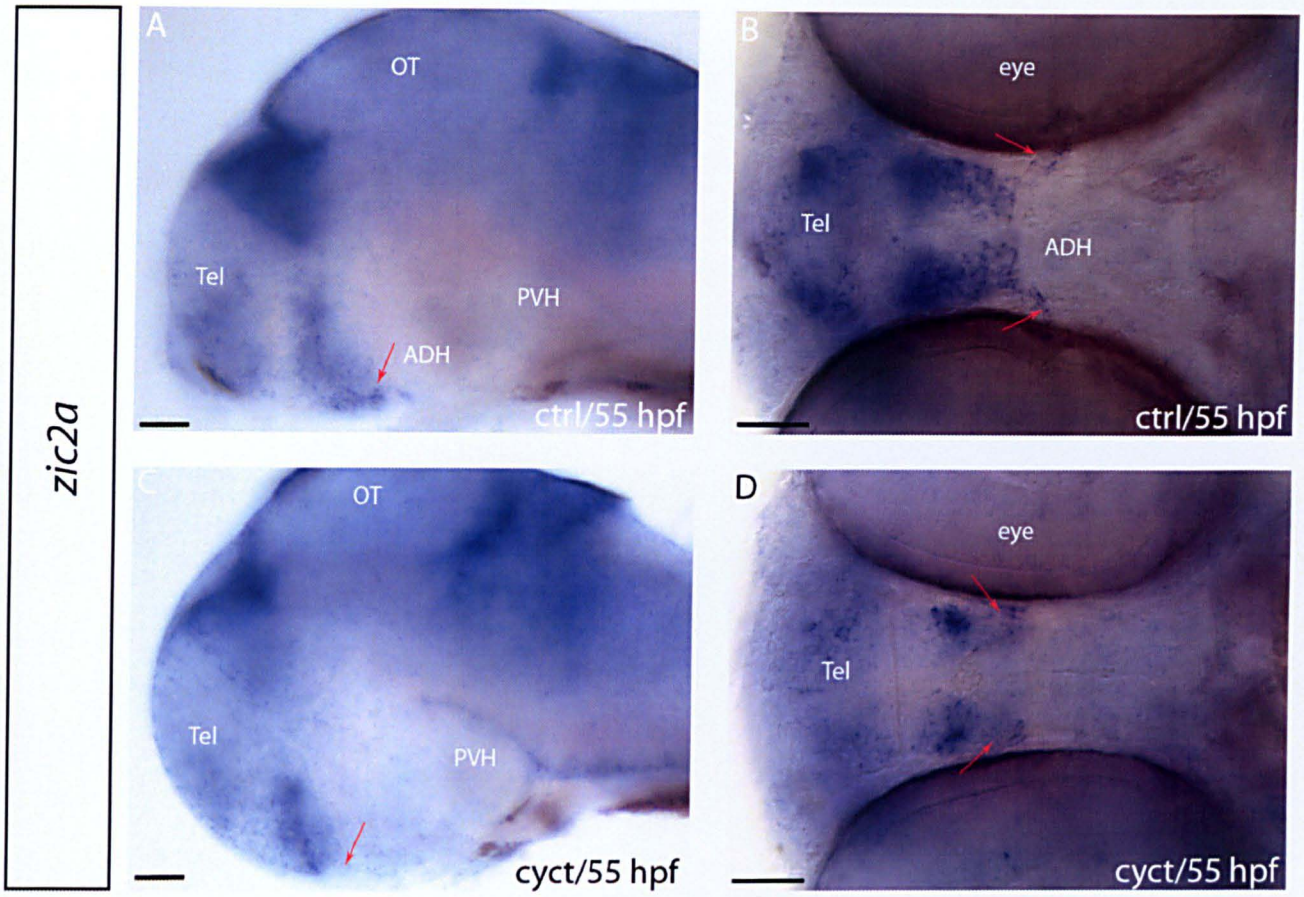

Figure 3.3 : Loss of *zic2a* expression at the optic chiasm of cyclopamine treated embryos. (A,B) Control treated embryos showing the normal formation of the optic chiasm (red arrows), whilst only the remnant *zic2a* expression in the optic chiasm can be seen in cyclopamine treated embryos (red arrows). (A and D) Lateral views. (B and D) Anterior views. Scale bars represent 50 μm.

both early and late time points for proper patterning of the hypothalamus. Early loss of Shh signalling prevents the appearance of anterior territories (i.e. the ADH) Later, maintained Shh signalling appears to be required to maintain anterior territories at the expense of posterior tissue, including regions around the 3rd ventricle.

3.2.2 *shh* regulates the specification of *pomc* cells

I next asked the pertinent question of whether maintained Shh signalling is required for the expression of *pomc* cells in the arcuate nucleus, by exposing 30 hpf embryos to cyclopamine , as described above. The number of *pomc* positive cells was significantly reduced in the arcuate nucleus of cyc-t embryos (arrowheads in Figure 3.4A,B). This implies a role for *shh* in regulating the number of *pomc* positive cells at the arcuate nucleus. Since cyclopamine treatment allows for temporal but not spatial inhibition of *shh* pathway, I tested the expression of tyroxine-hydroxylase (TH), which labels dopaminergic neurons to determine if the reduction of *pomc* positive cells is a specific effect. Some of the *th* positive neurons are found at the posterior *shh* expressing basal plate near the posterior tuberculum[89]. The data obtained (Figure 3.4C,D) show no observable changes in the distribution of *th* positive neurons at this region and no significant changes in the number of *th* positive cells. However a slight decrease in *th* positive cells is detected especially those distributed at the basal plate (arrowhead Figure 3.4D), where *shh* is expressed. The latter serves as positive control to show that *th* positive cells at the basal plate are affected by the inhibition of Shh signalling as well.

3.2.3 *shh*/Shh regulates progenitor cell markers in the hypothalamus

In the previous chapter, I noted that the reduction in *rx3* resulted in an enhanced proliferation (phos-H3 cells) and enhanced *isl1* expression. However, as suggested in chapter 2, these effects could be due to changes in *shh* expression in the ADH as well as the 3rd ventricle, detected in *rx3* morphants. To investigate this, I first examined whether attenuation of *shh* signalling affected neural progenitor cells

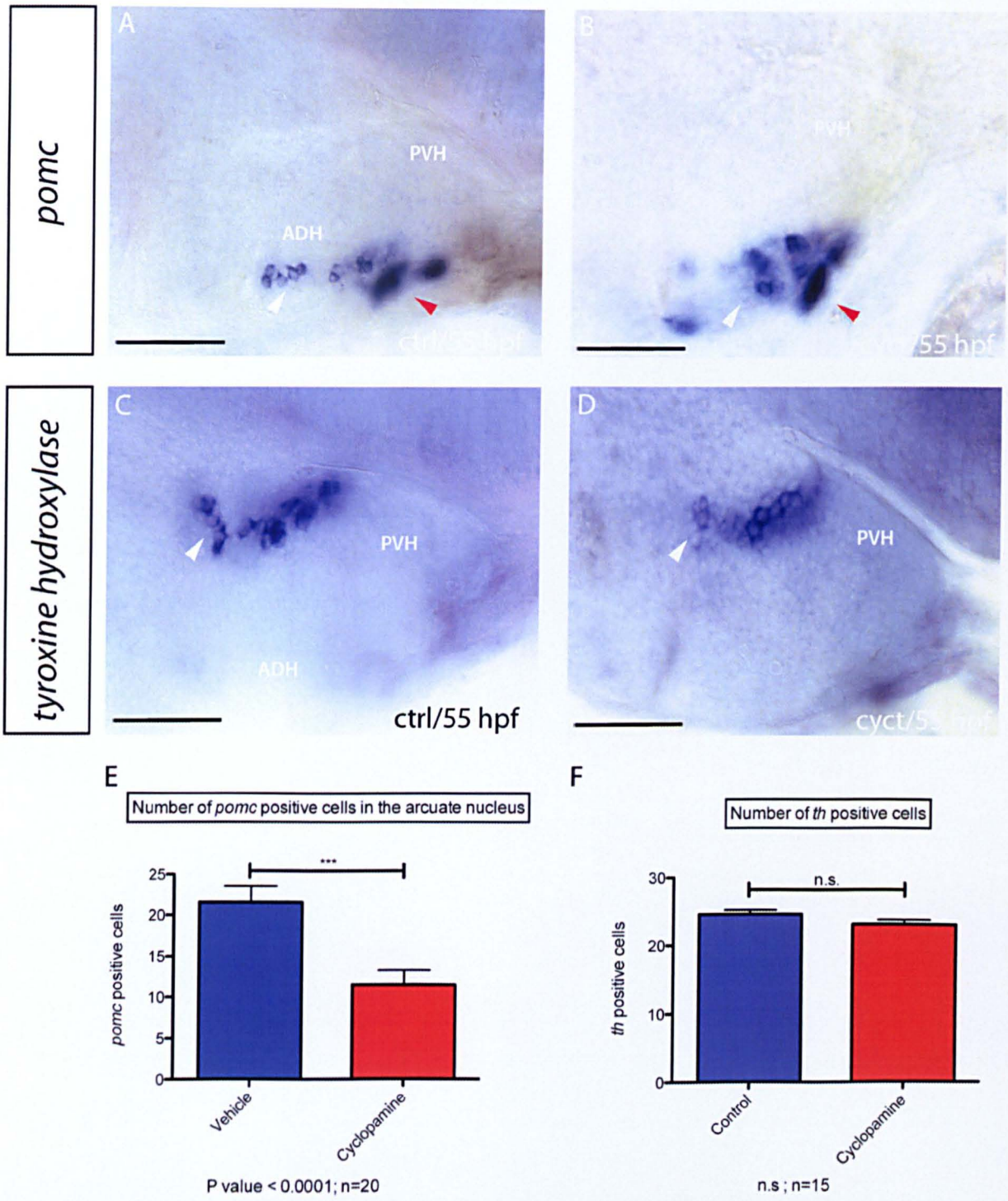

Figure 3.4 : *pomc* positive cells are reduced in the arcuate nucleus through the loss of Shh signalling.(A,B) In situ hybrdization analysis of *pomc* positive cells shows its reduction at the arcuate nucleus (white arrowhead), but not in the hypophysis (red arrowhead). (C,D) analysis of *th* positive cells at the posterior tuberculum shows a slight reduction in the number of cells although not statistically significant. (E,F) graphical representation of the changes in the number of *pomc* and *th* positive cells respectively. All embryos are viewed laterally. Scale bar represents 50 μm.

distributed in and around the ADH and 3rd ventricle. To do so, I examined expression of *sox2* and *sox3*, which are well-established markers for neural progenitor cells. The result interestingly shows increases in labelling of *sox3* but not, *sox2*, suggesting that reduction in *shh* signalling results in an accumulation of neural progenitor cells labelled by *sox3* (Figure 3.5). Close examination reveals that the expression patterns of *sox2* differ from that of *sox3* although they both label neural progenitor cells. In the cyc-t embryos, *sox2* labelled cells do not show much change in expression at the corresponding ADH (cor-ADH) region as well as the PVH (red arrowhead Figure 3.5D) whereas *sox3* labelled cells accumulates at the mid-ventral and PVH region (green and white arrowheads respectively in Figure 3.5B), noticeably at the ventricular region. Only a slight increase in *sox3* expression is observable in the cor-ADH of the cyc-t embryos compared to the control treated embryos (red arrowhead Figure 3.5B). In fact the main upregulation of *sox3* is observed in the more posterior tissues (i.e. the PVH) (Figure 3.5B) and *sox3* being expressed in PVH[90], supports the 'posteriorisation' of the hypothalamus (as proposed in section 3.2.1) at the expense of the ADH resulting from the loss of *shh* signalling.

To further examine this, I investigated if newly born neurons are affected through the loss of *shh* signalling at the cor-ADH region of the cyc-t embryo. I detected these cells through *isl1* ISH, which labels newly born neuronal cells. As shown in Figure 3.5, *isl1* expression is upregulated in the areas surrounding the cor-ADH and ventricle. This data potentially suggest an accumulation of early born neurons that would normally give rise to the neurons in areas surrounding the ADH including *pomc* expressing neurons in the arcuate nucleus. The increase in *isl1* expression is also observable in the ventral hypothalamic region (white arrowhead in Figure 3.5F), which suggest accumulation of early born neurons in the PVH as well. Apart from *isl1*, I have also tested the expression HuC/D through immunohistochemistry, which also labels for early born neurons, to detect if similar observation to isl1 can be made using HuC/D. Unfortunately however, no staining can be detected throughout the embryo most probably due to technical issues with the immunohistochemistry protocol.

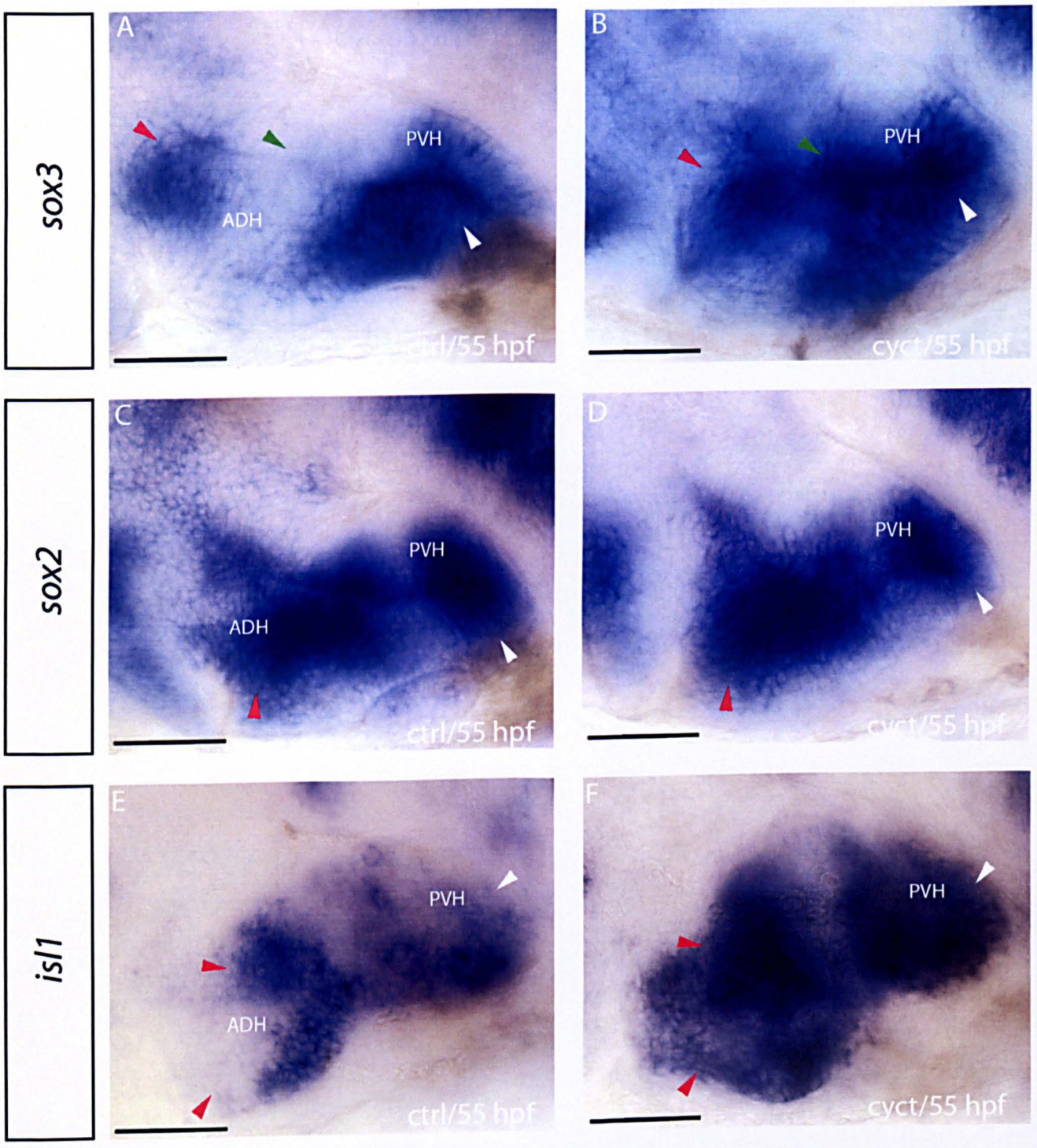

Figure 3.5 : Analysis of neural progenitor cells (*sox2/3*) and early neurons (*isl1*) in the ADH of Shh signalling attenuated embryos. (A,B) *sox3* expression is slightly increased at the corresponding ADH (cor-ADH) (red arrowhead), medial hypothalamic region (green arrowhead) at the PVH (white arrowhead). (C.D) *sox2* expression shows no change in expression (red arrowhead). (E,F) *isl1* expression shows a significant amount of upregulation at the cor-ADH (red arrowheads) and PVH (white arrowheads) as well of cyclopamine treated embryos. All embryos are viewed laterally. Scale bars represent 50 μm.

3.3 Discussion

3.3.1 Role of *shh* in development and establishment of the ADH/3rd ventricle

The function of *shh* expression at the ADH is still poorly understood. It was demonstrated that Shh at the ADH is required for the patterning and eventually the maintenance of Prolactin (PRL)-secreting cells in the adenohypophysis[67]. The ADH also demarcate the border between the prethalamus and hypothalamus of the developing embryo [69, 91]. In result chapter 1 (Figure 1.1), I have demonstrated that *shh* expression is maintained in the ADH at least until 100 hpf in the zebrafish embryos. The data in Figure 1.7, shows the co-localized expression of *shh* and *rx3* at that ADH suggesting that *shh* might play an important role in the development and establishment of the ADH along with *rx3*. Data in the previous chapter shows the regulation of *shh* expression at the ADH by *rx3*; loss of *rx3* function in the ADH led to the diminished *shh* expression in the ADH. As discussed in the same chapter, the result suggests that *rx3* acts upstream in a cell-autonomous fashion to regulate the expression of *shh* in the ADH. Through this chapter, I tested if Shh can act to regulate the expression of *rx3*. Interestingly early blockade of Shh signalling led to a reduced expression of *rx3* in the ADH, but a late blockade show a maintained but mis-patterned expression of *rx3* at the 3rd ventricle. These suggest that Shh and *rx3* exert regulatory effects on each other through a feedback loop during the specification of the ADH. The loop inter-regulation between Shh and transcription factors that patterns the CNS has been documented in the neural tube[7] and my data suggest that a similar mode of regulation between Shh and *rx3* in the ADH. The early role for Shh in the development of the ADH is consistent with a study[13] that reported a reduced ADH domain identified through *rx3* expression in the *smu* mutants analysed at 28 hpf. Interestingly, they also reported an expansion of *emx2* expression suggesting the ventro-posterorisation of the anterior hypothalamic region in the absence of Shh signalling. Interestingly, the latter finding is also consistent with my data that shows an increase in both expression and domain of *emx2* in the PVH. Altogether, *shh* appears to have different temporal roles that together are crucial for the proper development and establishment of the ADH. The reduction in *pomc* positive cells after reduction in Shh signalling could, therefore, be a consequence of the mis-specification of the ADH and its surrounding tissue

including the arcuate nucleus However, I cannot exclude the possibility that Shh (along with *rx3*) plays a role in promoting the differentiation of neural progenitor cells towards the *pomc* cell fate.

3.3.2 *shh* is required for the specification of NPCs to the *pomc* cell fate

Similar to the loss of *rx3* function (Chapter 2), the loss of Shh signalling sees a perturb development of functional cells at the region ventral to the ADH (i.e the arcuate nucleus) through the failure of cells to be specified and differentiate towards the terminal neuronal fates (i.e. *pomc* positive cells). The accumulation of *sox3* positive cells along in regions along the ventricle as shown in Figure 3.5B reflects; i) the posteriorisation of the anterior hypothalamus or the expansion of the PVH region at the expense of the ADH, and ii) failure of neural progenitor cells (NPCs) to be specified to neurons that could include the neurosecretory neurons at regions around the ADH including *pomc* positive cells in the arcuate nucleus. It can be postulated from evidence presented in this chapter that Shh from the ADH might be non-cell autonomously specifying the NPCs to the *pomc* cell fate.

However, the possibility remains that Shh might be negatively regulating the maintenance of the NPC population and not directly involved in the *pomc* cell specification. The blockade of Shh signalling led to the increased in the NPC number reflected by the increase in *sox3* as well as *isl1* expressions.

3.3.3 Loss of anterior hypothalamic domain affects the optic nerve development

Attenuation of *shh* signalling at the latter stage also affected the development of the optic nerve through the loss of the descussating optic chiasm as reflected in the loss of *zic2a* expression (Figure 3.3). This would normally suggests a loss of peripheral vision with the retention of central vision in the affected embryos[92]. This condition is better known as 'tunnel-vision' and it will be exciting to see if the embryos really do develop this condition and if upregulating Shh signalling is sufficient to rescue this phenotype. The optic chiasm can be found antero-dorsal to the hypothalamus and is an evolutionary conserved structure in vertebrates. Closer observation shows that the loss of *zic2a* expression that labels for the optic

chiasm may have been caused by the loss of the anterior hypothalamic region. Therefore, Shh signalling is also required for the maintenance of the anterior domains of the hypothalamus in the forebrain.

In summary, it was demonstrated through this chapter that the inhibition of Shh signalling in the early phase affected the development of the ADH region seen through the drastic reduction of *rx3* expression, but inhibition at a later stage affected the patterning of the ADH and 3rd ventricle as seen through *rx3* expression. As discussed above, these suggest that Shh and *rx3* operate in a feedback loop to mutually regulate/control the expression of each other. More importantly, the inhibition of Shh signalling saw the reduction of *pomc* expressing cells in the arcuate nucleus as hypothesised in the preceding chapter. Concomitantly, an accumulation of progenitor cells labelled by *sox3* and early born neurons by *isl1* was also observed. Together these data suggest that Shh and *rx3* acts to specify and promotes the differentiation of the progenitor cells towards the *pomc* cell fate in the arcuate nucleus.

In the next chapter, I will investigate the interaction between *rx3* and Fgf signalling based on the data reported in result chapter 1.

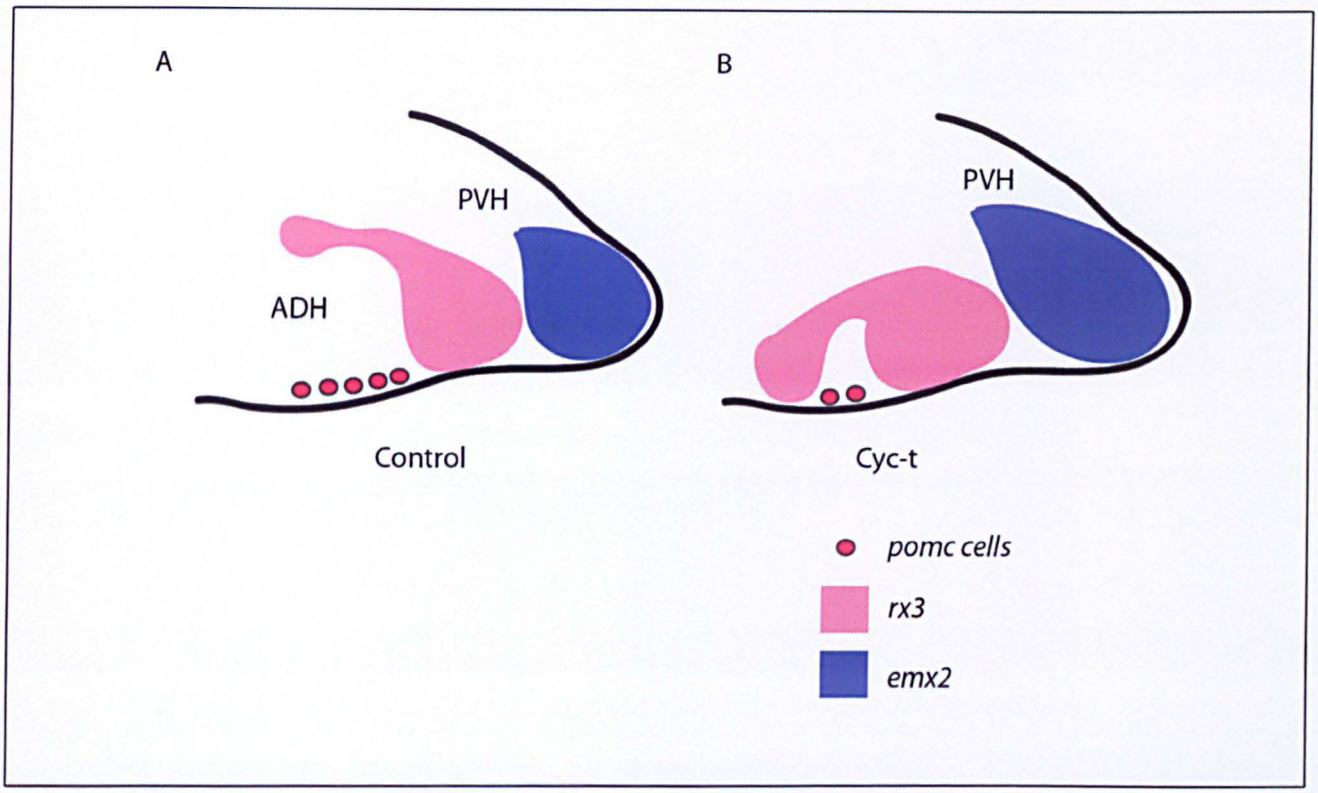

Figure 3.6 : Summary cartoon highlighting the key changes in the cyc-t embryo compared to the control treated embryo. Reduced ADH domain is observed concomitant with the mis-patterned expression of *rx3*. Concomitantly, an expansion of the PVH marker *emx2* is also seen. Similar to the *rx3* morphant, a reduced number of *pomc* positive cells is observed in the cyc-t embryos.

Chapter 4

Chapter 4: Fgf acts upstream of *rx3* to determine the number of *pomc* positive cells

4.1 Introduction

My expression analyses in chapter 1 show expression of *fgf3* in the PVH (Figure 1.4). The ETS-transcription factor *pea3* is also expressed broadly in the PVH, but, additionally, shows a partial overlap with *rx3 in the* ADH (Figure 1.8D). As described in chapter 2, the loss of *rx3* function in *rx3* morphants does not result in the loss of *fgf3* nor *pea3* indicating that *rx3* does not regulate the expression of *fgf3* nor the *fgf* signalling pathway. Thus, the reduction in *rx3*, and its potential effects mediated through reduction in Shh signalling, appears not to affect Fgf signalling. Nonetheless, this does not preclude a role for Fgf signalling in the regulation of *rx3*; Fgf could operate upstream of *rx3*.

Fgfs are key signalling molecules involved in the proliferation and differentiation of an array of tissues. They play a key role in early embryonic patterning and in the later specification of particular organs[93]. For instance, Fgfs govern proliferation of neural progenitor cells in the embyronic neural tube[94], and are key drivers of limb bud development in vertebrates[95], and fin development in zebrafish[96]. In the forebrain, *fgf* signalling has been implicated in the development of the adenohypophysis (the anterior pituitary) through studies performed in the zebrafish embryo[64]. In the hypothalamus however, the role of Fgfs is still very poorly understood compared to their role in the development of the pituitary. In the mouse, Fgf10 has been implicated in the control of hypothalamic neural progenitor cells[66]. However, in zebrafish, Fgf10 is not expressed in the forming hypothalamus as see in result chapter 1.

To begin to examine if Fgf interact with *rx3* in the hypothalamus, I tested whether Fgf signalling governs *rx3* expression and through it, its affect the number of *pomc* positive cells in the arcuate nucleus. To do so I used the chemical SU5402, which is an established Fgf signalling pathway inhibitor, to inhibit Fgf signalling in the zebrafish embryos. SU5402 works by binding to and inhibiting the tyrosine kinase domain of Fgf receptors, thus preventing Fgfs from signalling[97]. Like cyclopamine

(used in the previous chapter) SU5402 allows for the temporal inhibition of Fgf signalling in the zebrafish embryos, which bypasses any potential patterning defects from mutant embryos such as the *lia* or *fgf3* mutant line[98].

4.2 Results

4.2.1 Loss of *fgf* signalling through SU5402 reduces the expression of *rx3* and the number of *pomc* positive cells.

To inhibit the activity of Fgfs in the hypothalamus, I treated zebrafish embryos with SU5402 at stage following the late cyclopamine treatment regime as described in result chapter 3 and analysed them at 55 hpf (refer to Materials and Methods for more details). To analyze the efficacy of the SU5402 treatment, I studied the expression of *pea3* in SU5402 treated embryos (SU embryos), which, as described previously, is commonly used as the molecular read-out for Fgf signalling. My results show a significantly reduced expression of *pea3* after SU5402 treatment (Figure 4.1B).

I next examined whether the reduction in Fgf signalling governs *rx3* expression in the 3rd ventricle where *rx3* is expressed at 55 hpf. In SU-treated embryos I detected much-reduced expression levels of *rx3* in the 3rd ventricle, compared to control-treated embryos (DMSO treated) (Figure 4.1C,D). To examine whether the decrease in *rx3* expression affected *pomc* expressing cells, I performed *pomc* ISH on SU-treated embryos. Consistent with the data reported in chapter 2, suggesting a requirement for *rx3* in differentiation to the *pomc* cell fate, the number of *pomc* positive cells was reduced in the SU embryos (Figure 4.2A,B) in which the expression of *rx3* is reduced and its function is compromised. Similar to that reported in chapters 2 and 3, the inhibition of Fgf signalling pathway affects the *pomc* positive cells in the arcuate nucleus. However inhibiting Fgf signalling also seems to have an effect on the expression of *pomc* positive cells in the adenohypophysis as well.

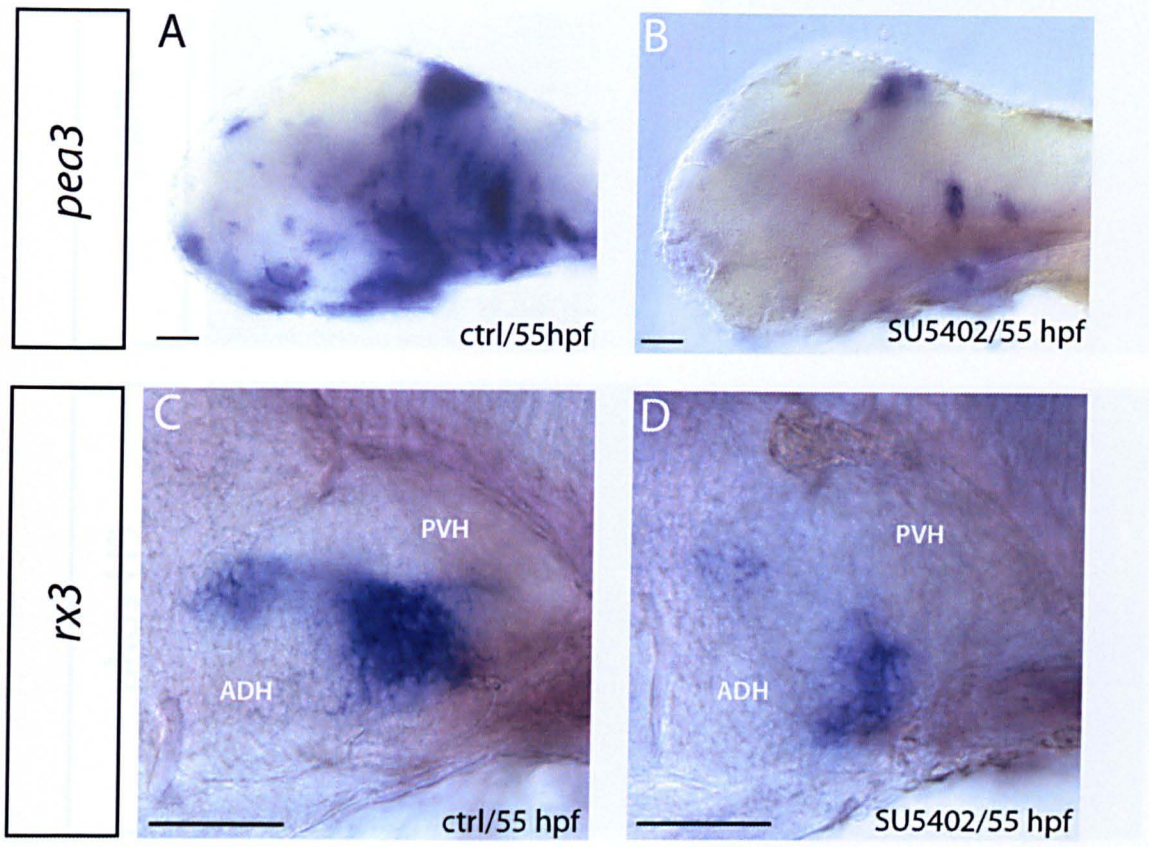

Figure 4.1 : *rx3* expression is reduced in SU5402 treated embryo. (A,B) Levels of *pea3* expression is significantly decreased after SU5402 treatment. (C,D) Expression of *rx3* is reduced in the 3rd ventricle of the SU5402 treated embryo. All embryos are viewed laterally with C,D showing only the hypothalamus. ctrl, control treated embryo. Scale bars represent 50 μm.

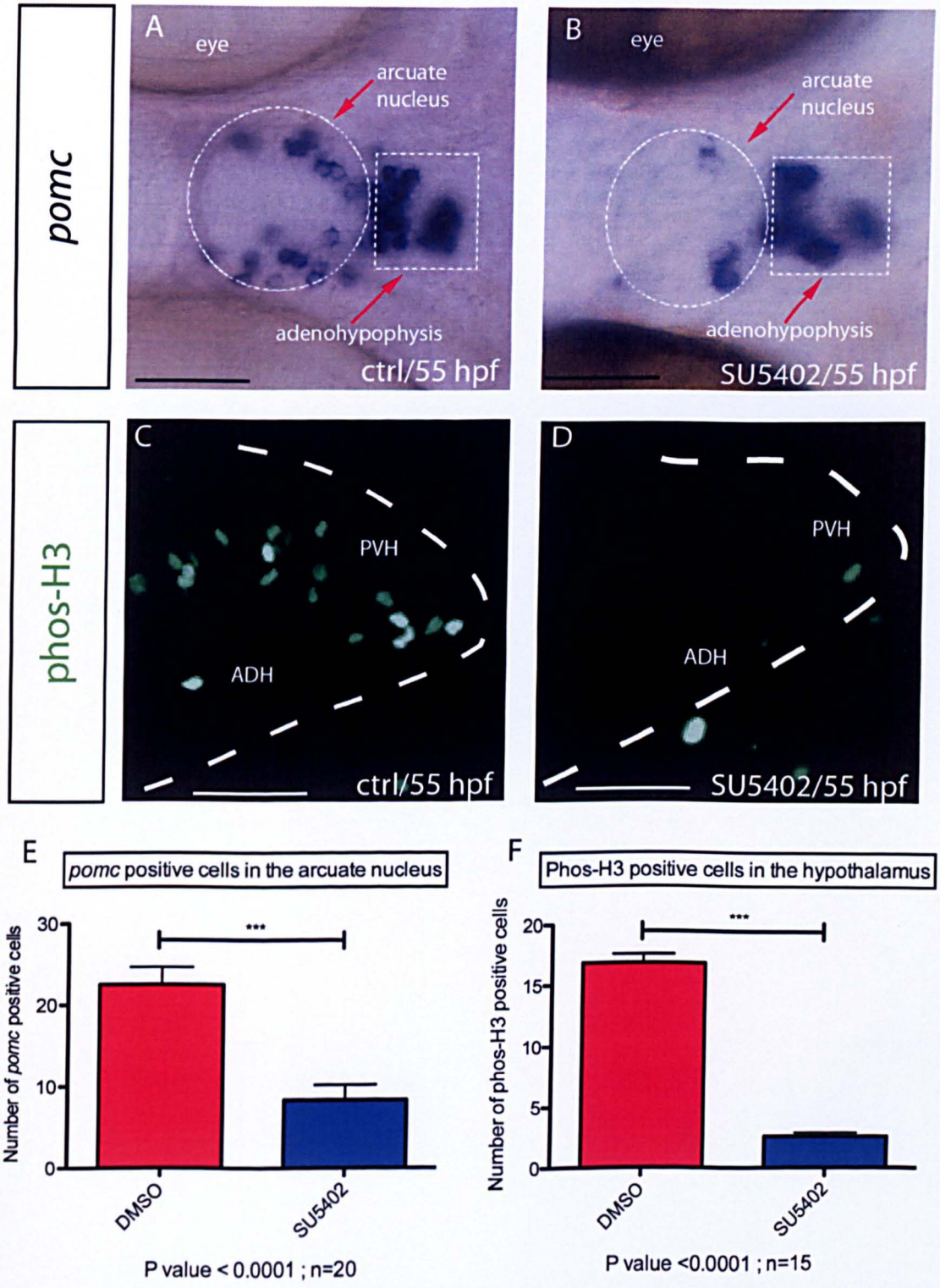

Figure 4.2 : The number of *pomc* and phos-H3 positive cells are reduced in SU5402 treated embryos. (A,B) Anterior view of the hypothalamus showing the reduction of *pomc* positive cells in the arcuate nucleus (white circle). Graph representing the reduction of *pomc* positive cells (E). (C,D) Lateral view of the hypothalamus showing a reduction in proliferating progenitor cells in the hypothalamus (phos-H3 positive) can be seen after SU5402 treatment. (F) Graph representing this reduction. Scale bars represent 50 μm.

4.2.2 Fgfs controls the number of proliferating cells in the hypothalamus

Proliferating cells in the embryonic zebrafish hypothalamus are found distributed along the ventricular region of the 3rd ventricle and are mainly found within the *rx3* expression domain in 55 hpf embryos. Since the expression of *rx3* is reduced when Fgf signalling is inhibited by SU5402, I investigated if this would affect the proliferating cells. To detect these, I used phos-H3 antibody similar to that used in chapter 2. The data obtained show a decrease in the number of phos-H3 labelled cells in the hypothalamus including the 3rd ventricle of SU embryos compared to the control treated embryos (Figure 4.2C,D).

4.2.3 Overexpression of *fgf3*

Temporal inhibition of the Fgf signalling pathway through SU5402 resulted in the decreased expression of *rx3* as well as *pomc* in the arcuate nucleus. The number of proliferating cells labelled by phos-H3 is significantly reduced as well. As described in result chapter 1, the expression of *fgf3* lies in close proximity to the ADH and the arcuate nucleus at 30 hpf. To investigate if Fgf3 can induce the expression of *pomc* cells at the arcuate nucleus given its close proximity of expression, I employed the use of the inducible *fgf3* hypermorphic mutant (kindly shared by Dr. Henry Roehl, CDBG). This mutant carries the hypermorphic *fgf3* gene driven by a heat-shock promoter, which will allow a temporal activation of the *fgf3* gene through incubation of the embryos at 38°C (please see Materials and Methods for more details). This method allows for the increase in Fgf3 to be controlled temporally. To test if the Fgf3 signalling pathway is overactivated as a result of the increase in Fgf3 levels, I analysed the expression of *pea3* and the data shows an increase in the mutant heat-shock embryos (Figure 4.3B). Interestingly, an increased *fgf3* signalling does not show a significant change in the number of *pomc* expressing cells at the arcuate nucleus (Figure 4.3C,D,E). The number of *pomc* positive cells is similar between the SU embryos and the control treated embryos.

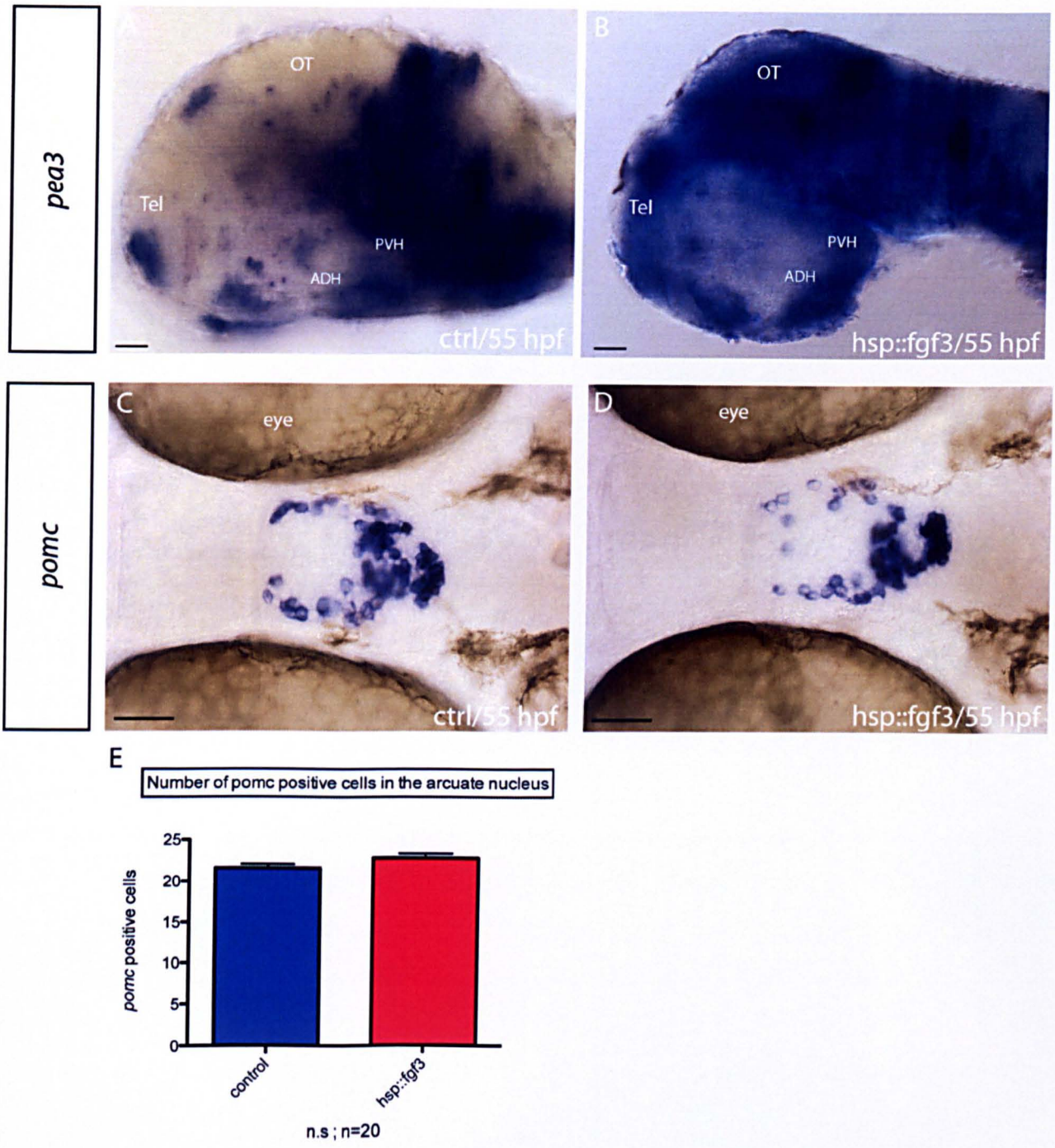

Figure 4.3: No change in the number of *pomc* expressing cells in the arcuate nucleus of the *hsp::fgf3* mutant embryo. (A,B) *pea3* expression level is increased in the *hsp::fgf3* embryo. (C,D) The increase Fgf3 signalling activity did not affect the expression of *pomc*. (E) Graph representation of C,D. Scale bars represent 50 μm.

4.3 Discussion

4.3.1 Fgf maintains *rx3* expression in the hypothalamus

The role of *fgfs* at the hypothalamus is still poorly understood and its role in the specification of the ADH and 3rd ventricle has not been described before. The data provided in this chapter clearly suggest an important function for Fgf signalling in regulating the expression of *rx3* in the hypothalamus. When Fgf signalling is attenuated in the embryos through SU5402 following the described regime, *rx3* expression is downregulated in the 3rd ventricle and the effects of this is seen in the reduced numbers of *pomc* positive cells in the arcuate nucleus. This supports the hypothesis that *rx3* is required for *pomc* positive cells specification as discussed in Chapter 2. It will be interesting to investigate if the reduction of Fgf signalling at an earlier stage (i.e. 10-30 hpf regime with SU5402) would have an effect on *rx3* expression in the ADH to address the question if Fgfs regulates the expression of *rx3* at the ADH. Given the time limitations on completing this thesis, I have tested the above regime once and using the same concentration of SU5402 (i.e. 5 μm) but found that the forebrain embryos were deformed to the extent of preventing further analysis. To address this, a lower concentration of SU5402 might be required to inhibit Fgf signalling without much deformity. The reduction in *rx3* expression suggests that Fgf acts upstream and is required for either the transcriptional initiation of *rx3* or the maintenance of *rx3* expression. However, as the embryos were only treated with SU5402 following the 30-55 hpf regime, the data above more accurately reflects a role of Fgfs in the maintenance of *rx3* expression at the 3rd ventricle.

I have showed through chapter 1 that *fgf3* is expressed in a close proximity to the ADH / 3rd ventricle where *rx3* is expressed and the arcuate nucleus. Although it might be tempting to postulate that Fgf3 is the functional Fgf acting upstream of *rx3*, it cannot be concluded that Fgf3 is the only Fgf responsible for the observed loss of *rx3* expression in the SU-embryos as above. This is based on the fact that there are 25 *fgf* genes in the zebrafish and the possibility remains that there might be other *fgfs* apart from *fgf3* (except *fgf8* and *fgf10*) that might be expressed at, near and influence the expression of *rx3*. It is hence worth investigating if there are

other *fgfs* that are expressed in the or in regions adjacent to the ADH/3rd ventricle that could potentially be regulating the expression of *rx3*. It will also be interesting to see if the overexpression of Fgf3 using the *hsp::fgf3* line have an effect on the levels of *rx3* expression to further substantiate the requirement for Fgf3 in regulating the expression of *rx3* in the hypothalamus.

4.3.2 Fgf controls proliferation of progenitor cells

There are published evidence to suggest a role for Fgfs in promoting the proliferation of neural progenitor cells[99, 100]. Evidence provided in this chapter suggests a similar role for *fgfs* in the control of progenitor cells proliferation in the hypothalamus as well. The disappearance of phos-H3 positive cells throughout the entire hypothalamus suggests that the function of *fgfs* is not domain restricted when control of proliferation is involved. Hence the function of *fgfs* on the proliferation process can be uncoupled from its regulation of *rx3* expression maintenance in the hypothalamus.

4.3.3 Fgfs regulates *pomc* population in the arcuate nucleus as well as in adenohypophysis

As shown in the results, the downregulation of *rx3* expression in the 3rd ventricle of SU embryos affected the number of *pomc* positive cells. The data in Figure 4.2 shows a reduced number of *pomc* positive cells in the SU embryos, corroborating the data and evidences provided in Chapter 2 that highlights the requirement for *rx3* in the specification of *pomc* positive cells in the arcuate nucleus. This observation strongly suggests a requirement of Fgf signalling for *rx3* cell expression, which in turn is required for the specification of *pomc* positive cells in the arcuate nucleus. Intriguingly however, the attenuation of Fgf signalling also affected the *pomc* positive cells in the adenohypophysis of the SU embryos. The *pomc* positive cells appear clustered and reduced in overall number at the adenohypophysis consistent with a previous study in the zebrafish, which demonstrates the reduced population of *pomc* expressing cells at the adenohypophysis of the *fgf3* mutant *lia*, demonstrating the requirement for *fgf3* in establishing *pomc* positive cells at the adenohypophysis[64]. They nevertheless

reported a normal expression of *pomc* in the arcuate nucleus but did not provide any quantitative evidence (i.e. the number of *pomc* positive cells), which may explain their failure to detect the changes in the number *pomc* positive cells at the arcuate nucleus as shown in Figure 4.2. The effect seen in both the *pomc* positive populations in the arcuate nucleus as well as the adenohypophysis in the *lia* mutant supports the argument for a role of Fgf3 in the regulation of *pomc* cells. It also suggests a wider role for Fgf3 in the regulation of *pomc* expression in both the arcuate nucleus and the adenohypophysis that have not been previously described.

Of course the possibility remains that Fgfs in particular Fgf3 may be non-autonomously regulating the *pomc* positive cells independently from its upstream regulation of *rx3*. To address this question, a rescue experiment is required whereby *rx3* mRNA can be injected into one-cell stage *lia* mutant embryos to see if the number of *pomc* positive cells in the arcuate nucleus (apart from the adenohypohysis) can be rescued to their normal levels.

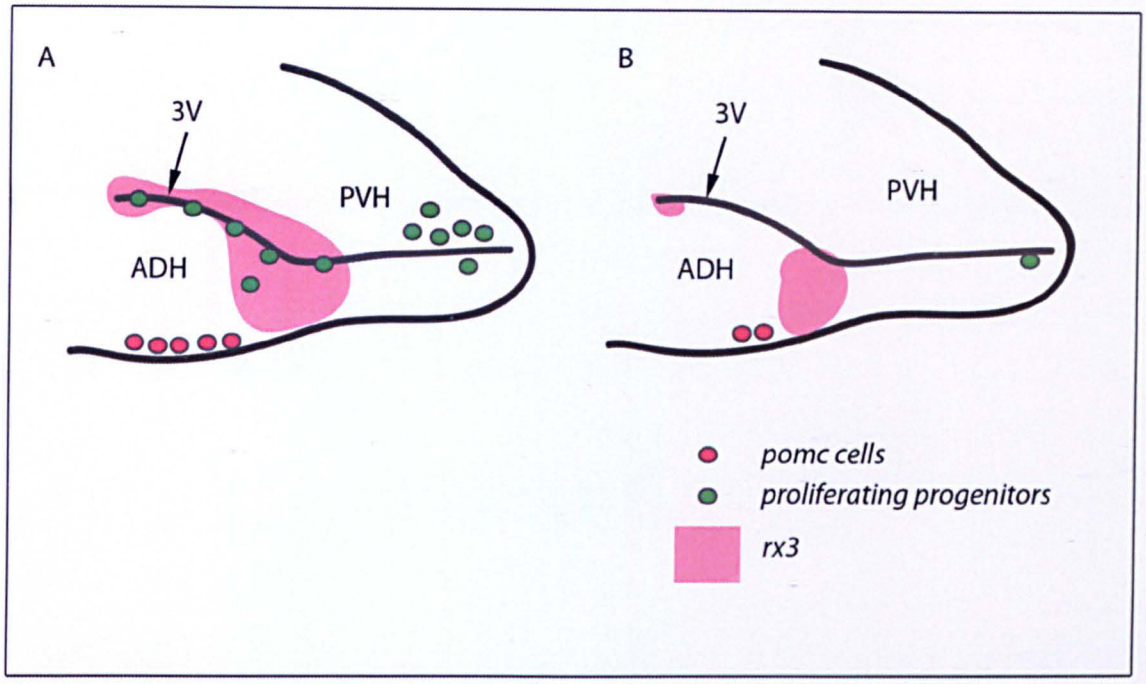

Figure 4.4 : Summary cartoon describing the key differences in SU5402 treated embryo compared to the control embryo. Expression of *rx3* is significantly reduced. Loss of pomc cells and proliferating progenitor cells is also observed in the SU5402 treated embryo.

Chapter 5

Chapter 5: Maintenance of *shh* and *fgf* expression in the adult hypothalamus and role in regulating neural stem/progenitor cells

5.1 Introduction

In the previous chapters, I have shown the expression of *shh* and *fgfs* in the embryonic hypothalamus and demonstrated that they play a role in the development/patterning of the anterior dorsal hypothalamus and differentiation of cells in the arcuate nucleus. I next wished to study if these signalling molecules continue to be expressed in the hypothalamus of the adult zebrafish and whether they may play roles in the adult. In this final results chapter, I analysed the expression profiles of *shh* and *fgf3* in the adult medial hypothalamic region, where a recently-characterised population of neural stem/progenitor cells are believed to reside in other species[50]. I wished to determine, first and foremost, whether I could identify this niche in the medial hypothalamic region of the adult zebrafish hypothalamus and second, to assess whether there might be a role for Shh and Fgfs in the behaviour of cells within the niche. Since there are no established markers that allow for the distinction of neural stem cells from neural progenitor cells in the zebrafish, this analysis did not attempt to distinguish between them, and throughout, I will use the abbreviation NPCs to represent both cell types.

In the mouse and the rat, NSCs and NPCs are restricted to the medial hypothalamic region, in a region lying just dorsal to the median eminence, a region that forms the boundary between the hypothalamus and the anterior pituitary. The zebrafish adult hypothalamus shows marked differences to the adult mammalian hypothalamus. First, as described in section 1.3.2, the median eminence does not exist in the adult zebrafish. Second, two lobes (superior and inferior) are found in the adult zebrafish hypothalamus, and it remains unclear how these relate to defined structures in the hypothalamus of adult mammals (Figure 5.1A). However, I wished to determine whether, despite these differences, a NPC niche does exist in the medial hypothalamus of the adult zebrafish. Given the fact that neurogenesis can occur in the adult fish, I also

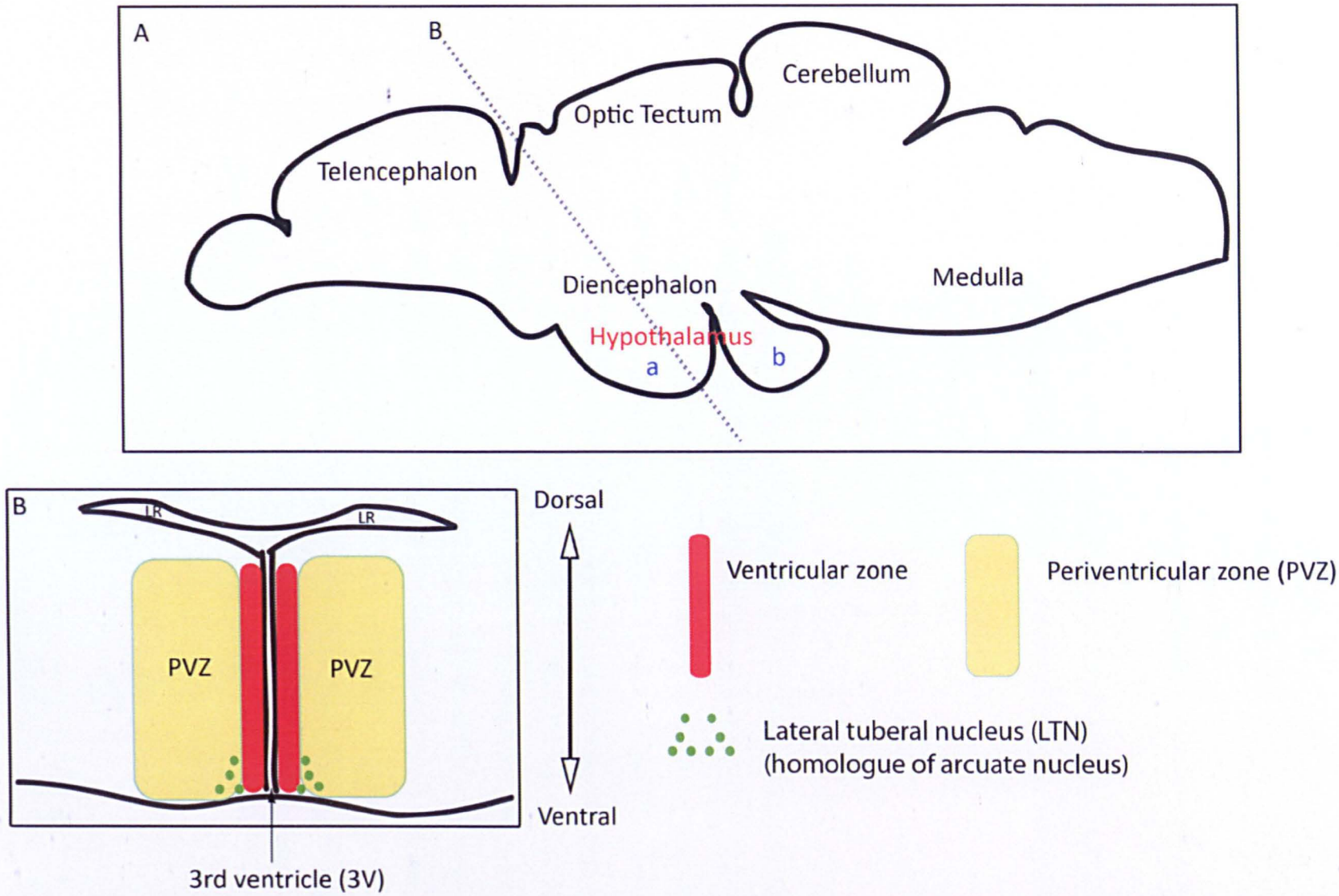

Figure 5.1: Schematic view of the adult zebrafish brain. (A) Lateral view showing the hypothalamus at the ventral diencephalon (a) superior, (b) inferior lobes of the hypothalamus. (B) Anterior view of the medial hypothalamic section obtained through the sectioning plane of the adult brain as shown in A. LR; lateral recesses of the 3rd ventricle

wished to determine whether I could find evidence to suggest the birth of neurons from the neural stem cell niche (i.e. neurogenesis) in this region. I focused in particular on neurons that might give rise to those in the lateral tuberal nucleus (LTN), proposed as the homologue of the mammalian arcuate nucleus[101, 102]. In the zebrafish, the LTN is located at the ventral most region of the medial hypothalamus[101]. This region is the focus of my investigation in this chapter.

In order to analyse the role of Shh in the behaviour of NPCs, I established a novel technique, attenuating Shh signalling in the adult zebrafish using cyclopamine.

5.2 Results

5.2.1 Expression of *shh* and *fgf3*

The medial hypothalamic region in the adult zebrafish can be bilaterally divided into different domains around the 3rd ventricle, the ventricular zone and the periventricular zone; in addition, a dorso-ventral axis can be recognised (Figure 5.1). The identification and recognition of these domains in my data is based on published work describing similar regions in the adult zebrafish brain and hypothalamus[103, 104]. Analysis of *shh* expression in tissue sections (sectioning plane is shown in Figure 5.1A) of the medial hypothalamus of the adult zebrafish shows a highly restricted expression of *shh* in the ventral domain of the ventricular zone (Figure 5.2A). *shh* expression is not detected elsewhere within the medial hypothalamus. By contrast expression of *fgf3* is restricted to the dorsal domain of the ventricular zone, and appears to precisely abut the expression of *shh* (Figure 5.2B). Intriguingly, *fgf3* appears to be expressed asymmetrically, one side showing more *fgf3* expression dorsally (arrowhead Figure 5.2B).

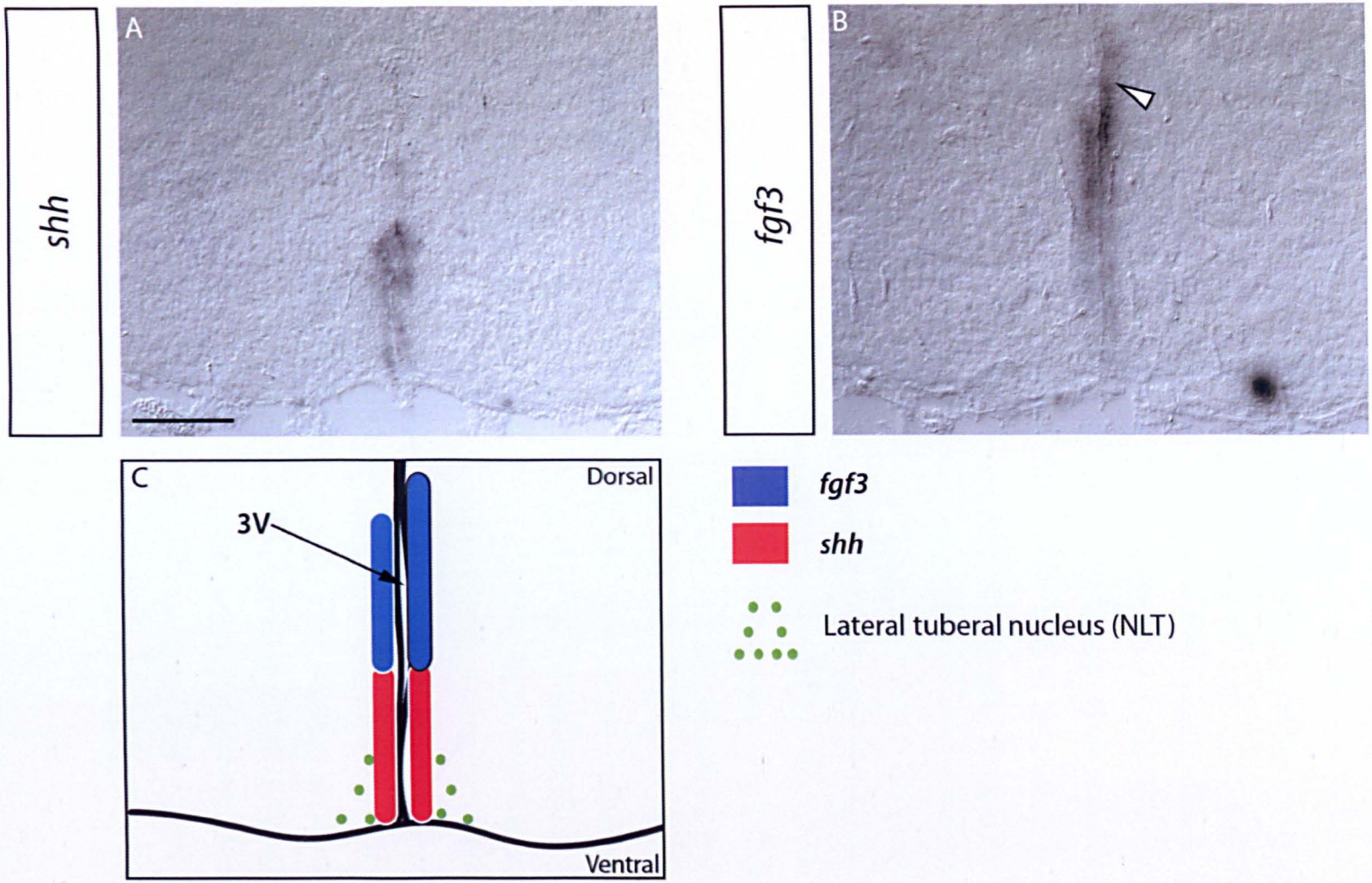

Figure 5.2: Distribution of *shh* and *fgf3* expressions in the adult medial hypothalamic section. (A,B) *shh* is expressed at the ventral regions of the medial hypothalamus and *fgf3* is expressed dorsally to the expression of *shh*. *fgf3* appears to be expressed asymmetrically; its dorsal most tip (arrowhead in B). (C) Cartoon showing the abutting expressions of *shh* and *fgf3* lining the 3rd ventricle (3V) and *shh* expression adjacent to the NLT. (A-C) Dorsal is up, ventral is down ; all sections are viewed anteriorly. Scale bar represent 20 μm.

5.2.2 Identifying NPCs in the medial hypothalamic region

As outlined in this chapter's introduction, the medial hypothalamic region of the mouse has recently been shown to harbour a NSC/ NPC niche in the ventricular zone of the 3rd ventricle[49-51, 105]. To study whether the *shh* or *fgf3* positive regions that I identified in the adult zebrafish may form part of a niche for NPCs, I examined the expression of Nestin in the medial hypothalamic region, through the analysis of GFP in a *nestin* promoter-driven GFP expressing zebrafish[106]. The result shows a very clear and distinct expression of Nestin at the ventricular zone of the medial hypothalamus (Figure 5.3C). Interestingly, Nestin appears to be expressed in a similar region to that of *shh*, i.e. in the ventral region of the medial hypothalamus. A closer observation of the Nestin expression reveals basally-extending projections emanating from the Nestin positive cells at the ventricular zone towards the ventral periventricular region (red arrowheads in Figure 5.3C). Thus, the Nestin positive cells have the appearance of radial glial-like tanycytes, that in the mouse and rat, have been shown to exhibit NSC and NPC characteristics[46, 52]. To investigate if the Nestin positive NPCs in the zebrafish are capable of proliferation, I analysed the expression patterns of MCM5 and BrdU, which label late G1 phase and S-phase of the cell cycle, and hence can identify proliferating NPCs. These analyses reveal that a population of proliferating NPCs labelled by MCM5 and BrdU exist within the Nestin positive and *shh* positive expressing domain (compare Figures 5.2 and 5.4). Some of the proliferating cells are labelled positive for both BrdU and MCM5 (arrowhead Figure 5.4H'). I simultaneously performed an analysis of the distribution of MCM5 and BrdU positive cells along the antero-posterior axis of the zebrafish hypothalamus. This data shows that the vast majority of these cells are found in the medial hypothalamus consistent to what have been described in the mouse and rat. A few BrdU and MCM5 positive cells can be found in the posterior hypothalamus, but none can be found in the anterior hypothalamus (Figure 5.4). (I was not able to able to perform BrdU injections into *nestin*::GFP line as it was still not permitted under Home Office regulations at the time of writing of this thesis.)

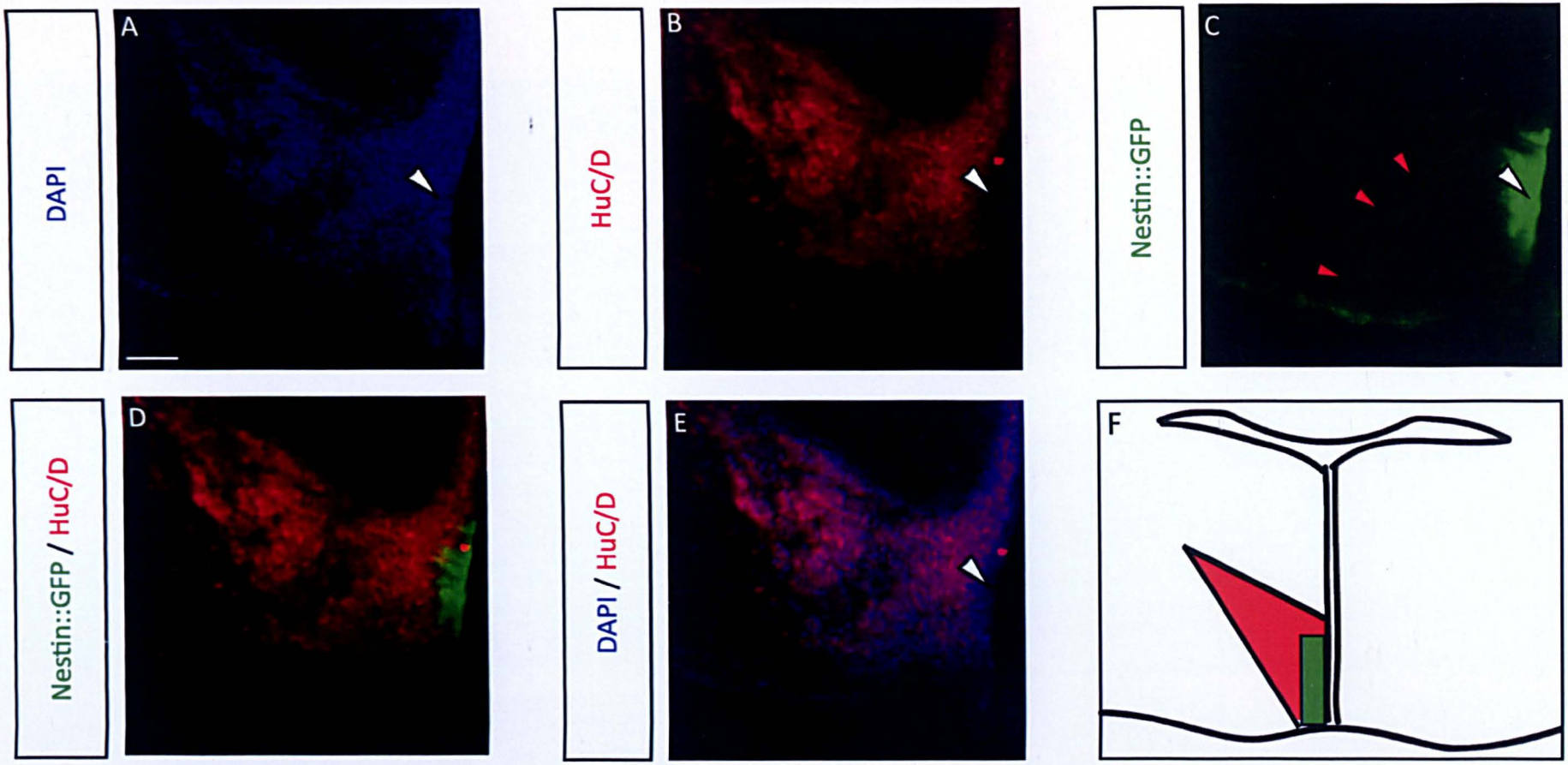

Figure 5.3 : Identification of neural stem cell niche and early born neurons through Nestin::GFP labelling and HuC/D. (A) DAPI labelling of cells showing the ventricular region where Nestin is expressed and not HuC/D (compare white arrowheads in A,B,C and E).(C) Nestin expression indicating the presence of neural stem cells in the ventral region. Projections are seen to emanate from the Nestin positive cells to the periventricular region suggesting a glial identity of these cells (red arrowheads). (D) Early born neurons labelled by HuC/D exist at the periventricular region adjacent to the Nestin positive cells and do not exist at all at the ventricular zone. (E) No HuC/D positive cells can be seen at the ventricular zone where Nestin positive neural stem cells are residing. (A-E) All images are left-side transverse view of the medial hypothalamus as described in F (green box represents Nestin ; red triangle represents HuC/D). Scale bar represent 10 μm.

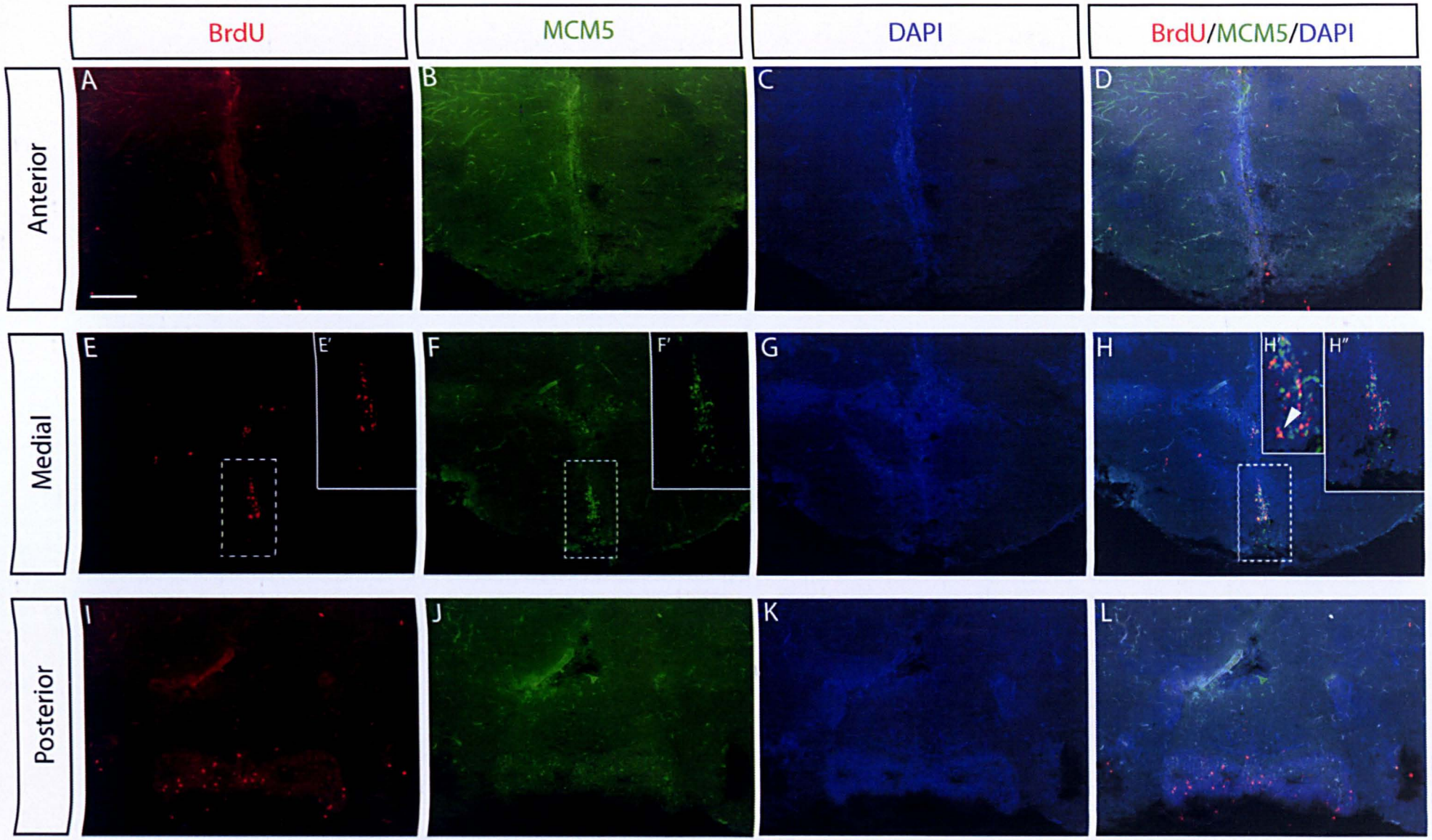

Figure 5.4 : Distribution of proliferating NPCs in the hypothalamus labelled by MCM5 and BrdU. A majority of these cells are found in the medial hypothalamic region (E-H). (I-L) Few proliferating cells can be found at the posterior hypothalamus, but none are found at the anterior hypothalamus (A-D). All images are transverse view of the medial hypothalamus. Scale bar represent 50 μm.

As outlined above, the Nestin positive cells have long basally-extending processes, suggesting they may be tanycytes. To confirm this, I analysed the expression of the tanycytic marker, Vimentin. My data reveals that cells positive for Vimentin are present in the medial hypothalamic region lining the ventral ventricular zone (Figure 5.5C) similar to that shown in the mouse (Figure 5.5J). Comparison of vimentin-labelling with Nestin-GFP suggests that they are expressed in similar domains and might even be expressed by the same cells. Technical difficulties currently prevent double labelling of Vimentin and Nestin-GFP as explained in the Discussion below. Additionally, double labelling of vimentin and MCM5 shows the distribution of proliferating cells within and dorsal to the vimentin expressing domain (Figure 5.5D,D'). Together, these observations show that similar cells are found in the zebrafish to those found in the mouse, and suggest the presence of a NPC niche in the medial hypothalamus of the zebrafish.

5.2.3 Neurogenesis at the medial hypothalamic region

In addition to examining markers that allowed me to identify the NPC niche, I also investigated if the NPCs have the potential to undergo neurogenesis. To do this, I analysed the expression of the protein HuC/D, which is expressed in newly born neurons and immature neurons. I did this by performing double immunolabelling of HuC/D along with, first Nestin, then MCM5. The double labelling of HuC/D and Nestin (through GFP labelling) clearly shows early born neurons (HuC/D positive) at the medial hypothalamus adjacent to but not overlapping with, Nestin positive neural stem cells (Figure 5.3D). Comparison of Figures 5.3 A,B,C and E (white arrowheads), shows DAPI/Nestin positive NPCs in the ventricular zone and shows that these do not express HuC/D. Early born neurons derived from NPCs would eventually lose their capability to proliferate after undergoing neurogenesis. I investigated if this is true for the HuC/D cells observed by performing double labelling with MCM5. The majority of MCM5 positive cells are found close to the VZ, with far fewer in HuC/D positive cells. MCM5 expression in HuC/D cells appears to be restricted to those closest to the VZ, that are most likely to be proliferating progenitors (Figure 5.5G,H,H').

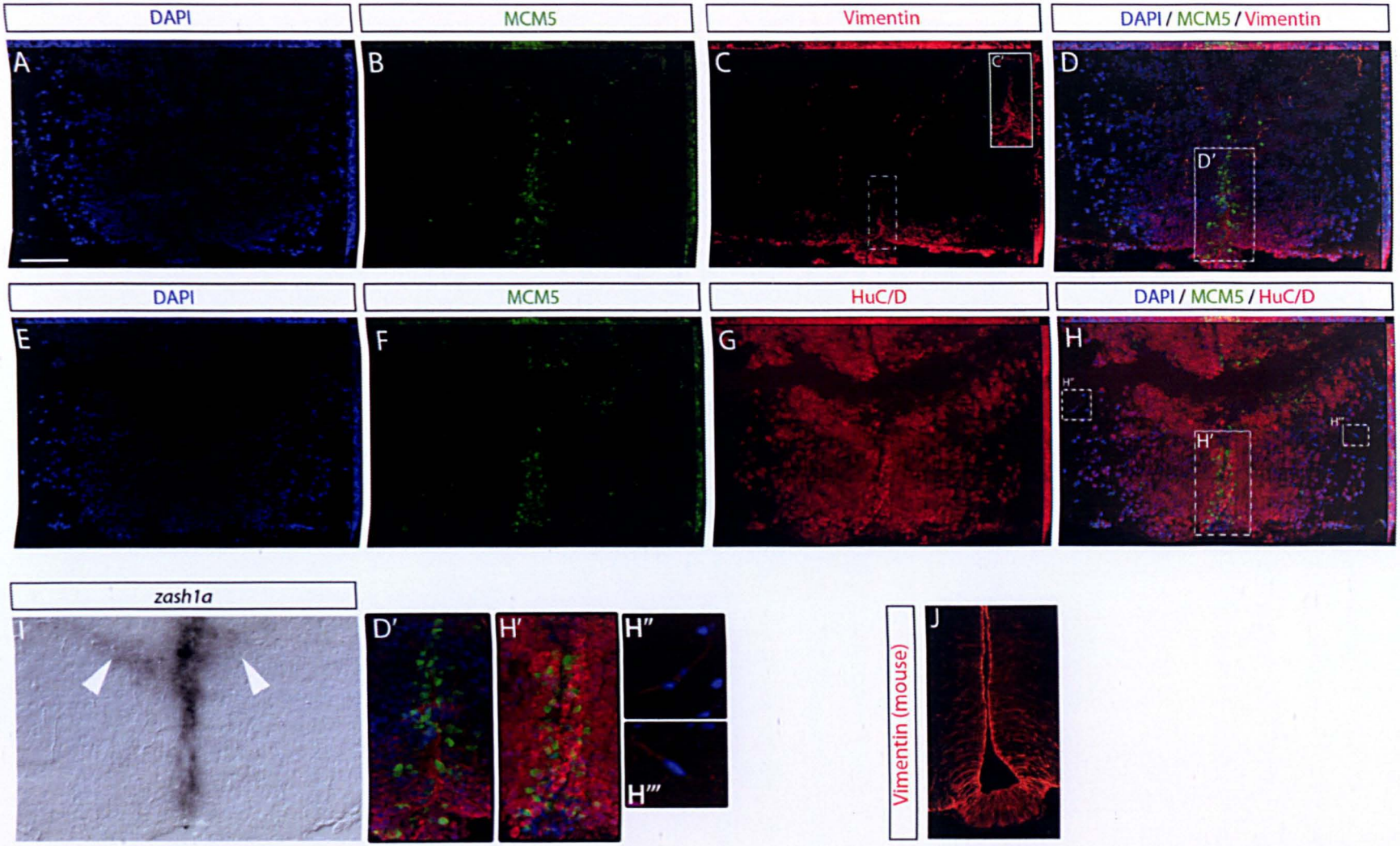

Figure 5.5 : Tanycytic cells can be found in the medial hypothalamic region. (C) These cells are labelled by Vimentin and reside at the ventral most region (boxed); blown up in C'. (D) Distribution of proliferating cells labelled by MCM5 (B) are observed within the same region as the tanycytes (D'). (E-H) Early born neurons labelled by HuC/D do not express the proliferating marker MCM5. The cells located closest to the ventricular zone show highest expression of HuC/D (H') whilst cells farthest away show the weakest expression and resemble fully-developed neurons showing neurite outgrowth (H'',H'''). Scale bar represent 50 μm.

Further away, cells weakest in HuC/D expression are beginning to resemble mature neurons, exhibiting neurite outgrowth (Figure 5.5H",H'").

The molecular marker, *zash1a* labels cells undergoing neurogenesis in the CNS of the zebrafish. To confirm that NPCs might undergo neurogenesis, I performed *zash1a* ISH on the medial hypothalamic section and found that *zash1a* is expressed in cells at the ventricular zone in a 'salt-and-pepper' distribution (Figure 5.5I). Its expression lines the ventricle and appears to be expressed in cells lining the lateral recesses as well (arrowheads Figure 5.5I).

5.2.4 Attenuation of Shh signalling affects proliferation

As described in the previous sections, *shh* is expressed in ventral cells lining the 3rd ventricle, i.e. in the region where NPCs can undergo proliferation and neurogenesis. I therefore wished to examine if *shh* exerts any control on the behaviour of the NPCs at the medial hypothalamic of the adult zebrafish. In the embryonic neural tube and adult neural stem cell niches of the dentate gyrus and subventricular zones, Shh is known to govern cell proliferation. I therefore hypothesised that Shh may govern the proliferation of NPCs in the adult zebrafish medial hypothalamus. To investigate this, I innovated a novel way to attenuate Shh signalling in the adult zebrafish as detailed in the Materials and Methods chapter. I employed the use of cyclopamine in the adult zebrafish through intraperitoneal injection (IP). As outlined in the chapter introduction, the need for this stems from the fact that there are no inducible mutants that would allow for Shh signalling to be genetically attenuated in the adult zebrafish.

To validate if the method worked and if cyclopamine could attenuate Shh signalling in the adult, I analysed expression of *ptc1* in the medial hypothalamus. Excitingly, the result shows a robust and consistent reduction of *ptc1* in the hypothalamus of adult zebrafish treated with cyclopamine compared to controls that were ethanol treated (Figure 5.6) (both n=5). However, this effect might not be specific to the hypothalamus since IP-injected cyclopamine is distributed throughout the zebrafish via the bloodstreams. I proceeded to study if the

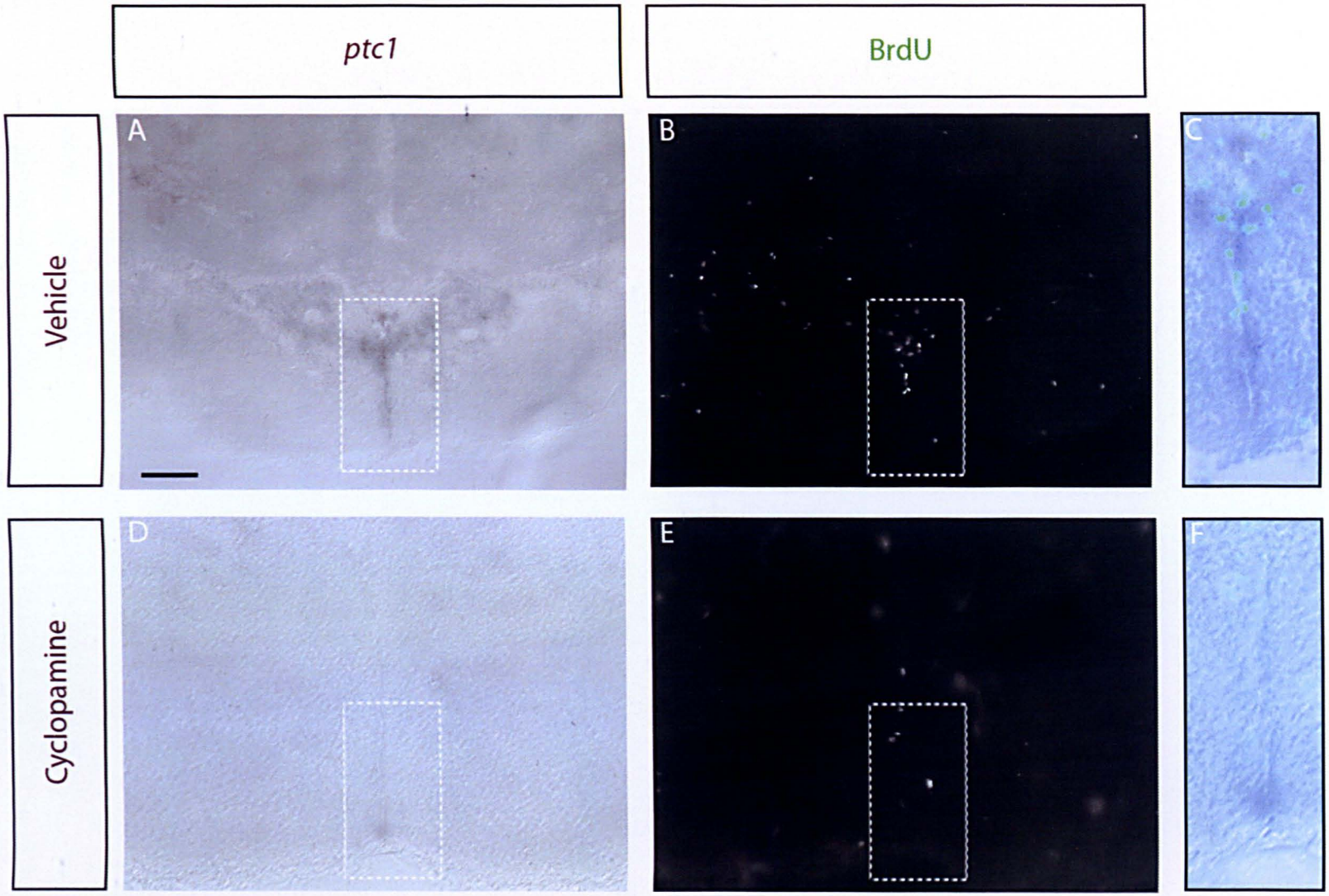

Figure 5.6 : The levels of *ptc1* is significantly decreased in the medial hypothalamus of the cyclopamine injected zebrafish. (A,B,D,E) Double labelling through *ptc1* in situ hybridisation and BrdU immunohistochemistry shows the reduction of BrdU labelled cells concomitant with the reduction in *ptc1* expression levels. (C) Enlarged merged images of A and B. (F) Enlarged merged images of D and E. All sections are transverse view of the medial hypothalamus. Scale bar represent 50 μm.

proliferation of the NPCs is affected by examining markers of G1 and S phase. These results showed that both MCM5 and BrdU showed a significant reduction in the medial hypothalamus of cyclopamine-treated fish (Figure 5.6B,E and Figure 5.7). Statistical analyses reveal a 75% decrease in BrdU+ cells and a 40% decrease in G1-phase cells (Figure 5.6D,H).

5.3 Discussion

5.3.1 NPCs exist in the medial hypothalamus of the adult zebrafish

The data detailed in this chapter show that NPCs exist in the adult zebrafish hypothalamus, and are largely restricted to the medial hypothalamic region. This is the first characterisation of NPCs in the adult zebrafish hypothalamus, although the existence of this niche has been proposed before, along with several other uncharacterized NPC niches in the adult zebrafish brain[47]. Almost all of our knowledge on NPCs in the adult hypothalamus stems from research in the mouse. One of the key issues limiting research on NPCs in the hypothalamus of the adult mouse is the difficulty in detecting cell proliferation *in situ* under endogenous conditions. However, emerging evidence (as outlined in the Introduction) is beginning to show that there are indeed proliferating stem and progenitor cells in the medial hypothalamic region of the adult mouse, but that these proliferate at a low rate compared to the adult zebrafish[52].

In the adult zebrafish, progenitor cell proliferation (i.e. MCM5 and BrdU positive cells) can be detected without difficulty in the medial hypothalamus, as shown in this chapter, suggesting that NPCs in this region do normally proliferate. Clearly, more work needs to be performed in order to fully demonstrate the existence of a NSC-containing niche: to qualify as a neural stem cell niche, one needs to demonstrate the ability of cells to give rise to newly born neurons or glia (i.e. multipotency). The data in Figures 5.3 and 5.5 indicates the ability of the NPCs in the medial hypothalamus to give rise to newly born neurons, labelled by HuC/D. However, a more elaborate demonstration is required before this niche can be fully established as a functional neural stem cell niche in the adult zebrafish

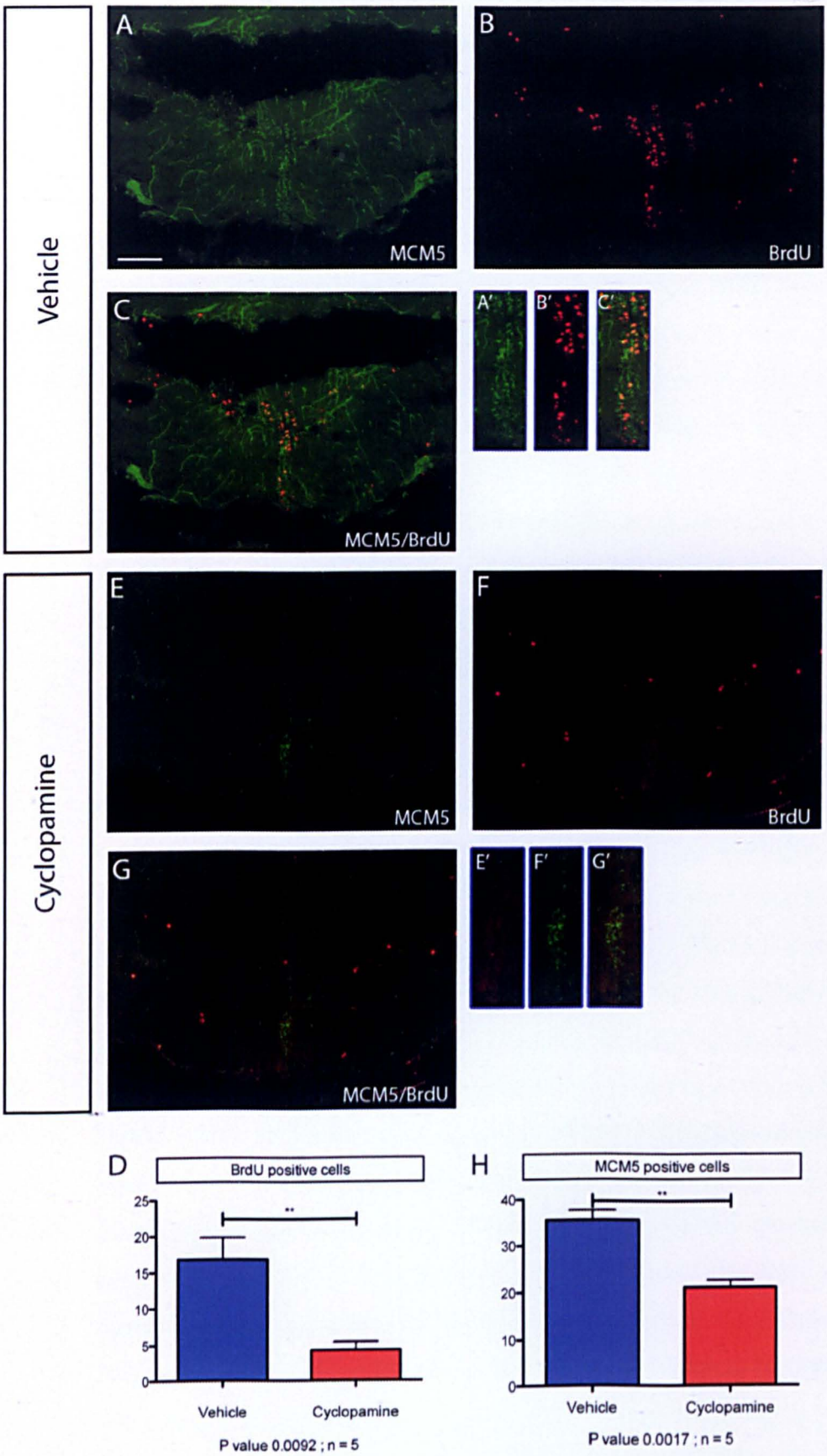

Figure 5.7: Reduction of proliferative cells in cyclopamine injected adult zebrafish. (A-C) Vehicle (ethanol) injected. (E-F) Cyclopamine injected. (D,H) Graph representing the reduction in BrdU and MCM5 labelled cells in Vehicle and Cyclopamine injected zebrafish. Both the reductions are statistically significant. Scale bar represent 50 μm.

brain. This includes demonstrating that NPCs in the niche are multipotent, and can give rise to both newly born glial-cells as well as neurons. Such a demonstration could result from detailed lineage tracing experiments, to trace the NPCs from the multipotent state through differentiation into fully functional neurons or glia. This could be achieved through the genetic labelling of the neural stem cells using a neural stem cell marker gene (i.e. *nestin*) driven by a detectable tag (i.e. GFP or Kaede). Labelled neural stem cells would ideally retain the expressed tag although *nestin* is no longer expressed, throughout the process of differentiation and maturation into functional neurons or glias allowing for the lineage tracing of the neural stem cells to its terminal differentiation. The Nestin-GFP line used in this thesis is not suitable for lineage tracing since it was designed to produce a fusion Nestin-GFP protein product (i.e. in-frame exonic fusion of the GFP into the Nestin ORF[106]) that would degrade when Nestin is no longer expressed and functional in the cells (i.e. early neuronal cells).

The expression of the proneural gene *zash1a* close to the ventricular zone of the medial hypothalamus provides additional evidence that NPCs undergo neurogenesis to differentiate towards neuronal fates. The basic helix-loop-helix (bHLH) transcription factor *zash1a* is the homologue of the achaete-scute gene of *D.melanogaster* that is required for neurogenesis[107] and its expression in the post-embryonic brain has been demonstrated to exist in similar regions to *Mash1* (the homologue gene) in the mouse[108] allowing for direct comparison for the gene expression and function between the zebrafish and the mouse. In the mouse, Mash1 has been shown to promote the differentiation of committed neural progenitors[109] and is required for neurogenesis in the adult rat dentate gyrus after transient forebrain ischemia[110]. *Mash1* is detected in the adult mouse hypothalamus, and a study has shown the role of *Mash1* for neurogenesis and specification of functional neurons in the developing mouse hypothalamus[111]. My evidence for *zash1a* expression in the medial hypothalamus of the adult zebrafish is the first demonstration of hypothalamic expression of this gene in the fish, and suggests a role for *zash1a* gene in neurogenesis in the adult vertebrate hypothalamus. Further investigation to corroborate the above would require a temporal *zash1a* gene knockout that could be achieved through the Cre-Lox inducible system[112].

5.3.2 Tanycytes as the potential neural stem cells in the hypothalamus

A key and fundamental issue in neural stem cell biology is the ability to pinpoint the exact identity of the neural stem cells. In the medial hypothalamus, NPCs or to be more specific neural stem cells are regarded to exist at the cell walls in the ventricular zone lining the 3rd ventricle. The 3rd ventricle, together with an abundant supply of portal capillary vessels in the close vicinity, potentially serve as primary sources of signalling and growth factors that might be required for the neural stem cells to proliferate, self-renew and maintain their niche. Tanycytes are the likely candidates to serve as neural stem cells since they morphologically resemble the radial glia cells, which are the neural stem cells in the embryos and has been demonstrated in the adult rat to display characteristics of neural progenitor cells[46]. Tanycytes are neurosecretory neurons that have basal projections and contact blood vessels in the median eminence, but some of these are believed to retain multipotency and neurogenecity[46]. They are thought to be the mature and functional version of the radial glia cells in the adult brain. I hence investigated if the adult zebrafish hypothalamus harbours any tanycytic cells and showed that there are indeed tanycytes located at the ventral region of the medial hypothalamus. These cells are positive for Vimentin (an intermediate filament protein) and appear to be lining the 3rd ventricle with projections into the periventricular zone probably making contacts with the blood vessels. These features are consistent with the description of tanycytes in the adult mouse and rat hypothalamus albeit the non-existence of the median eminence in the zebrafish. Although my data is the first to show the existence of tanycytes in the adult zebrafish brain, it is definitely not the case for the wider teleosts as the existence of tanycytes has been reported before in the teleost *Clarias batrachus-like*[113]. Suprisingly, the tanycytes were reported to be in the median eminence of the *Clarias batrachus-like* which is atypical of the teleosts.

In the mouse, tanycytic neural stem cells express both Vimentin and Nestin[114, 115]. In fact, Nestin has been shown to be able to interact and form heteropolymers with vimentin[116]. In this chapter, I have shown that Nestin-expressing cells exist in the same domain as the tanycytes (i.e. Vimentin positive cells) in the ventro-medial

hypothalamus. The Nestin positive cells even exhibit tanycytic-like projections towards the ventral periventricular region as well. Although this strongly suggest similar identities between the tanycytes and Nestin positive neural stem cells, it does not conclusively prove that they are the same cells. Demonstrating this would require double immunolabelling of GFP and Vimentin that I have not yet performed. Vimentin detection requires an antigen-retrieval technique, where the tissue sample is first treated with sodium citrate at 95°C prior to labelling. This treatment itself degrades the GFP antigen in the tissue making it extremely difficult to detect Nestin-expressing cells. Nevertheless I am now currently experimenting with different techniques to try and achieve this,

As shown in Figure 5.4, proliferating cells labelled by MCM5 are found interspersed with Vimentin-expressing cells, suggesting the possible derivation of MCM5-positive cells from the tanycytes. It is difficult to observe if the tanycytes themselves are labelled with MCM5 at this resolution since Vimentin do not label the cell nucleus. Nevertheless tanycytes are believed to be quiescent neural stem cells that are not actively proliferating[117], hence eliminating the possibility to detect tanycytic cells that label positive for both MCM5 and Vimentin. It will be interesting however to detect if the tanycytes show the expression of G0 cell phase or growth arrest phase molecular markers like Gas1 (growth arrest-specific 1). Gas1 is expressed in cells that are cell cycle arrested[118]. Interestingly, it has also been demonstrated that Gas1 expression is downregulated when human NPCs are induced to differentiate to astrocytes *in vitro*[119].

5.3.3 *shh* controls the proliferation of NPCs

In this chapter, I have described the expression of the signalling molecule *shh* in the ventro-medial hypothalamus. This expression is seen in the same region where Nestin, Vimentin and the proliferation markers MCM5 and BrdU are expressed, although the latter two markers are positive in cells at the dorso-medial hypothalamus and at the lateral recesses as well. This suggests the likelihood that *shh* might be regulating a NPC population(s) at the ventro-medial hypothalamus. To test this, I attenuated *shh* signalling in the adult zebrafish. As briefly outlined in section 5.2.4, I performed this through intraperitoneal (IP) injection of

cyclopamine into the adult 1-year old zebrafish. IP injection has been widely used to deliver substances such as BrdU into the zebrafish as well as the mouse. In fact, delivery of cyclopamine through IP injection has been performed before in the mouse in a study analysing the effects of cyclopamine on medulloblastoma[120]. However, cyclopamine delivery in the adult fish has never been performed, more so through IP injection. After the initial phase of optimization, the method worked very well and *ptc1* expression was greatly reduced in cyclopamine-injected samples, indicating attenuation of the *shh* signalling pathway. This technique could arguably bypass the requirement for a mutant or compliment results obtained through future mutant studies.

As *shh* has been shown to be a positive regulator of the cell cycle and promote cell proliferation including neural precursor cells[121-123], I tested the markers MCM5 and BrdU. BrdU is an artificial analogue of thymidine. It works by incorporating into newly synthesized DNA strand, substituting for thymidine during cell division in the S-phase of the cell cycle[124] that can be later detected using BrdU specific antibody. MCM5 or mini chromosome maintenance complex is a member of the MCM family of chromatin-binding proteins that is upregulated in cells in the late G1 phase of the cell cycle reflecting the requirement for MCM5 in active cell proliferation[125, 126].

The result shows that both markers are reduced in terms of positive cell numbers in the cyclopamine-injected fish. This indicates that the proliferative capacity of NPCs in the medial hypothalamic region is governed by *shh*. Intriguingly however, BrdU positive cells show a greater percentage of reduction (75% reduction) compared to the MCM5 positive cells (40% reduction). An interesting yet logical speculation to explain this observation is that the NPCs are arrested at the G1 phase of the cell cycle when *shh* signalling is attenuated. It has been described before that *shh* is required for the inhibition of p21, a cyclin-dependent protein kinase (CDK) regulator that directly regulates cell proliferation through the inhibition of DNA replication[127, 128]. Hence, when Shh signalling is attenuated, DNA replication may fail to occur in the NPCs, preventing the incorporation of BrdU. This is consistent with previous findings that show a reduction in BrdU-positive cells when p21 is overexpressed in human cell lines (U2OS cells)[127], and might

explain why BrdU positive cells are reduced in far greater numbers compared to MCM5 positive cells.

Given the limited time to undertake these studies, I have not yet analysed a potential role for *fgf3* in the proliferation of the NPCs. It has been demonstrated that ICV (intracerebroventricular) FGF infusion in the adult mouse results in an increase in BrdU positive cells in tanycytes in the medial hypothalamic region[105]. Moreover, FGFs play a role in the embryonic neural tube in the maintenance for proliferating Sox progenitors[129]. Fgfs also cooperate with Shh to control cell proliferation in the fin-bud of the developing zebrafish[130]. It will therefore be crucial in future studies to assess whether FGFs govern proliferation of the NSCs in the hypothalamus of the adult zebrafish.

Overall Discussion

Overall Discussion

Prior to the work outlined in this thesis, the homeobox transcription factor *rx3/Rax* was mainly studied through its role in eye development. The loss of *rx3/Rax* function leads to the loss of eye phenotype, which is manifested as anophthamia or microphthalmia in humans. Studies on the mechanism underlying these phenotypes have characterised a role for *rx3* in optic vesicle versus telencephalic morphogenesis[29] and a role in the specification of retinal pigment epithelium fate[131]

In this final part of the thesis, I will discuss the overall findings of the first four results chapters and outline possible mechanism(s) to describe the role of *rx3* in embryonic hypothalamic development, through its interaction with the *shh* and *fgf* pathways. I will discuss modes that might explain the findings in this thesis. I will also discuss the importance of studying the maintenance of these signalling molecules in the adult hypothalamus and discuss my findings in the fifth result chapter in the context of the first four. Additionally, I will also highlight experiments that need to be performed to support the existing data as well as future work to extend the findings made in this thesis. Limitations of my work and data will also be discussed along with a brief critique on the suitability of the zebrafish as a model to study hypothalamic development.

rx3 regulates the expression of *shh* in the ADH and vice-versa

In chapter 1, I described the overlapping expression domains of *shh* and *rx3,* first in the ADH and then in the 3rd ventricle. To investigate the regulatory role of *rx3* on *shh*, I analysed the expression of *shh* in *rx3* morphants and found that expression of *shh* is diminished in the ADH. In chapter 3, I showed that inhibition of *shh* signalling resulted in drastically reduced rx3 expression in the ADH during early stage inhibition (Figure 3.2), suggesting that *shh* acts to regulate the expression of *rx3* during the establishment of the ADH. Together the data show a previously undescribed feedback loop between *shh* and *rx3*. Feedback loops between *shh* and downstream transcription factors has been described in the posterior neural tube, studies supporting the idea that HD proteins induced along the D-V axis of the

neural tube in response to Shh, themselves contribute to the Shh output. Thus, early studies showed that Shh induces Foxa1 expression in the floor plate, which in turn enhances Shh expression in the floor plate[132]. More recently, studies show that the Nkx genes, which are induced lateral to Shh-expressing floor plate cells, feed-forward to strengthen Shh signalling[7, 133]. My data reveal that a *shh*-HD transcription factor loop is similarly operating during the early establishment of the ADH, suggesting that such a strengthening mechanism might operate more widely within the CNS, and through HD proteins other than the Nkx genes. In the spinal cord, this mechanism has been suggested to be crucial in converting a Shh gradient into a step-like gradient, leading to sharp thresholds of Shh signalling, each able to specify a distinct response. Future studies, examining expression of other HD proteins that are expressed adjacent to the ADH are required to address whether a similar mechanism operates in the hypothalamus, but my data begin to suggest that it might.

Shh from the ADH patterns the anterior hypothalamus and telencephalon

Numerous past studies have shown that Shh is required for development and patterning of the hypothalamus[68, 69]. However, since Shh is expressed in prechordal mesoderm, in the hypothalamic floor plate, and then in the basal plate, these studies do not address, specifically, whether Shh from the ADH plays any role in the normal specification and maintenance of hypothalamic tissue. Two recent studies in the mouse have begun to address this. The selective deletion of Shh from the basal plate including the ADH reveals that Shh is essential for anterior hypothalamic patterning[69]. This study reported that loss of *shh* in that region resulted in the loss of *Pomc* positive cells in the arcuate nucleus, but a maintained *Rax* expression which draws remarkable similarity to my data produced in result chapter 3 where inhibition of Shh signalling saw a reduced number of *pomc* positive cells in the arcuate nucleus and a maintained *rx3* expression in the 3rd ventricle (Figures 3.2 and 3.4). Similarly, transgenic approaches in the mouse, coupled with in vitro experiments show that neural Shh coordinates anteroposterior and dorsoventral patterning in the hypothalamus and in the diencephalon-telencephalon junction (DTJ)[68]. These experiments reveal also that neural Shh is necessary for the lateral hypothalamus to attain its proper size and is

required for the specification of hypocretin/orexin cells. My studies in the zebrafish support and extend these findings, showing that Shh that derives from the ADH is necessary for the proper patterning of the hypothalamus. Reduction of Shh expression, either mediated indirectly via *rx3* knockdown, or directly through early cyclopamine treatment, led to an expansion of posterior and medial markers into more anterior regions: thus, *sox*, *isl1*, *rx3*, *emx* all extended anteriorly. The expansion of posterior markers was accompanied by a loss of anterior markers, including the ADH itself (as judged through the mis-patterned expression of *rx3*) and the loss of *zic2a*, a marker of the optic chiasm. Intriguingly, the loss of function of *rx3* caused a downregulation of *shh* in the ADH, but not in the 3rd ventricle. Together, these results suggest that Shh in the ADH, but not the 3rd ventricle, govern the anterior patterning of the hypothalamus.

In keeping with results in the mouse[68], my studies show that the loss of *shh* expression in the ADH appears to result in the secondary (non cell-autonomous) loss of Shh in the telencephalon (Figure 2.6). In other species, Shh from the diencephalon appears to induce *Shh* in the telencephalon[12] and my results suggest a similar model in zebrafish. Thus, the loss of *Shh* in the ADH appears to have profound effects on the patterning of both the diencephalon and telencephalon.

Rx3 and Shh govern the specification and differentiation of progenitor cells to *pomc* positive cells in the arcuate nucleus

Studies in the mouse show that a reduction in Shh expression in the hypothalamus leads to the loss of a specific hypothalamic neuron, the hyprocretin/orexin positive neuron. My results similarly reveal that the loss of Shh in the ADH, mediated either through loss function of *rx3* and through direct inhibition of Shh signalling, leads to the reduction of *pomc* expressing cells in the arcuate nucleus. The loss of *pomc* positive cells in the arcuate nucleus leads me to hypothesise that Shh is required for the specification of these cells, and to hypothesise that Shh could operate at a number of levels to govern this specification.

i) *rx3*/Shh may be required for the early patterning of *pomc* progenitors.

First, as outlined above, Shh from the ADH appears to pattern the anterior hypothalamus. This raises the possibility that Shh may establish an early *pomc* progenitor. Although I have not examined expression of *nkx2.1*, this gene is a potential candidate. In both mouse and chick, Nkx2.1 is a known direct target of the Shh signalling pathway[134] and sustained Shh signalling is required for expression of Nkx2.1[12, 135]. Importantly, elegant lineage-tracing experiments in the mouse show that POMC positive cells in the arcuate nucleus arise from Nkx2.1 positive progenitor cells in the hypothalamus[136]. Together, this raises the possibility that Shh governs Nkx2.1 progenitor cells, which in turn, can give rise to *pomc* positive neurons. In keeping with this model is the observation that although *nkx2.1b* expression appears upregulated in the posterior hypothalamus of *chokh* mutants, its expression appears downregulated in cells immediately adjacent to the ADH, including regions likely to harbour arcuate nucleus progenitors[29]. Clearly, further studies are required to test this, and in future, I aim to analyse expression of the *nkx* genes more closely.

ii) *rx3*/Shh may govern progenitor cell behaviour in the 3rd ventricle

A second possibility is that *rx3*/Shh in the 3rd ventricle plays a role in governing the transition of neural progenitor cells to differentiate towards *pomc* positive fates in the arcuate nucleus. In all species, differentiating neurons migrate to lateral/mantle layers of the CNS from stem/progenitor cells in the ventricular zone, and migration of POMC progenitors from the ventricle towards the arcuate nucleus has been described in the mouse[137]. My data are consistent with the possibility that appropriate expression of *rx3* and Shh in progenitor cells in the 3rd ventricle is a prerequisite for normal differentiation of *pomc* positive cells. In the *rx3* morphant embryos, proliferating progenitors increase in the 3rd ventricle, this increase accompanied by elevated levels of *shh* and *rx3* expression. My studies however do not establish the relationship between the proliferating progenitors, the *rx3* positive and the *shh* positive cells. In the mouse, Rax positive progenitors in the hypothalamus are also positive for Nestin and Sox1 (SoxB1) expression suggesting the idea that *rx3* may mark an early 'stem-like' or progenitor cell, and

play a cell-intrinsic role in its behaviour[138]. Similarly, other studies in the mouse show that Shh marks early stem/progenitor cells in the subventricular zone, its activity governing their behaviour[121, 139]. Thus, imbalance of *rx3*, or Shh activity, could lead to an altered behaviour of progenitor cells, leading, for instance, towards elevated levels of self renewal and concomitant decrease in differentiation.

My studies do not preclude other possibilities. For instance, *rx3* may function as a competence factor for progenitor cells to respond to Shh from the 3rd ventricle. In this model, progenitor cells in the 3rd ventricle, destined to assume a *pomc* positive identity, are incompetent to differentiate to the *pomc* cell fate through the loss of *rx3* function, hence their accumulation detected through phos-H3 expressions and their inability to respond to Shh in the 3rd ventricle of the *rx3* morphant.

Alternatively, *rx3* may be cell-autonomously required for the segregation of *pomc*-destined progenitor cells from the rest of the progenitor cell pool in the ventricle. The potential 'cell sorting' function of *rx3* is postulated through a study performed in chimeric mouse that demonstrates cell autonomous role of *rx* in segregating wild type cells from *rx-/-* cells during morphogenesis of the retina/pituitary[31]. Inappropriate segregation might, in turn, lead to an altered capacity to differentiate.

iii) Late effect of ADH-derived Shh on specification of pomc

A third possibility is that ADH-derived Shh drives the late specification and differentiation of progenitor cell to the *pomc* expressing fate, once they have migrated into the arcuate nucleus. In chapter 1, I showed that *ptc1*, a downstream read-out of Shh signalling is detected in the arcuate nucleus, where hypothalamic *pomc* positive cells are found (white arrowhead Figure 1.3B: the arcuate nucleus is located just adjacent to the ADH Figure 2.2). Although there is no evidence that Shh operates directly on the *pomc* gene to enhance its expression, previous work has described an indirect activation of *pomc* expression in the adult pituitary by Shh signalling through the Gli1 transcription factor[82]. This raises the possibility that Shh may operate at late phases of *pomc* cell specification.

Together, then, my results could suggest that *rx3*/Shh play a role in establishing either *pomc* progenitor cells, or *pomc* expression itself. Of course, these possibilities are not mutually exclusive. It is possible that *pomc* progenitors first express *rx3* to be Shh competent, begin to express *nkx2.1* upon activation by shh in the ADH/3rd ventricle, and then require Shh again at a late phase for *pomc* expression. In order to begin to distinguish these possibilities, I now intend to perform an analysis of a broader range of markers, including performing lineage-tracing experiment using caged-dextran method as described in the literature[29]. Such studies will allow me to begin to understand where the *pomc* progenitor cells lie at distinct phases of development, the markers they express as they differentiate, and their relationship to *rx3* positive and *shh* positive cells.

A second issue that I would like to address in future studies is to firmly establish whether Shh signalling is important in two phases: a first phase in which Shh is required for the induction and establishment of the ADH and its adjacent region including arcuate nucleus progenitors, and a second phase in which Shh is required for the specification and differentiation of *pomc* positive cells in the arcuate nucleus. Such a distinct temporal function of SHH has been reported before in the neural tube, where SHH is first required to convert naive neural plate cells into a progenitor state, and in which subsequent SHH signalling mediates the differentiation to motor neurons[140]. I intend to now demonstrate whether a similar operation of Shh occurs in the generation of *pomc* positive cells in the arcuate nucleus, suggesting a conserved function and mechanism of *shh* in the generation of neurons along the A-P axis of the vertebrate neural tube, for instance, either through further conditional experiments using cyclopamine, or through the use of light-activated morpholinos.

Caveats

An outstanding question is that of why *pomc* positive cells are still found in the arcuate nucleus of the *rx3* morphant embryos albeit in significantly lower numbers. This occurs despite the apparent loss of the ADH/*shh* expression in the ADH. There are at least three reasons that could account for this:

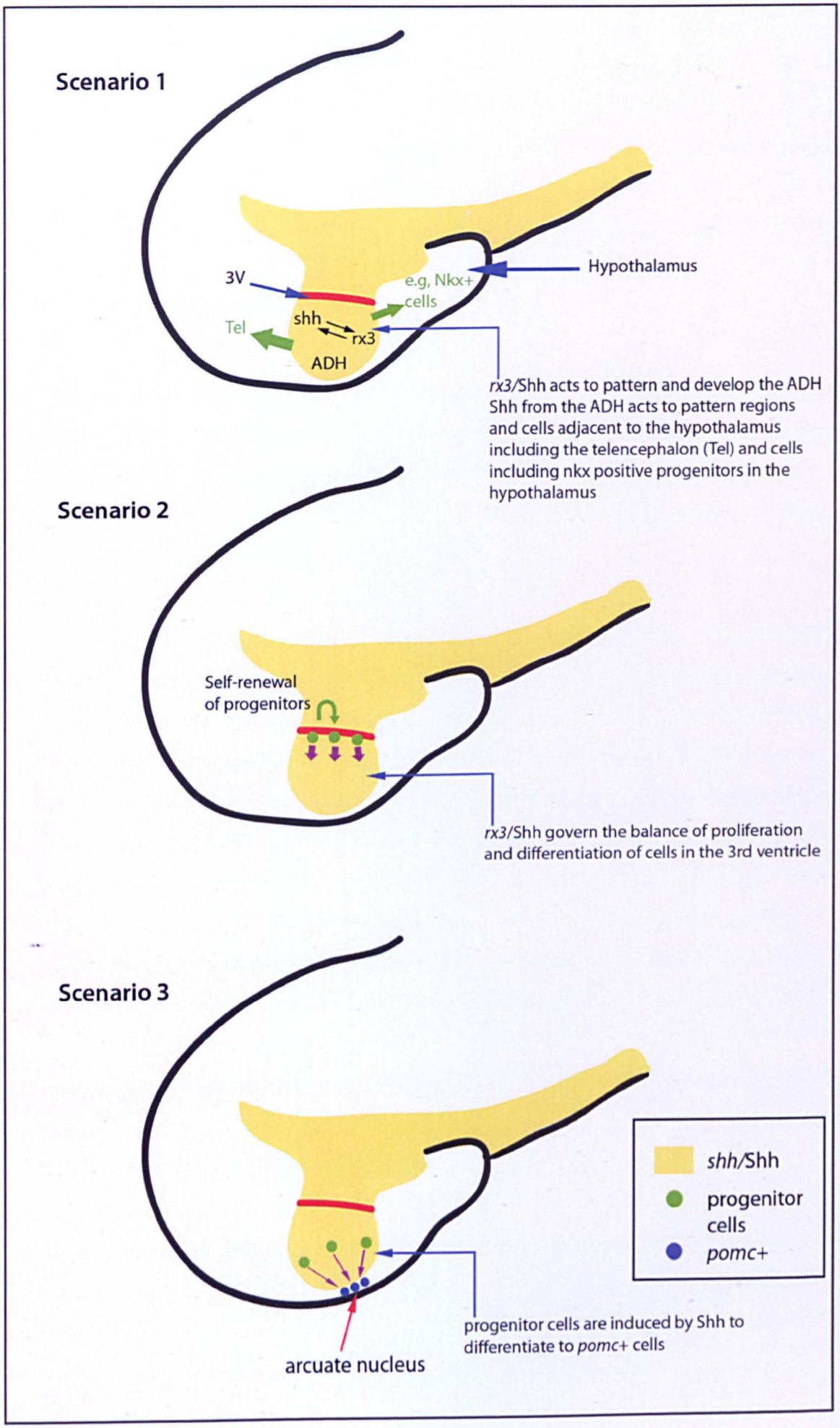
Scenario 1
3V
Tel
shh
rx3
ADH
e.g, Nkx+
cells
Hypothalamus
rx3/Shh acts to pattern and develop the ADH
Shh from the ADH acts to pattern regions
and cells adjacent to the hypothalamus
including the telencephalon (Tel) and cells
including nkx positive progenitors in the
hypothalamus
Scenario 2
Self-renewal
of progenitors
rx3/Shh govern the balance of proliferation
and differentiation of cells in the 3rd ventricle
Scenario 3
shh/Shh
progenitor
cells
pomc+
progenitor cells are induced by Shh to
differentiate to pomc+ cells
arcuate nucleus

First, it is possible that there are other factors apart from Shh and *rx3* governing *pomc* cell differentiation. For instance, in the adult mouse hypothalamus, the differentiation of neural progenitor cells from the 3rd ventricle to a *Pomc* cell fate in the arcuate nucleus requires FGF signalling[49]. My studies show that i) Inhibition of Fgf signalling led to the reduction of *pomc* positive cells in the arcuate nucleus and ii) Fgf signalling appears largely unaffected in the hypothalamus after *rx3* or Shh signalling reduction in *rx3* morphant embryos. Thus, it is possible that Fgf plays some role in *pomc* differentiation.

Second, since the analyses were performed using *rx3* morphants, there is a chance that the inhibitory effectof the morpholinos dissipate as the embryos develop and mature. The gradual loss of morpholino knockdown effects in the developing zebrafish embryo is quite common. Hence, it will be vital to repeat some of these experiments using the *chokh* mutant embryos.

Thirdly, as *rx3* morphant embryos have lost *rx3* function from the one-cell stage, it is possible that some of the observed effects are indirect effects resulting from the early loss of telencephalic/diencephalic subdivisions. In future, I would therefore like to perform a conditional analysis of *rx3* function. Although a conditional *rx3* knock-down mutant can be generated, a quicker way would be to attenuate *rx3* function through the use of light-activated morpholinos or photomorph[141]. This new method incorporates the design of mRNA specific targeted morpholino (i.e. *rx3*) in the same way as a regular morpholino but embedded within a caging molecule that will degrade upon exposure to a 405 nm laser wavelength. Using a confocal, this laser can be directed to specifically degrade the cage and release the morpholino in a site-specific manner. This technique hence not only allows for temporal, but spatial control as well and can almost eliminate non-specific effects.

Regulation of *rx3* expression by Fgfs

In addition to demonstrating that *rx3* is likely to operate in concert with Shh, my data reveals a potential role for Fgf as an upstream regulator of *rx3* expression. This finding supports previous studies, demonstrating that Fgf acts upstream of soxB1 gene (sox2/3) expression during retinal development[142] and that soxB1

genes regulate expression of rx3 during early embryogenesis[143] .Together these analyses suggest a possible molecular route, in which upstream Fgf signalling indirectly regulates the expression of *rx3* through *soxB1* genes. In future experiments, I would like to address this by examining *soxB1* expression in SU-treated embryos, and examining *rx3* expression in *soxB1* knock-out embryos (i.e. *sox2* or *sox3* morpholino knockdown).

Maintenance of *shh* and *fgf3* in the adult zebrafish hypothalamus

The expression of signalling factors in the adult environment is beginning to attract active research as these molecules may play pertinent roles in the maintenance of adult systems. Mis-regulation of SHH signalling has been implicated in the onset of tumours including basal cell carcinoma (BCC)[144, 145] and medulloblastoma[146, 147] whilst mis-regulated FGF signalling has been implicated in the growth of astrocytomas[148]. These findings clearly suggest that both *shh* and *fgfs* are important in the adult as 'system maintenance' factors without which disease states will begin to manifest.

In result chapter 5, I have demonstrated the maintenance of *shh* and *fgf3* in the adult zebrafish medial hypothalamus, and demonstrated that, in the adult medial zebrafish hypothalamus, *shh* may be crucial for the proliferation of NPCs. In future, I would like to examine if *rx3* is still expressed in the adult zebrafish hypothalamus and if it is regulating *shh* expression as in the embryos. Interestingly, *rx3* is reported to be expressed in the hypothalamus of the adult Medaka fish (*Oryzias latipes*)[131] suggesting the strong likelihood of detecting *rx3* expression in the hypothalamus of the adult zebrafish.

Additionally, the expression of *fgf3* detected in the adult zebrafish hypothalamus warrants a further investigation into the role of *fgf3* in the potential regulation of NPCs and a potential involvement in *rx3* maintenance. Unfortunately, the *chokh* mutant line is juvenile lethal and would not survive until adulthood, making it impossible for loss-of-function *rx3* study in the adult. Nevertheless, it might still be informative to study the above using heterozygous *chokh* mutant embryos.

Suitability of the zebrafish as model for hypothalamic study

As outlined in the thesis Introduction, the zebrafish has many unique features, which facilitates its use as an emerging model system for developmental biology research. However as with any other model system, there are both advantages and limitations to the zebrafish model. In this section I will highlight some of the advantages and limitations of using the zebrafish to study the hypothalamus from my own experimentation experience gained through this thesis.

i) Advantages

One of the most useful advantages of using the zebrafish is the relative ease of performing whole-mount ISH and immunohistochemistry during embryonic development, especially at the early stages. It is not as easy to perform whole-mount ISH using chick and mouse embryos due to their large size and thick ectodermal layers that prevent the easy penetration of ISH probes and antibodies. In these model systems, ISH is normally performed on hypothalamic sections or semi-wholemounts, where the embryos are cut into half along their neuroaxes. However, whole mount visualization of ISH labelling often provides invaluable information through an absolute observation of gene expression in the hypothalamus. Also, established methods such as PTU and bleaching that allows for the removal of melanocytes which cause pigmentation from the mid-staged embryos onwards, are available and easily performed in the zebrafish embryos. The availability of pigment-less mutants like *nacre* and *golden* provides an alternative to the above and can be crossed to other mutant lines as well, to produce pigment-less embryos. Apart from that, removal of the eyes to allow visualization of the hypothalamus is quite a straightforward technique which can be done manually using fine needles or chemically through dispase treatment as described in Materials and Methods.

ii) Disadvantages

The hypothalamus of the zebrafish embryo is extremely small relative to the chick and mouse embryos. This makes the characterisation and manipulation of the

hypothalamus challenging. Whilst the hypothalamus is anatomically similar to the chick and mouse at very early stages of development, it begins to look different from late embryonic stage onwards into adult. A clear example of this is the existence of two hypothalamic lobes (i.e. the superior and inferior lobes) in the adult zebrafish, which does not exist in the adult rodent models. Another example is the appearance of the lateral recesses of the 3rd ventricle (or diencephalic ventricle) in the adult hypothalamus, which is not seen in the rodent models. As yet, the function of these recesses is still currently unknown. Also as outlined in the result chapters, the zebrafish does not have infundibulum or median eminence structures. Nevertheless, despite these anatomical differences, the zebrafish hypothalamus is still by and large functionally similar to those of the higher vertebrates and shares conserved patterning and development as seen through this thesis.

Conclusion and Application

The data presented in this thesis is the first to describe the novel role of *rx3* in the hypothalamus. It is also the first to show *rx3* as a regulator of the *shh* pathway, and vice-versa, and the upstream control of *rx3* expression by *fgf*.

Pomc is a key gene involved in feeding behaviour and this suggests that anopthalmic patients (where loss of function *Rx/Rax* is described) might suffer from a dysregulated feeding function, which is worth investigating. The *Rx/Rax* gene is thus potentially useful as a therapeutic target not only for anopthalmia but also for feeding-related problems.

Apart from that, the data provided in this thesis also show the maintenance of *shh* and *fgf3* in the adult hypothalamus. Evidence suggests that *shh* functions to control the proliferation of adult neural progenitor cells. These findings provide further support to the importance of studying maintained signalling factors in the adult environment. Additionally, the technique to introduce chemicals through IP injection as developed through this thesis could be extremely useful to study a variety of signalling factors in the adult zebrafish.

References

References:

1. Butler, A. B. & Hodos, W. Comparative Vertebrate Neuroanatomy (Evolution and Adaptation) (Wiley, 2005).
2. Liu, F. & Placzek, M. in prep. (2010).
3. Spemann, H. Embryonic development and induction (Hafner, New York, 1938).
4. Catala, M., Teillet, M. A., De Robertis, E. M. & Le Douarin, M. L. A spinal cord fate map in the avian embryo: while regressing, Hensen's node lays down the notochord and floor plate thus joining the spinal cord lateral walls. Development 122, 2599-610 (1996).
5. Dessaud, E., McMahon, A. P. & Briscoe, J. Pattern formation in the vertebrate neural tube: a sonic hedgehog morphogen-regulated transcriptional network. Development 135, 2489-503 (2008).
6. Briscoe, J., Pierani, A., Jessell, T. M. & Ericson, J. A homeodomain protein code specifies progenitor cell identity and neuronal fate in the ventral neural tube. Cell 101, 435-45 (2000).
7. Ribes, V. & Briscoe, J. Establishing and interpreting graded Sonic Hedgehog signaling during vertebrate neural tube patterning: the role of negative feedback. Cold Spring Harb Perspect Biol 1, a002014 (2009).
8. Strahle, U., Lam, C. S., Ertzer, R. & Rastegar, S. Vertebrate floor-plate specification: variations on common themes. Trends Genet 20, 155-62 (2004).
9. Placzek, M. & Briscoe, J. The floor plate: multiple cells, multiple signals. Nat Rev Neurosci 6, 230-40 (2005).
10. Le Douarin, N. M. & Halpern, M. E. Discussion point. Origin and specification of the neural tube floor plate: insights from the chick and zebrafish. Curr Opin Neurobiol 10, 23-30 (2000).
11. Ohyama, K., Das, R. & Placzek, M. Temporal progression of hypothalamic patterning by a dual action of BMP. Development 135, 3325-31 (2008).
12. Placzek, M. personal communications.
13. Mathieu, J., Barth, A., Rosa, F. M., Wilson, S. W. & Peyrieras, N. Distinct and cooperative roles for Nodal and Hedgehog signals during hypothalamic development. Development 129, 3055-65 (2002).
14. Manning, L. et al. Regional morphogenesis in the hypothalamus: a BMP-Tbx2 pathway coordinates fate and proliferation through Shh downregulation. Dev Cell 11, 873-85 (2006).
15. Jeong, Y. & Epstein, D. J. Distinct regulators of Shh transcription in the floor plate and notochord indicate separate origins for these tissues in the mouse node. Development 130, 3891-902 (2003).
16. Muthu, V. & Placzek, M. unpublished data.
17. Kapsimali, M., Caneparo, L., Houart, C. & Wilson, S. W. Inhibition of Wnt/Axin/beta-catenin pathway activity promotes ventral CNS midline tissue to adopt hypothalamic rather than floorplate identity. Development 131, 5923-33 (2004).
18. Tessmar-Raible, K. et al. Conserved sensory-neurosecretory cell types in annelid and fish forebrain: insights into hypothalamus evolution. Cell 129, 1389-400 (2007).
19. Furukawa, T., KOZAK, C. A. & CEPKO, C. L. rax, a novel paired-type homeobox gene, shows expression in the

anterior neural fold and developing retina. Proc. Natl. Acad. Sci. USA 94, 3088-3093 (1997).
20. Billeter, M. et al. Determination of the nuclear magnetic resonance solution structure of an Antennapedia homeodomain-DNA complex. J Mol Biol 234, 1084-93 (1993).
21. Ensembl.
22. Thompson, J. D., Gibson, T. J., Plewniak, F., Jeanmougin, F. & Higgins, D. G. The ClustalX windows interface: flexible strategies for multiple sequence alignment aided by quality analysis tools. Nucleic Acids Research 25, 4876-4882 (1997).
23. Page, R. D. M.
24. Lequeux, L. et al. Confirmation of RAX gene involvement in human anophthalmia. Clin Genet 74, 392-5 (2008).
25. Mathers, P. H., Grinberg, A., Mahon, K. A. & Jamrich, M. The Rx homeobox gene is essential for vertebrate eye development. Nature 387, 603-7 (1997).
26. Loosli, F. et al. Loss of eyes in zebrafish caused by mutation of chokh/rx3. EMBO Rep 4, 894-9 (2003).
27. Andreazzoli, M., Gestri, G., Angeloni, D., Menna, E. & Barsacchi, G. Role of Xrx1 in Xenopus eye and anterior brain development. Development 126, 2451-60 (1999).
28. Loosli, F. et al. Medaka eyeless is the key factor linking retinal determination and eye growth. Development 128, 4035-44 (2001).
29. Stigloher, C. et al. Segregation of telencephalic and eye-field identities inside the zebrafish forebrain territory is controlled by Rx3. Development 133, 2925-35 (2006).
30. Zhang, L., Mathers, P. H. & Jamrich, M. Function of Rx, but not Pax6, is essential for the formation of retinal progenitor cells in mice. Genesis 28, 135-42 (2000).
31. Medina-Martinez, O. et al. Cell-autonomous requirement for rx function in the mammalian retina and posterior pituitary. PLoS One 4, e4513 (2009).
32. Chuang, J. C., Mathers, P. H. & Raymond, P. A. Expression of three Rx homeobox genes in embryonic and adult zebrafish. Mech Dev 84, 195-8 (1999).
33. Dickmeis, T. et al. Glucocorticoids play a key role in circadian cell cycle rhythms. PLoS Biol 5, e78 (2007).
34. Thompson, J. A. e. a. Embryonic Stem Cell Lines Derived from Human Blastocysts. Science 282, 1145-1147 (1998).
35. NIH.
36. Spradling, A., Drummond-Barbosa, D. & Kai, T. Stem cells find their niche. Nature 414, 98-104 (2001).
37. Palasz, A. & Kaminski, M. Stem cell niche in the Drosophila ovary and testis; a valuable model of the intercellular signalling relationships. Adv Med Sci 54, 143-9 (2009).
38. Alvarez-Buylla, A., Garcia-Verdugo, J. M. & Tramontin, A. D. A unified hypothesis on the lineage of neural stem cells. Nat Rev Neurosci 2, 287-93 (2001).
39. Morshead, C. M. et al. Neural stem cells in the adult mammalian forebrain: a relatively quiescent subpopulation of subependymal cells. Neuron 13, 1071-82 (1994).
40. Weiss, S. et al. Multipotent CNS stem cells are present in the adult mammalian spinal cord and ventricular neuroaxis. J Neurosci 16, 7599-609 (1996).

41. Bedard, A. & Parent, A. Evidence of newly generated neurons in the human olfactory bulb. Brain Res Dev Brain Res 151, 159-68 (2004).
42. Gould, E., Vail, N., Wagers, M. & Gross, C. G. Adult-generated hippocampal and neocortical neurons in macaques have a transient existence. Proc Natl Acad Sci U S A 98, 10910-7 (2001).
43. Gould, E., Reeves, A. J., Graziano, M. S. & Gross, C. G. Neurogenesis in the neocortex of adult primates. Science 286, 548-52 (1999).
44. Zhao, M. et al. Evidence for neurogenesis in the adult mammalian substantia nigra. Proc Natl Acad Sci U S A 100, 7925-30 (2003).
45. Eccles, J. C. Neurogenesis and morphogenesis in the cerebellar cortex. Proc Natl Acad Sci U S A 66, 294-301 (1970).
46. Xu, Y. et al. Neurogenesis in the ependymal layer of the adult rat 3rd ventricle. Exp Neurol 192, 251-64 (2005).
47. Kaslin, J., Ganz, J. & Brand, M. Proliferation, neurogenesis and regeneration in the non-mammalian vertebrate brain. Philos Trans R Soc Lond B Biol Sci 363, 101-22 (2008).
48. Grandel, H., Kaslin, J., Ganz, J., Wenzel, I. & Brand, M. Neural stem cells and neurogenesis in the adult zebrafish brain: origin, proliferation dynamics, migration and cell fate. Dev Biol 295, 263-77 (2006).
49. Kokoeva, M. V., Yin, H. & Flier, J. S. Neurogenesis in the hypothalamus of adult mice: potential role in energy balance. Science 310, 679-83 (2005).
50. Kokoeva, M. V., Yin, H. & Flier, J. S. Evidence for constitutive neural cell proliferation in the adult murine hypothalamus. J Comp Neurol 505, 209-20 (2007).
51. Pierce, A. A. & Xu, A. W. De novo neurogenesis in adult hypothalamus as a compensatory mechanism to regulate energy balance. J Neurosci 30, 723-30.
52. Robins, S. (*unpublished data*).
53. Streisinger, G. SEGREGATION ANALYSES AND GENE-CENTROMERE DISTANCES IN ZEBRAFISH. Genetics 112 (1986).
54. White, R. M. et al. Transparent adult zebrafish as a tool for in vivo transplantation analysis. Cell Stem Cell 2, 183-9 (2008).
55. Nusslein-Volhard, C. & Dahm, R. Zebrafish: A Practical Approach (2002).
56. Kimmel, C. B., Ballard, W. W., Kimmel, S. R., Ullmann, B. & Schilling, T. F. Stages of embryonic development of the zebrafish. Dev Dyn 203, 253-310 (1995).
57. InvitrogenPrimerDesignTool.
58. Sambrook, J., Fritsch, E. F. & Maniatis, T. Molecular Cloning: A Laboratory Manual (Plainview, New York: Cold Spring Harbor Laboratory Press, 1989).
59. BLAST(NCBI).
60. NEBcutterV2.0.
61. Bijlsma, M. F. et al. Repression of smoothened by patched-dependent (pro-)vitamin D3 secretion. PLoS Biol 4, e232 (2006).
62. Pontecorvi, M., Goding, C. R., Richardson, W. D. & Kessaris, N. Expression of Tbx2 and Tbx3 in the developing hypothalamic-pituitary axis. Gene Expr Patterns 8, 411-7 (2008).
63. Sleeman, M. et al. Identification of a new fibroblast growth factor receptor, FGFR5. Gene 271, 171-82 (2001).
64. Herzog, W. et al. Fgf3 signaling from the ventral diencephalon is required for early specification and subsequent survival of the zebrafish adenohypophysis. Development 131, 3681-92 (2004).

65. Pearson, C. Unpublished data (*unpublished data*).
66. Hajihosseini, M. K. et al. Localization and fate of Fgf10-expressing cells in the adult mouse brain implicate Fgf10 in control of neurogenesis. Mol Cell Neurosci 37, 857-68 (2008).
67. Sbrogna, J. L., Barresi, M. J. & Karlstrom, R. O. Multiple roles for Hedgehog signaling in zebrafish pituitary development. Dev Biol 254, 19-35 (2003).
68. Szabo, N. E. et al. Role of neuroepithelial Sonic hedgehog in hypothalamic patterning. J Neurosci 29, 6989-7002 (2009).
69. Shimogori, T. et al. A genomic atlas of mouse hypothalamic development. Nat Neurosci 13, 767-75 (2010).
70. Palma, V. et al. Sonic hedgehog controls stem cell behavior in the postnatal and adult brain. Development 132, 335-44 (2005).
71. Kengaku, M. & Okamoto, H. Basic fibroblast growth factor induces differentiation of neural tube and neural crest lineages of cultured ectoderm cells from Xenopus gastrula. Development 119, 1067-78 (1993).
72. Regan, J. C., Concha, M. L., Roussigne, M., Russell, C. & Wilson, S. W. An Fgf8-dependent bistable cell migratory event establishes CNS asymmetry. Neuron 61, 27-34 (2009).
73. Ohuchi, H. et al. FGF10 acts as a major ligand for FGF receptor 2 IIIb in mouse multi-organ development. Biochem Biophys Res Commun 277, 643-9 (2000).
74. Challis, B. G. et al. A missense mutation disrupting a dibasic prohormone processing site in pro-opiomelanocortin (POMC) increases susceptibility to early-onset obesity through a novel molecular mechanism. Hum Mol Genet 11, 1997-2004 (2002).
75. Krude, H. et al. Severe early-onset obesity, adrenal insufficiency and red hair pigmentation caused by POMC mutations in humans. Nat Genet 19, 155-7 (1998).
76. de Souza, F. S. et al. Identification of neuronal enhancers of the proopiomelanocortin gene by transgenic mouse analysis and phylogenetic footprinting. Mol Cell Biol 25, 3076-86 (2005).
77. Placzek, M., Jessell, T. M. & Dodd, J. Induction of floor plate differentiation by contact-dependent, homeogenetic signals. Development 117, 205-18 (1993).
78. Agren, M., Kogerman, P., Kleman, M. I., Wessling, M. & Toftgard, R. Expression of the PTCH1 tumor suppressor gene is regulated by alternative promoters and a single functional Gli-binding site. Gene 330, 101-14 (2004).
79. Watanabe, K. et al. Directed differentiation of telencephalic precursors from embryonic stem cells. Nat Neurosci 8, 288-96 (2005).
80. Martinez-Morales, J. R., Signore, M., Acampora, D., Simeone, A. & Bovolenta, P. Otx genes are required for tissue specification in the developing eye. Development 128, 2019-30 (2001).
81. Briscoe, J. & Ericson, J. The specification of neuronal identity by graded Sonic Hedgehog signalling. Semin Cell Dev Biol 10, 353-62 (1999).
82. Vila, G. et al. Sonic hedgehog regulates CRH signal transduction in the adult pituitary. Faseb J 19, 281-3 (2005).
83. Barresi, M. J., Stickney, H. L. & Devoto, S. H. The zebrafish slow-muscle-omitted gene product is required for Hedgehog signal transduction and the development of slow muscle identity. Development 127, 2189-99 (2000).
84. van Eeden, F. J. et al. Mutations affecting somite formation and patterning in the zebrafish, Danio rerio. Development 123, 153-64 (1996).

85. Schauerte, H. E. et al. Sonic hedgehog is not required for the induction of medial floor plate cells in the zebrafish. Development 125, 2983-93 (1998).
86. Incardona, J. P., Gaffield, W., Kapur, R. P. & Roelink, H. The teratogenic Veratrum alkaloid cyclopamine inhibits sonic hedgehog signal transduction. Development 125, 3553-62 (1998).
87. Cooper, M. K., Porter, J. A., Young, K. E. & Beachy, P. A. Teratogen-mediated inhibition of target tissue response to Shh signaling. Science 280, 1603-7 (1998).
88. Chen, J. K., Taipale, J., Cooper, M. K. & Beachy, P. A. Inhibition of Hedgehog signaling by direct binding of cyclopamine to Smoothened. Genes Dev 16, 2743-8 (2002).
89. Bellipanni, G., Rink, E. & Bally-Cuif, L. Cloning of two tryptophan hydroxylase genes expressed in the diencephalon of the developing zebrafish brain. Mech Dev 119 Suppl 1, S215-20 (2002).
90. Lee, J. E., Wu, S. F., Goering, L. M. & Dorsky, R. I. Canonical Wnt signaling through Lef1 is required for hypothalamic neurogenesis. Development 133, 4451-61 (2006).
91. Jeong, J. Y. et al. Patterning the zebrafish diencephalon by the conserved zinc-finger protein Fezl. Development 134, 127-36 (2007).
92. Medterms. http://www.medterms.com/script/main/art.asp?articlekey=24514.
93. Bottcher, R. T. & Niehrs, C. Fibroblast growth factor signaling during early vertebrate development. Endocr Rev 26, 63-77 (2005).
94. Cayuso, J. & Marti, E. Morphogens in motion: growth control of the neural tube. J Neurobiol 64, 376-87 (2005).
95. Tanaka, E. M. & Gann, A. F. Limb development. The budding role of FGF. Curr Biol 5, 594-7 (1995).
96. Lee, Y., Grill, S., Sanchez, A., Murphy-Ryan, M. & Poss, K. D. Fgf signaling instructs position-dependent growth rate during zebrafish fin regeneration. Development 132, 5173-83 (2005).
97. Mohammadi, M. et al. Structures of the tyrosine kinase domain of fibroblast growth factor receptor in complex with inhibitors. Science 276, 955-60 (1997).
98. Herzog, W. et al. Genetic analysis of adenohypophysis formation in zebrafish. Mol Endocrinol 18, 1185-95 (2004).
99. Kosaka, N. et al. FGF-4 regulates neural progenitor cell proliferation and neuronal differentiation. Faseb J 20, 1484-5 (2006).
100. Sato, T. et al. FRS2alpha Regulates Erk Levels to Control a Self-Renewal Target Hes1 and Proliferation of FGF-Responsive Neural Stem/Progenitor Cells. Stem Cells.
101. Forlano, P. M. & Cone, R. D. Conserved neurochemical pathways involved in hypothalamic control of energy homeostasis. J Comp Neurol 505, 235-48 (2007).
102. Cerda-Reverter, J. M., Ling, M. K., Schioth, H. B. & Peter, R. E. Molecular cloning, characterization and brain mapping of the melanocortin 5 receptor in the goldfish. J Neurochem 87, 1354-67 (2003).
103. Berberoglu, M. A., Dong, Z., Mueller, T. & Guo, S. fezf2 expression delineates cells with proliferative potential and expressing markers of neural stem cells in the adult zebrafish brain. Gene Expr Patterns 9, 411-22 (2009).

104. Topp, S. et al. Fgf signaling in the zebrafish adult brain: association of Fgf activity with ventricular zones but not cell proliferation. J Comp Neurol 510, 422-39 (2008).
105. McNay, D., Robins, S., Flier, J. S. & Placzek, M. in prep (2010).
106. Lam, C. S., Marz, M. & Strahle, U. gfap and nestin reporter lines reveal characteristics of neural progenitors in the adult zebrafish brain. Dev Dyn 238, 475-86 (2009).
107. Villares, R. & Cabrera, C. V. The achaete-scute gene complex of D. melanogaster: conserved domains in a subset of genes required for neurogenesis and their homology to myc. Cell 50, 415-24 (1987).
108. Wullimann, M. F. & Mueller, T. Expression of Zash-1a in the postembryonic zebrafish brain allows comparison to mouse Mash1 domains. Brain Res Gene Expr Patterns 1, 187-92 (2002).
109. Sommer, L., Shah, N., Rao, M. & Anderson, D. J. The cellular function of MASH1 in autonomic neurogenesis. Neuron 15, 1245-58 (1995).
110. Kawai, T., Takagi, N., Nakahara, M. & Takeo, S. Changes in the expression of Hes5 and Mash1 mRNA in the adult rat dentate gyrus after transient forebrain ischemia. Neurosci Lett 380, 17-20 (2005).
111. McNay, D. E., Pelling, M., Claxton, S., Guillemot, F. & Ang, S. L. Mash1 is required for generic and subtype differentiation of hypothalamic neuroendocrine cells. Mol Endocrinol 20, 1623-32 (2006).
112. Sauer, B. Inducible gene targeting in mice using the Cre/lox system. Methods 14, 381-92 (1998).
113. Sathyanesan, A. G. & Joy, K. P. A micromorphological and histoenzymological study on the third ventricular ependyma of the teleost Clarias batrachus (L.). Z Mikrosk Anat Forsch 92, 700-22 (1978).
114. Drapeau, J. et al. Nestin-expressing neural stem cells identified in the scar following myocardial infarction. J Cell Physiol 204, 51-62 (2005).
115. Doetsch, F., Garcia-Verdugo, J. M. & Alvarez-Buylla, A. Cellular composition and three-dimensional organization of the subventricular germinal zone in the adult mammalian brain. J Neurosci 17, 5046-61 (1997).
116. Steinert, P. M. et al. A high molecular weight intermediate filament-associated protein in BHK-21 cells is nestin, a type VI intermediate filament protein. Limited co-assembly in vitro to form heteropolymers with type III vimentin and type IV alpha-internexin. J Biol Chem 274, 9881-90 (1999).
117. Chiasson, B. J., Tropepe, V., Morshead, C. M. & van der Kooy, D. Adult mammalian forebrain ependymal and subependymal cells demonstrate proliferative potential, but only subependymal cells have neural stem cell characteristics. J Neurosci 19, 4462-71 (1999).
118. Del Sal, G., Ruaro, M. E., Philipson, L. & Schneider, C. The growth arrest-specific gene, gas1, is involved in growth suppression. Cell 70, 595-607 (1992).
119. Obayashi, S., Tabunoki, H., Kim, S. U. & Satoh, J. Gene expression profiling of human neural progenitor cells following the serum-induced astrocyte differentiation. Cell Mol Neurobiol 29, 423-38 (2009).
120. Sanchez, P. & Ruiz i Altaba, A. In vivo inhibition of endogenous brain tumors through systemic interference of Hedgehog signaling in mice. Mech Dev 122, 223-30 (2005).
121. Machold, R. et al. Sonic hedgehog is required for progenitor cell maintenance in telencephalic stem cell niches. Neuron 39, 937-50 (2003).

122. Bambakidis, N. C. et al. Endogenous stem cell proliferation induced by intravenous hedgehog agonist administration after contusion in the adult rat spinal cord. J Neurosurg Spine 10, 171-6 (2009).
123. Bambakidis, N. C., Wang, R. Z., Franic, L. & Miller, R. H. Sonic hedgehog-induced neural precursor proliferation after adult rodent spinal cord injury. J Neurosurg 99, 70-5 (2003).
124. Gallagher, E., Enzler, T., Matsuzawa, A. & Karin, M. 5-bromo-2-deoxyuridine (BrdU) and 7-amino-actinomycin (7-AAD) staining for cell proliferation assay. Nature Protocols (2007).
125. Chen, Y., Hennessy, K., Botstein, D. & Tye, B. CDC46/MCM5, a yeast protein whose subcellular localization is cell cycle-regulated, is involved in DNA replication at autonomously replicating sequences. Proc Natl Acad Sci U S A 89, 10459-63 (1992).
126. Ryu, S. & Driever, W. Minichromosome maintenance proteins as markers for proliferation zones during embryogenesis. Cell Cycle 5, 1140-2 (2006).
127. Soria, G., Speroni, J., Podhajcer, O. L., Prives, C. & Gottifredi, V. p21 differentially regulates DNA replication and DNA-repair-associated processes after UV irradiation. J Cell Sci 121, 3271-82 (2008).
128. Fan, H. & Khavari, P. A. Sonic hedgehog opposes epithelial cell cycle arrest. J Cell Biol 147, 71-6 (1999).
129. Rogers CD, Archer TC, Cunningham DD, Grammer TC & EM, C. Sox3 expression is maintained by FGF signaling and restricted to the neural plate by Vent proteins in the Xenopus embryo. Developmental Biology 313, 307-319 (2008).
130. Prykhozhij, S. V. & Neumann, C. J. Distinct roles of Shh and Fgf signaling in regulating cell proliferation during zebrafish pectoral fin development. BMC Dev Biol 8, 91 (2008).
131. Rojas-Munoz, A., Dahm, R. & Nusslein-Volhard, C. chokh/rx3 specifies the retinal pigment epithelium fate independently of eye morphogenesis. Dev Biol 288, 348-62 (2005).
132. Ruiz i Altaba A, Placzek M, Baldassare M, Dodd J & TM., J. Early stages of notochord and floor plate development in the chick embryo defined by normal and induced expression of HNF-3 beta. Developmental Biology 170, 299-313 (1995).
133. Ericsson, J. (2010).
134. Vokes, S. A. et al. Genomic characterization of Gli-activator targets in sonic hedgehog-mediated neural patterning. Development 134, 1977-89 (2007).
135. Ohyama, K., Ellis, P., Kimura, S. & Placzek, M. Directed differentiation of neural cells to hypothalamic dopaminergic neurons. Development 132, 5185-97 (2005).
136. Yee, C. L., Wang, Y., Anderson, S., Ekker, M. & Rubenstein, J. L. Arcuate nucleus expression of NKX2.1 and DLX and lineages expressing these transcription factors in neuropeptide Y(+), proopiomelanocortin(+), and tyrosine hydroxylase(+) neurons in neonatal and adult mice. J Comp Neurol 517, 37-50 (2009).
137. Jo, Y. H. & Chua, S., Jr. Transcription factors in the development of medial hypothalamic structures. Am J Physiol Endocrinol Metab 297, E563-7 (2009).
138. Wataya, T. et al. Minimization of exogenous signals in ES cell culture induces rostral hypothalamic differentiation. Proc Natl Acad Sci U S A 105, 11796-801 (2008).

139. Ahn, S. & Joyner, A. L. In vivo analysis of quiescent adult neural stem cells responding to Sonic hedgehog. Nature 437, 894-7 (2005).
140. Ericson, J., Morton, S., Kawakami, A., Roelink, H. & Jessell, T. M. Two critical periods of Sonic Hedgehog signaling required for the specification of motor neuron identity. Cell 87, 661-73 (1996).
141. Tomasini, A. J., Schuler, A. D., Zebala, J. A. & Mayer, A. N. PhotoMorphs: a novel light-activated reagent for controlling gene expression in zebrafish. Genesis 47, 736-43 (2009).
142. Ishii, Y., Weinberg, K., Oda-Ishii, I., Coughlin, L. & Mikawa, T. Morphogenesis and cytodifferentiation of the avian retinal pigmented epithelium require downregulation of Group B1 Sox genes. Development 136, 2579-89 (2009).
143. Okuda, Y., Ogura, E., Kondoh, H. & Kamachi, Y. B1 SOX coordinate cell specification with patterning and morphogenesis in the early zebrafish embryo. PLoS Genet 6, e1000936.
144. Oro, A. E. et al. Basal cell carcinomas in mice overexpressing sonic hedgehog. Science 276, 817-21 (1997).
145. Fan, H., Oro, A. E., Scott, M. P. & Khavari, P. A. Induction of basal cell carcinoma features in transgenic human skin expressing Sonic Hedgehog. Nat Med 3, 788-92 (1997).
146. Zurawel, R. H. et al. Analysis of PTCH/SMO/SHH pathway genes in medulloblastoma. Genes Chromosomes Cancer 27, 44-51 (2000).
147. Goodrich, L. V., Milenkovic, L., Higgins, K. M. & Scott, M. P. Altered neural cell fates and medulloblastoma in mouse patched mutants. Science 277, 1109-13 (1997).
148. Morrison, R. S. et al. Basic fibroblast growth factor and fibroblast growth factor receptor I are implicated in the growth of human astrocytomas. J Neurooncol 18, 207-16 (1994).
149. Abitua,. Wikipedia
150. Wasserman, B. Developmental Biology Page (http://www.luc.edu/faculty/wwasser/dev/devm.htm)
151. Brown, M. The Developing Brain (Oxford University Press).
152. Human Development Lecture ((http://www.utm.utoronto.ca/ ~w3bio380/lecture13.htm)
153. Ciruna, B., Jenny, A., Lee, D., Mlodzik, M., Schier, A.F. Planar cell polarity signalling couples cell division and morphogenesis during neurulation Nature 439, (2006).
154. Betrand, N., Castro, D.S., Guillemot, F. Proneural genes and the specification of neural cell types. Nature Reviews Neuroscience 3, (2002).
155. Gould, E. How widespread is adult neurogenesis in mammals?. Nature Reviews Neuroscience 8, (2007).